# Performance Optimization of Industrial Refrigeration Systems

By

Kyle A. Manske

A thesis submitted in partial fulfillment of

the requirements for the degree of

## Master of Science

(MECHANICAL ENGINEERING)

at the

University of Wisconsin-Madison

1999

Approved By:

_____

Date: _____

# Abstract

Industrial refrigeration systems can be found in applications ranging from ice making to food processing and preservation to industrial chemical processes. These systems typically consist of many different components, each component may be produced by a different manufacturer. The operational data provided by the different manufacturers for each component is used by system designers to specify installation and operational procedures of the system. Often times, the optimum control of an individual piece of equipment results in sub-optimal system performance due to unforeseen interactions between the different system components. It is important to identify and monitor key parameters of the system, such as power consumption and refrigeration effect, in order to optimize the performance.

The efforts of this research focused on modeling an operating, ammonia vapor compression, refrigeration system serving a two-temperature food storage and distribution facility located near Milwaukee, WI. This system utilized a combination of both single-screw and reciprocating compressors operating under single-stage compression, an evaporative condenser, and both liquid overfeed and direct expansion evaporators. The model was verified with experimental data recorded from the system and then used to identify alternative designs and operating techniques that lead to optimum system performance.

Changes in system operation such as variable frequency (VFD) or multi-speed motor control on condenser and evaporator fans, head pressure control, refrigerant temperature control, and aspects of load sharing between compressors were investigated. Also, the performance of several alternative system designs was investigated. The aspects of alternative system design that were examined are condenser sizing, two-stage compression, load separation by addition of another suction level, and thermosiphon.

A 31 percent reduction in annual energy usage and a 21 percent reduction in annual peak electrical demand over the current system operation is predicted to be possible with the most feasible of the optimization techniques and designs examined implemented.

# Acknowledgements

I would like to thank my family and friends for being so supportive throughout the process of this research. Without their advice, encouragement, and understanding this work would have never been completed.

I'd also like to especially thank my advisors Sandy and Doug for all their assistance with this research. Thank you Sandy for your extraordinary efforts and support with EES and thank you Doug for sharing your knowledge of ammonia refrigeration with me and allowing me to sit in on your design classes.

Several refrigeration professionals took some of their time and resources to assist me with this research and I would like to also mention their names:
Ruth Urban – Energy Center of Wisconsin
Mike Slawny – WEPCO
Mike Fisher – Vilter Manufacturing Company.
Jim Denkmann – Denkmann Thermal Storage, LTD.
Randy Kastello – J.F. Ahern Co.
Gordon Struder – Evapco
John Kollasch – Evapco

This research project has been sponsored by the Energy Service, Research, and Education Committee through a grant from the Energy Center of Wisconsin.

# List Of Figures

# List Of Tables

# Table Of Contents

# Abbreviation List

The following abbreviations are used extensively throughout this paper.

| | | |
|---|---|---|
| %FLC | -- | percent of full load capacity<br>= (actual capacity)/(available capacity)*100 |
| %FLP | -- | percent of full load power<br>= (actual power)/(power at full load available capacity)*100 |
| BHP | -- | brake horsepower [hp] |
| BPR | -- | back pressure regulator |
| CAP | -- | cooling capacity [ton] |
| COP | -- | coefficient of performance |
| DSR | -- | dry suction return line |
| dx | -- | direct expansion (coil) |
| EES | -- | Engineering Equation Solver |
| epsilon | -- | effectiveness |
| h | -- | enthalpy [btu/lbm] |
| hp | -- | horsepower [hp] |
| HRF | -- | heat rejection factor = (nominal capacity/actual capacity) |
| MBH | -- | 1000 btu/hr |
| OIL | -- | oil cooling load [MBH] |
| P | -- | pressure [psia] |
| P-h diagram | -- | pressure-enthalpy diagram |
| R-717 | -- | ammonia refrigerant |
| Re | -- | Reynolds number |
| s | -- | entropy [btu/hr-F] |
| SCT | -- | saturated condensing temperature [F] |
| SDT | -- | saturated discharge temperature [F] |
| SST | -- | saturated suction temperature [F] |
| T-s diagram | -- | temperature entropy diagram |
| T | -- | temperature [F] |
| TD | -- | temperature difference [F] = (Tair,in - Tref,sat) |
| ton | -- | 12000 btu/hr |
| txv | -- | thermal expansion valve |
| VFD | -- | variable frequency drive |
| WEPCO | -- | Wisconsin Electric Power Company |
| WSR | -- | wet suction return line |

# *Chapter 1 -Introduction*

## 1.1 Refrigeration Background

Industrial refrigeration systems can be found in nearly every developed location in the world. Applications for these systems include food preservation, heat removal from industrial processes such as chemical production, and numerous other special applications in the construction and manufacturing industries. Vapor compression refrigeration systems have been used to reduce the temperature of a particular substance or process for over one hundred years. However, the industrial refrigeration industry has historically paid very little attention to the energy needed to achieve the objectives of the refrigeration processes. As a result, industrial refrigeration system design and operation is more of an art form than a science. Often, even though a refrigeration system is producing the desired result, it may not be operating efficiently. Recent concerns about electrical usage and costs have prompted many in the refrigeration industry to re-evaluate the cost-effectiveness of their system design and operating strategies. Refrigeration system optimization can be defined as a process that produces the desired refrigeration effect for minimum cost (usually life-cycle cost). As energy and equipment become more expensive, the need for optimizing new and existing systems will continue to grow.

The biggest challenge most industrial refrigeration system designers and operators face is component diversity. All refrigeration systems consist of different components and often times each component will be produced by a different manufacturer. Examples of components include compressors, condensers, evaporators, heat exchangers, vessels, piping, expansion valves, pumps, and filters. The arrangement of all these components, in relation to each other, defines the system. The refrigeration system designer must select and arrange components to build-up a coherent and functional system. Often, designers have little information consisting only of performance characteristics of each individual component at a design condition. Basing system design decisions on individual component performance characteristics may lead to sub-optimum performance of the overall system in its as-operated condition. The effects that each of the components have

on each other and the system are often times confounded. The optimum performance of the system rarely occurs when each component is selected to operate at its optimum setting.

In cold food storage applications, the desired result of the refrigeration system is to maintain a food product at a temperature low enough to prevent premature spoilage. This often requires a refrigeration system to reduce the temperature of a warmer product that has been shipped to a refrigerated warehouse for storage and subsequent distribution in the future. The space inside the warehouse must be maintained at or below a particular temperature set point that depends on the product being stored. Humidity control for the storage space may be required as well. These cold storage facilities are generally very large and rely on refrigeration systems sized adequately to maintain the desired temperature. Depending upon the construction of the warehouse, the product shipping schedule, refrigeration system design, and system control, it is likely that the peak energy consumption of a cold storage facility will occur when electrical utilities have their highest demand for electricity.

## 1.2 Research Objectives

To gain further insight into identifying techniques that will lead to more efficient refrigeration systems, this study will baseline the performance of an existing industrial refrigeration system using readily available manufacturer's data and then explore different control strategies and system arrangements with a verified computer model. The information learned from this study will be applicable to other industrial refrigeration systems with similar design criteria. The following objectives identify the scope of this research project.

- To create a computer model of an existing industrial refrigeration system, based on typical manufacturer's data for major system components.
- Validate the model with data acquired from the actual operating system and establish a baseline of its operation.

- Simulate changes in the operating parameters of the system and compare the resulting system performance to the established baseline system performance and explore any additional performance improvement measures.
- Explore different system configurations including:
  - Two-stage compression
  - Split system operation including thermosiphon cooling opportunities
  - Variable and multi-speed motor controls
- Explore different system operating strategies including:
  - Head pressure control
  - Hot gas defrost
  - Load sharing
  - Intermediate pressure control
- Identify critical parameters of the system that designers and operators can use to optimize existing refrigeration systems.
- Present the results of the computer model in a yearly operating cost format and make recommendations on control strategies and system configurations that lead to optimal performance.
- Present performance measures of optimized systems for use in identifying inefficient refrigeration systems.
- Identify the necessary components of a basic instrumentation package that could be used to optimize the performance of an existing industrial refrigeration system.

## 1.3 Thesis Organization

This thesis follows nearly the same chronological progression that the research was completed in. Chapter 1 introduces the need for this work and states the specific objectives of the project. It also provides a detailed description of the particular system that was selected for the study. Chapter 2 details the modeling part of the research. Each major component of the system is introduced and described. Chapter 3 then goes on to verify the model with actual system data and concludes with some details learned from the modeling process. Chapter 4 describes how a yearlong simulation of the system is

accomplished and establishes performance measures for baseline operation of the current system. Chapter 5 investigates four different alternative system configurations and reports the performance of each alternative. Chapter 6 quantifies possible control strategy advantages and examines some of the confounding effects components have on overall system performance. Chapter 6 also contains the yearly simulation results from an optimized cold storage warehouse refrigeration system. Chapter 7 lists the parameters that need to be monitored in a system in order to optimize its performance. It then goes on to report a final comparison of some of the optimizing techniques and system arrangements used for this particular system. Finally it summarizes the major findings of this study and makes a recommendation on potential future research needed in this area.

## 1.4 System Description

The refrigeration system examined in this project is a cold storage warehouse facility located near Milwaukee, WI. The facility contains four types of refrigerated spaces. The size, temperature, and available insulation values of these spaces are summarized in Table 1.1. Building construction type is considered lightweight for all spaces. There is mostly insulation and very little mass in the walls and roofs.

| Space | Area | Temp. | RH | U-Value Roof [Btu/hr-ft²-F] | U-Value Wall [Btu/hr-ft²-F] | U-Value Perimeter [Btu/hr-ft²-F] |
|---|---|---|---|---|---|---|
| Freezer | 54,000 ft² | 0°F | 80% | 0.03022 | 0.03044 | n/a |
| Cooler | 32,200 ft² | 34°F | 87% | 0.03986 | 0.04024 | 1 |
| Cooler Dock | 5,700 ft² | 45°F | 65% | 0.03986 | 0.04024 | 1 |
| Banana Rooms | 4,000 ft² | 56-64°F | 80% | unavailable | unavailable | unavailable |
| Tomato Rooms | 4,000 ft² | 45-55°F | 80% | unavailable | unavailable | unavailable |

**Table 1.1 Conditioned Space Summary**

The freezer and cooler with its loading dock are separate buildings located adjacent to each other. The banana and tomato ripening rooms are located in a heated space adjacent to the cooler. A simplified schematic of the layout of the buildings is shown in Figure 1.1. This schematic was the basis for the load calculations detailed in Section 2.5.

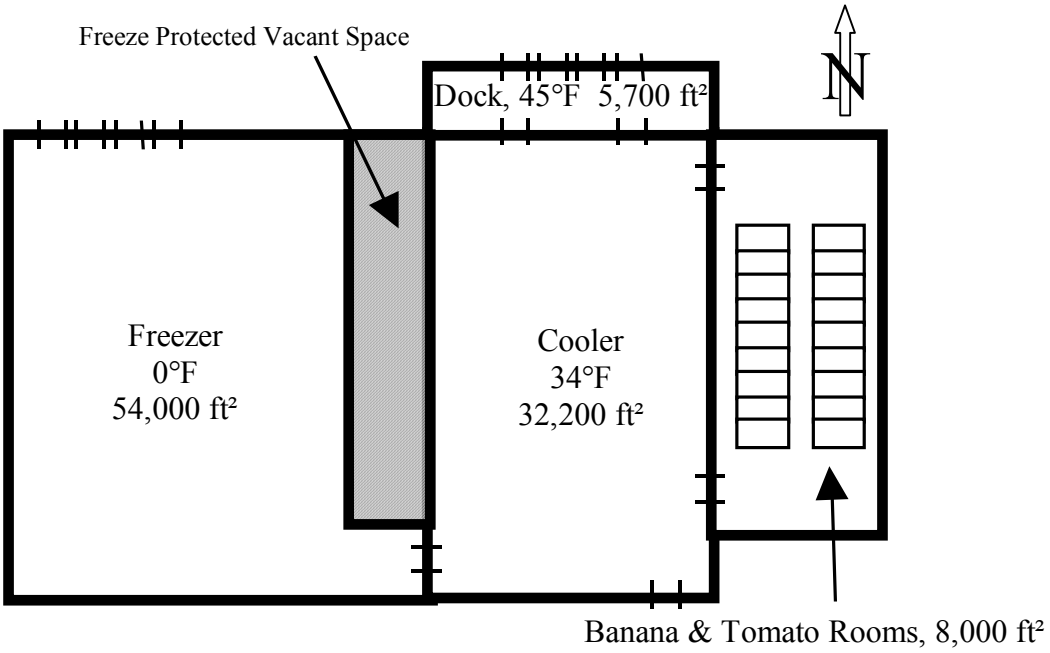


**Figure 1.1 Refrigerated Space Layout**

The refrigerant used in this system is ammonia (R-717). Evaporators in the freezer are top fed, pumped liquid overfeed. A greater quantity of liquid is pumped through the evaporator than the amount of refrigerant that is actually evaporated in pumped liquid overfeed evaporators. Cooler, and cooler dock evaporators are all bottom feed pumped liquid overfeed where as the evaporators in the banana and tomato ripening rooms are direct expansion controlled by thermal expansion valves and back pressure regulators.

All pumped liquid overfeed systems require receiver vessels. Receiver vessels are large tanks that hold two phase refrigerant. They have four main purposes:

1. Separate the liquid and vapor components of a two-phase flow.
2. Maintain a liquid level with suitable static head for the liquid pumps (even with moderate load fluctuations).
3. Store a reserve of refrigerant to smooth transient load fluctuations in the system.
4. Prevent liquid refrigerant surges in the system from damaging compressors (since gravity will separate the liquid from the vapor inside the vessel).

Figure 1.2 is a simplified diagram of the system's main refrigeration components.

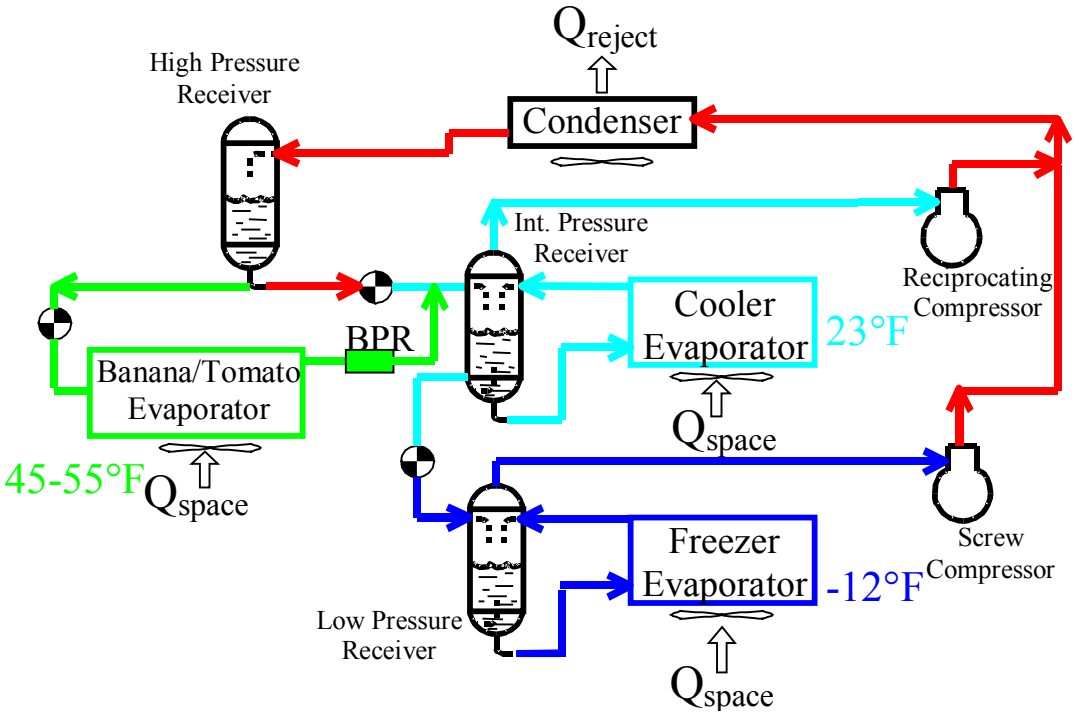


**Figure 1.2 Simplified System Diagram**

There are three main vessels in the system as shown in Figure 1.2. The first is the high pressure receiver where liquid refrigerant draining from the condenser is stored. Liquid refrigerant from the high pressure receiver is then throttled to either the intermediate pressure receiver or to the direct expansion evaporators in the banana and tomato ripening rooms. The temperature of the refrigerant in the banana/tomato room evaporators is regulated at a desired level by use of a back-pressure regulator. The back-pressure regulator then throttles the refrigerant gas to the intermediate pressure receiver which is at a lower temperature/pressure. Liquid in the intermediate pressure receiver is then either pumped to the cooler and cooler dock evaporators or throttled again to the low pressure receiver. Liquid refrigerant from the low pressure receiver is pumped to freezer evaporators with a mechanical liquid recirculating pump. Liquid levels in the intermediate and low pressure receivers are maintained at a near constant level by a pilot operated, modulating expansion valve controlled by a float switch located on the receiver tank (Phillips model# 701S).

A single-screw (Vilter model# VSS 451) and reciprocating compressor (Vilter model# VMC 4412) operate in parallel, each compressing to a common discharge header and a single evaporative condenser. The suction line from the low pressure receiver leads to the screw compressor. The suction line from the intermediate pressure receiver leads to the reciprocating compressor. Additional compressors, in parallel piping arrangements to the primary compressors, can be brought on-line if the load exceeds the capacity of the primary compressors.

Two coriolis effect mass flow meters from Schlumberger Industries Inc. ($\dot{m}$ ® Coriolis Force Mass Flow Meter (1 inch) ) are located in the liquid supply lines to the intermediate and low pressure receivers. The mass flow meters are connected to a data acquisition system that records the cumulative mass flow through the system. The flow meters require single-phase refrigerant to accurately determine mass flow. To ensure single-phase refrigerant, shell and tube heat exchangers are installed up stream of the flow meters to subcool the refrigerant in the liquid supply lines before it enters the mass flow meters. Exact locations of the flow meters are shown in Figure 2.1.

Evaporator coils in the freezer and cooler are defrosted with hot gas twice a day on a time scheduled basis. Loading dock evaporators are defrosted three times a day. Evaporator defrost cycles are staggered so that there is usually no more than one evaporator in defrost at a time. Hot gas is superheated refrigerant vapor. It is piped directly from the discharge headers of the compressors. Hot gas is also used in a shell and tube heat exchanger to heat a brine solution for use in sub-floor heating of the freezer space.

# *Chapter 2 -Modeling*

## 2.1 Software

The entire modeling for this project was done using the Engineering Equation Solver (EES) software developed by F-Chart Software [Klein and Alvarado, 1999]. EES is a non-linear equation solver that has built in procedures capable of calculating the thermodynamic properties of many commonly found substances such as air, water, and most refrigerants. The internal procedures of EES allow extremely convenient computer modeling of thermodynamic processes such as refrigeration systems. EES also allows the user to create procedures allowing very efficient customization of the program.

## 2.2 Modeling Scheme

As in all large industrial refrigeration systems, this warehouse refrigeration system consists of many different components all connected by pipes. The main components are listed in Table 2.2. To aid in the organization of the modeling process, a process flow diagram of the refrigerant or “wet” side of the refrigeration system was created. The process flow diagram is shown below in Figure 2.1. P-h diagrams of the processes are shown in Figure 2.2 - Figure 2.5.

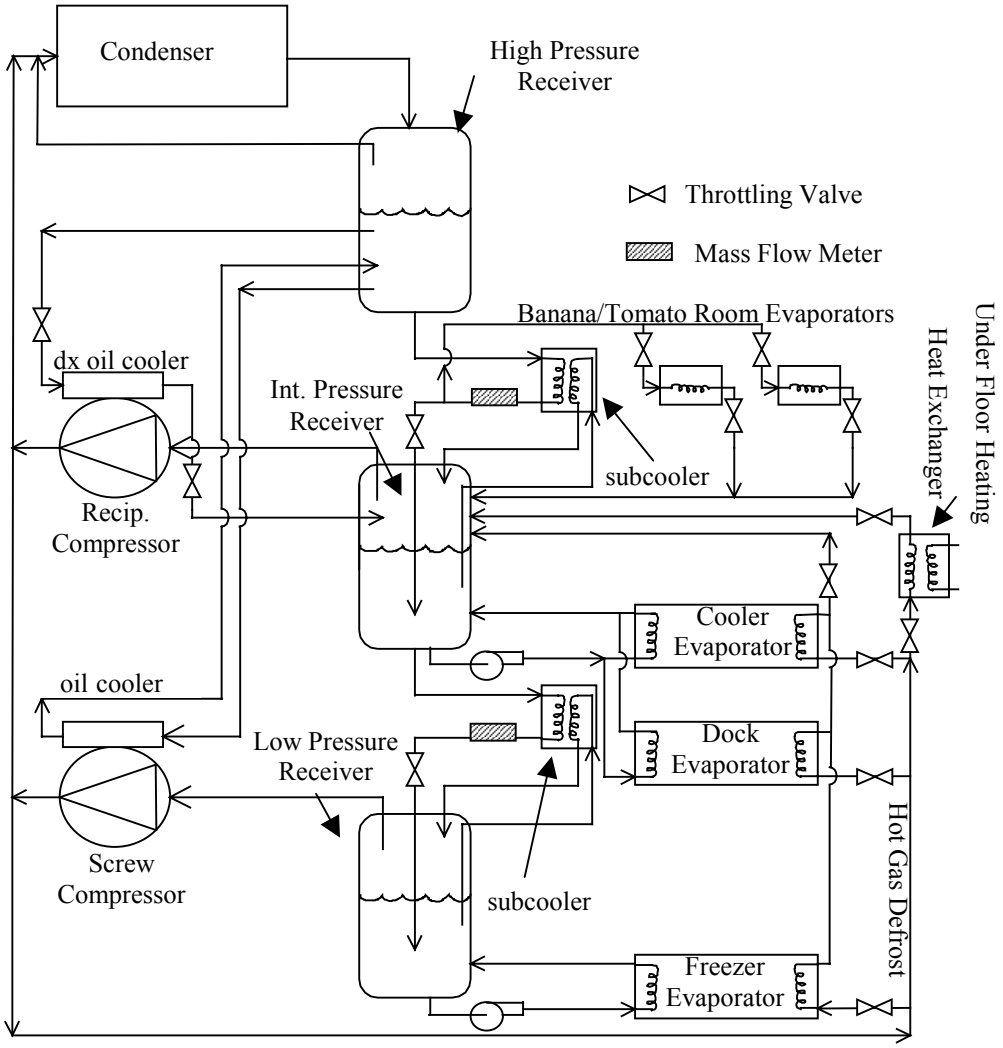


**Figure 2.1 Process Flow Diagram**

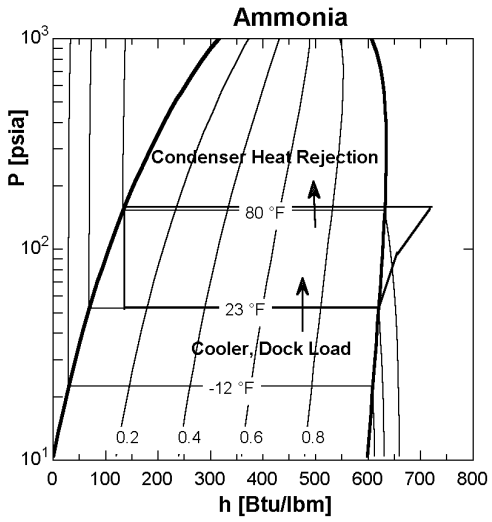


**Figure 2.2 P-h Dia. Cooler, Dock Load**

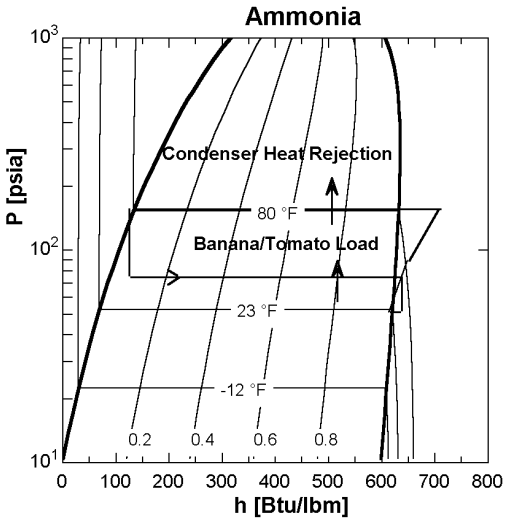


**Figure 2.4 P-h Dia. Banana/Tomato Load**

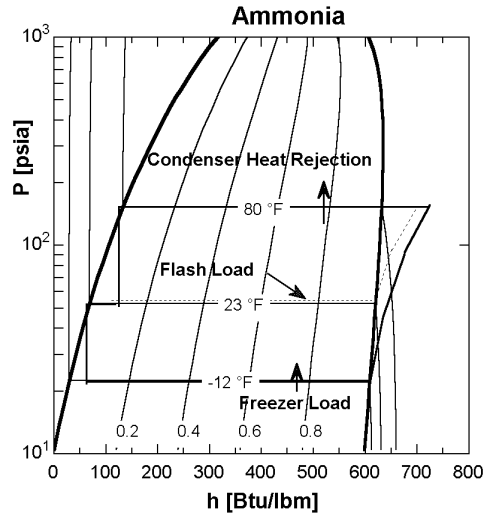


**Figure 2.3 P-h Dia. Freezer Load**

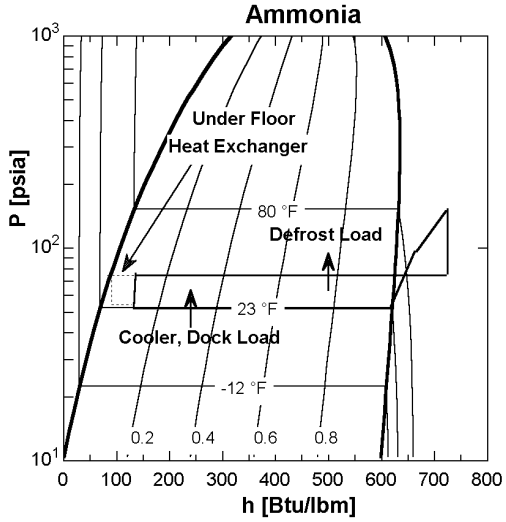


**Figure 2.5 P-h Dia. Defrost Load**

The most basic components in Figure 2.1 are the receiver vessels. Receiver vessels are big tanks placed in the system to separate the liquid and vapor phases of a two-phase refrigerant flow. Also, depending on the system, receiver vessels are used for liquid refrigerant or capacity storage Each tank has a controlled temperature/pressure and liquid level range. Each of the other components of the system either removes or replenishes vapor and/or liquid to or from these vessels to meet the needs of the load and control system set points. The idea of mass balances around the receiver vessels was the basic

philosophy behind the organization of the model. An internal EES procedure was created for each of the refrigeration components. Then, in the main body of the EES code, each component was linked to the receiver vessels with the appropriate vapor and/or liquid mass flows. Finally, the system equations were closed by applying energy and mass balances around the appropriate components. The main EES code can be found on the compact disc accompanying this thesis. An explanation of the file directory on this compact disc is provided in Appendix A.

## 2.3 Modeling Unit Choice

The entire system was modeled using English units. The English unit system was selected because most ammonia refrigeration experts use it as the industry standard. As a result, the majority of ammonia refrigeration literature, including the manufacturer's catalogs, is commonly found using the English unit system. As an additional factor in this project, all the historical experimental data acquired from the system were recorded using English units. Typical units for system parameters are listed in Table 2.1.

| System Parameter | Typical Unit |
|---|---|
| Pressure | [psia] |
| Temperature | [°F] |
| Mass flow | [lbm/hr] |
| Volume flow | [cfm] |
| Capacity | [Ton] or [Btu/hr] |
| Power | [HP] |
| Specific Enthalpy | [Btu/lbm] |

**Table 2.1 Typical English Units**

## 2.4 Component Modeling

Whenever possible, typical manufacturer's data were used to make a quasi-steady state model of each component. Procedures that model each component and are called by the main EES program can be found on the compact disc accompanying this thesis. Appendix A provides a description of the file directory on this compact disc. Table 2.2 lists the main components that were modeled for this system.

| Component | Manufacturer | Model Number | Type |
|---|---|---|---|
| Compressor | Vilter | AMC-A12K-4412-B<br>VSS-451-VVR-A-H-NEC-TH<br>VSS-751-VVR-A-H-NEC-TH | Reciprocating<br>Single Screw<br>Single Screw |
| Condenser | Evapco | PMCB-885 | Evaporative |
| Cooler Evaporator | Evapco | NTL2-4044-150P | Pumped Liquid Overfeed |
| Freezer Evaporator | Evapco | NTM2-3262-200L | Pumped Liquid Overfeed |
| Dock Evaporator | Evapco | NTX2-2300-N-033P | Pumped Liquid Overfeed |
| Banana Evaporator | Krack | DT2S-395-DXFARTA | Direct Expansion |
| Piping | | | Steel - Typical |
| Vessels | RVS | | Vertical |
| Thermal Expansion Valves | Unknown | DAE-5 | |
| Expansion Valves | Phillips | 701S | Pilot Operated, Modulating |
| Subcoolers | unknown | unknown | Shell and Tube |

**Table 2.2 Main System Components**

### 2.4.1 Compressors

#### 2.4.1.1 Correlations and Compressor Maps

In most industrial refrigeration applications, compressors consume the majority of the system total energy requirements. The three parameters that are of most interest to a refrigeration system designer or operator are the power required by the compressor, the amount of useful cooling (capacity) it provides, and the amount of oil cooling it needs. Most compressor manufacturers provide tables for each of their compressor models that

list these three requirements (brake horsepower, capacity [tons], and oil cooling load [MBH]) given saturated suction and saturated discharge temperature/pressure. Saturation temperature is defined as the temperature corresponding to the saturated vapor state of the refrigerant given a particular pressure. From the data in these tables, correlations of brake horsepower, capacity and oil cooling load can be developed as functions of saturated suction temperature (SST) [°F] and saturated discharge temperature (SDT) [°F]. As shown in a previous study on refrigeration [Brownell, 1998], a second order polynomial with cross term fits the manufacturer's data quite well. The linear regression results are correlations in the form of Equations (2.1)-(2.3). The power (P), capacity (C), and oil cooling load (O) coefficients along with RMS (root-mean-square) and $R^2$ (residual squared) statistics for each compressor modeled in this study are located in 7.4Appendix B.

$$BHP = P_1 + P_2 \cdot SST + P_3 \cdot SST^2 + P_4 \cdot SDT + P_5 \cdot SDT^2 + P_6 \cdot SST \cdot SDT \qquad [BHP] \quad (2.1)$$

$$CAP = C_1 + C_2 \cdot SST + C_3 \cdot SST^2 + C_4 \cdot SDT + C_5 \cdot SDT^2 + C_6 \cdot SST \cdot SDT \quad [tons] \quad (2.2)$$

$$OIL = O_1 + O_2 \cdot SST + O_3 \cdot SST^2 + O_4 \cdot SDT + O_5 \cdot SDT^2 + O_6 \cdot SST \cdot SDT \quad [MBH] \quad (2.3)$$

- SST & SDT in [°F]

Plotting the dependent variable of Equations (2.1)-(2.3) against the SST for different SDT's results in a plot that is commonly referred to as a compressor map. Figure 2.6 shows an example of a compressor map displaying capacity as a function of SST and SDT for a VSS-451 Vilter screw compressor.

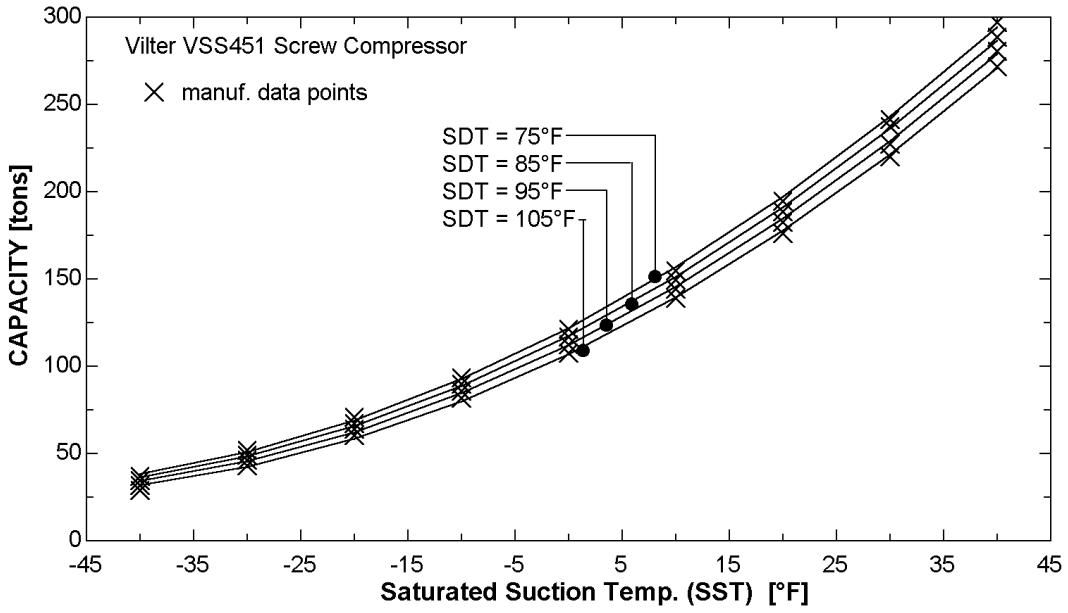


**Figure 2.6 Capacity Compressor Map**

When manufacturers rate their machines, the pressure is measured at the inlet and outlet flanges of the compressor. The saturated temperature corresponding to those measured pressures is also presented in the catalog data. Compressor ratings do not include pressure losses and the associated saturation temperature change due to valve trains or oil separators even though both are commonly included with the compressor package. It is also pertinent to point out that some manufacturers list saturated discharge temperature (SDT) as "saturated condensing temperature (SCT)" even though their measurements are at the discharge flange of the compressor and not in the condenser of the refrigeration cycle. The extra pressure drop due to the discharge side valve trains and oil separators was accounted for in the system model and is discussed in Section 2.4.4.

Caution should also be used when extrapolating compressor data outside the range provided in the manufacturer's catalogs. Extrapolation to lower discharge pressures was used when multi-level head pressure control was examined in Section 5.4.1. The extrapolated values were compared to actual values obtain from a manufacturer's representative. At most the error was three percent which is well within the general error associated with the manufacturer's data.

#### 2.4.1.2 Rated Verses Actual Capacity

The amount of useful cooling or the capacity rating [tons or Btu/hr] of the compressor needs to be carefully defined. The actual useful heat transfer takes place in the evaporators of the refrigeration system which are almost completely unrelated to the compressors and often located several hundred feet from the compressors. Capacity is defined by Equation (2.4) where we can see that it depends on the refrigerant mass flow [lbm/hr] and change in specific enthalpy [Btu/lbm] of the refrigerant across the evaporator.

$$Capacity = \dot{m} \cdot \left( h_{ref,out} - h_{ref,in} \right) \tag{2.4}$$

If any of the parameters that define capacity change in the evaporator, the capacity rating of the compressor must be adjusted to account for these changes. Operating conditions that change these parameters are discussed in the following paragraphs.

Screw and reciprocating compressors are both positive displacement devices. For each revolution of the motor, a given ***volume*** of vapor is compressed. The mass flow through a compressor operating at a constant speed will change as the specific volume of the inlet gas changes. The maximum mass flow occurs when the inlet gas is a saturated vapor. A measure that is commonly used to identify how far from this maximum flow operating point is called degrees of superheat. The more degrees of superheat that there are in the gas entering the compressor, the larger the specific volume of the gas and the lower the mass flow of the compressor.

Manufacturers must specify the nominal conditions to establish their base capacity ratings. Typically, the manufacturers provide a specified superheat (which governs the mass flow and specific enthalpy of the refrigerant at the evaporator outlet) and a specified subcooling (which governs the specific enthalpy of the refrigerant to the evaporator inlet). Refrigerant supplied to the evaporator as a subcooled liquid is defined as having some number, X, degrees of subcooling below its saturation temperature. Refrigerant that

enters the compressor as a superheated vapor is defined as having some number, Y, degrees of superheat above its saturation temperature. If any one of the parameters that define capacity (mass flow, or specific enthalpies of the refrigerant) change independently of the SST or SDT of the compressor, the capacity reported by the manufacturer must be corrected. For example, Manufacturer A states that their ratings are based on 10°F of superheat and 10°F of subcooling. The actual system provides refrigerant with only 4°F of superheat and 15°F of subcooling. The calculated capacity will have to be increased to account for the extra 5°F of sensible cooling provided by the additional subcooling. Capacity must also be increased because of the increase in mass flow. Mass flow increases because the lower superheat means a lower specific volume inlet condition. However because the refrigerant has less superheat, the capacity must be reduced slightly because the 6°F of superheat did not contribute to useful refrigeration from the load. Equation (2.5) is a compact expression that can be used for the adjustment of the capacity.

$$CAP_{actual} = CAP_{mfr} \cdot \frac{v_{mfr}}{v_{actual}} \cdot \frac{\Delta h_{actual}}{\Delta h_{mfr}} \tag{2.5}$$

**where:**

$v_{mfr}$ = specific volume of inlet gas based on manufacturer's specified conditions.

$v_{mfr}$ (SST,superheat)$_{mfr}$

$v_{actual}$ = actual specific volume of inlet gas in application. $v_{actual}$ (SST,superheat)$_{actual}$

$\Delta h_{mfr}$ = difference in specific enthalpies of refrigerant between manufacturer's rated compressor suction and rated evaporator inlet. $h_{suc}$(SST,superheat)$_{mfr}$, $h_{in}$(SCT, subcooling)$_{mfr}$

$\Delta h_{actual}$ = actual difference in specific enthalpies of refrigerant between compressor suction and evaporator inlet. $h_{suc}$ (SST,superheat)$_{actual}$, $h_{in}$ (SCT, subcooling)$_{actual}$

Brake horsepower and oil cooling load are only dependent on the difference between the discharge pressure and the suction pressure (pressure lift) and internal construction of the

compressor and do not need to be adjusted for different mass flow rates, superheat, and subcooled conditions that define the capacity at the evaporator.

#### 2.4.1.3 Compressor Unloading

Since screw and reciprocating compressors are both positive displacement devices, the approach for modeling them, up until now, has been identical. The main difference in modeling these two different kinds of compressors arises when they are operated at part-load conditions. The proper positioning of two slide valves along the screw unloads a screw compressor from 10 to 100% of its available capacity. One slide valve controls the volume of gas that is admitted to the compression chamber. The other varies the location of the discharge port and therefore controls the pressure lift of the compressor.

Reciprocating compressors are unloaded by reducing the number of cylinders that are providing active gas compression. As cylinders are unloaded, the compressor circulates less refrigerant and its capacity is reduced. The capacity of a reciprocating compressor can be reduced in step sizes equal to the number of cylinders unloaded at a time divided by the total number of cylinders. To achieve a capacity less than that of full load, or percent full load capacity (%FLC) between the steps, cylinders are cycled on and off. This cycling of cylinders on and off essentially produces a linear unloading profile without the “staircase” effect, as shown in Figure 2.7.

As compressors are unloaded, their power and oil cooling requirements decrease as well, but not proportionally. Unloading curves for both the screw and reciprocating compressors are shown in Figure 2.7. These curves give the operator an indication of the fraction of full load power (%FLP) the compressor will use at a specific percent of its full load capacity (%FLC sometimes known as the part-load ratio). The compressor model assumes the oil cooling requirements are reduced in the same proportion as the power.

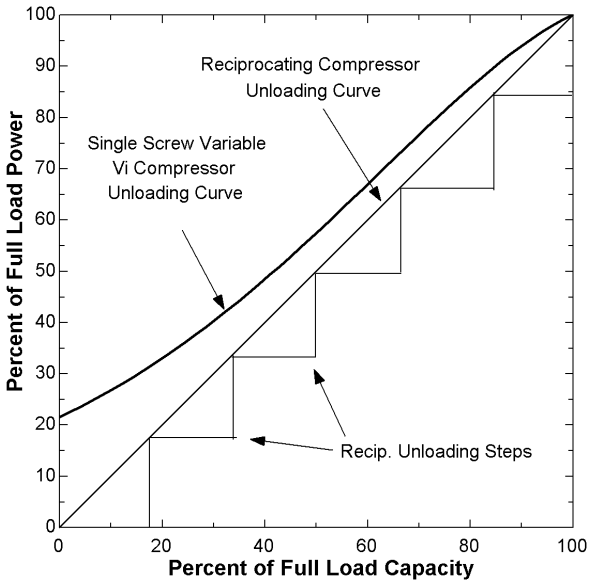


**Figure 2.7 Compressor Unloading Curves**

A regression equation of the screw unloading curve was obtained from a representative of the Vilter Manufacturing Corporation and is presented in Equation (2.6) [Fisher,1998].

$$\%FullLoadPower = 21.5733 + 0.465983 \cdot \%FLC + 0.00544201 \cdot \%FLC^2 - 5.55343 \cdot 10^{-6} \cdot \%FLC^3 + 7.40075 \cdot 10^{-8} \cdot \%FLC^4 - 2.43589 \cdot 10^{-9} \cdot \%FLC^5 \quad (2.6)$$

## 2.4.2 Evaporative Condenser

### 2.4.2.1 Evaporative Condenser Description

Evaporative condensers are another major power consumer in industrial refrigeration systems. Evaporative condensers reject energy from the high pressure, hot compressor discharge refrigerant to the ambient air. As energy is removed from the hot gas, a change in state from vapor to liquid occurs. A diagram of an evaporative condenser is shown in Figure 2.8.

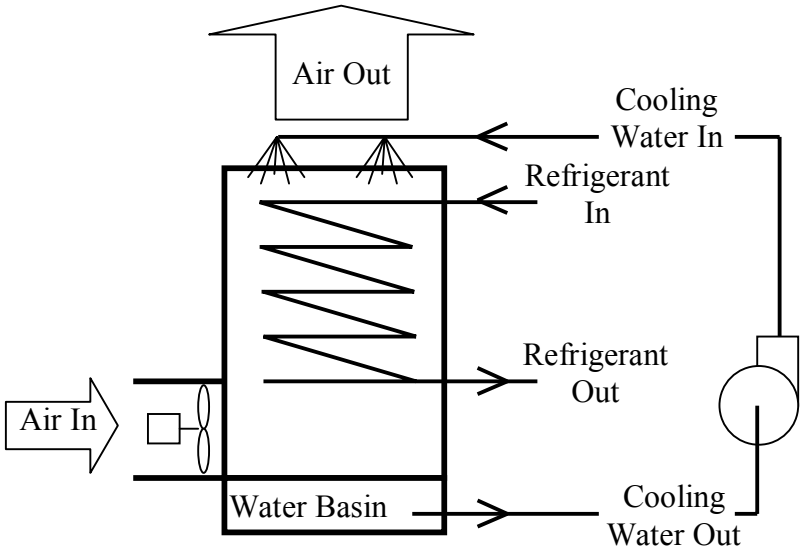


**Figure 2.8 Evaporative Condenser Diagram**

Superheated refrigerant vapor enters the coils of the evaporative condenser at the top of the unit. Water from a basin is pumped up to the top of the unit and sprayed down over the outside of the coils as outside air is drawn or blown through the unit by fans. As the water pours over the coils and evaporates into the air stream, the exterior heat exchanger surface tends to approach the outside air wet bulb temperature. Also as the water pours over the coils, energy is transferred from the high temperature refrigerant to the cold water resulting in a phase change and condensing the refrigerant into a liquid (still at high pressure). Nearly saturated air leaves the top of the condenser at a temperature near the refrigerant's saturated condensing temperature (SCT). The SCT is the refrigerant's saturation temperature corresponding to the pressure inside the condenser. The refrigerant then leaves the condenser as a saturated or perhaps slightly subcooled liquid. An evaporative condenser rejects energy by both heat and mass transfer on the outside surface of the condenser tubes. The main component of energy rejected by the condenser comes from evaporating the water, so an evaporative condenser is mainly a wet bulb sensitive device.

#### 2.4.2.2 Manufacturer's Ratings

Typically, manufacturers provide the nominal volumetric air flow, the nominal heat rejection capacity, and a variable load multiplier that is referred to as the heat rejection factor (HRF). The HRF is a function of the outside air wet bulb and the refrigerant SCT. The actual heat rejected by the evaporator is calculated by dividing the nominal heat rejection capacity by the HRF. (Equation (2.7))

$$Capacity = \frac{Nominal\ Capacity}{HRF\left(T_{wb}, SCT\right)} \tag{2.7}$$

Evapco provided HRF's for wet bulb temperatures between 50°F and 86°F and for saturated condensing temperatures (SCT) between 85°F and 110°F. Dry bulb temperature was not specified and can be assumed to have negligible effects on evaporative condenser performance. An explanation of the rating process for evaporative condensing units was provided in a conversation with an engineer at Evapco [Kollasch, 1999]. Varying inlet conditions are adjusted by mixing outside air with some of the moisture laden exhaust air exiting out the top of the evaporator until the desired inlet air wet bulb temperature is reached. The inlet air dry bulb is not controlled and is allowed to float.

#### 2.4.2.3 Enthalpy Effectiveness

An effectiveness approach was used to model the evaporative condenser. This approach was used in a previous study with good results [Brownell, 1998]. Since evaporative condensers reject energy with both mass and heat transfer mechanisms, an effectiveness must be enthalpy based. Effectiveness is defined in Equation (2.8).

$$Effectiveness = \frac{Cond.Capacity}{Max.Cond.Capacity} = \frac{\dot{m}_{air} \cdot \left( h_{air,out}\big|_{T_{air,out},Sat} - h_{air,in} \right)}{\dot{m}_{air} \cdot \left( h_{air,out}\big|_{T_{refrigerant},Sat} - h_{air,in} \right)} \tag{2.8}$$

Effectiveness is displayed graphically in Figure 2.9.

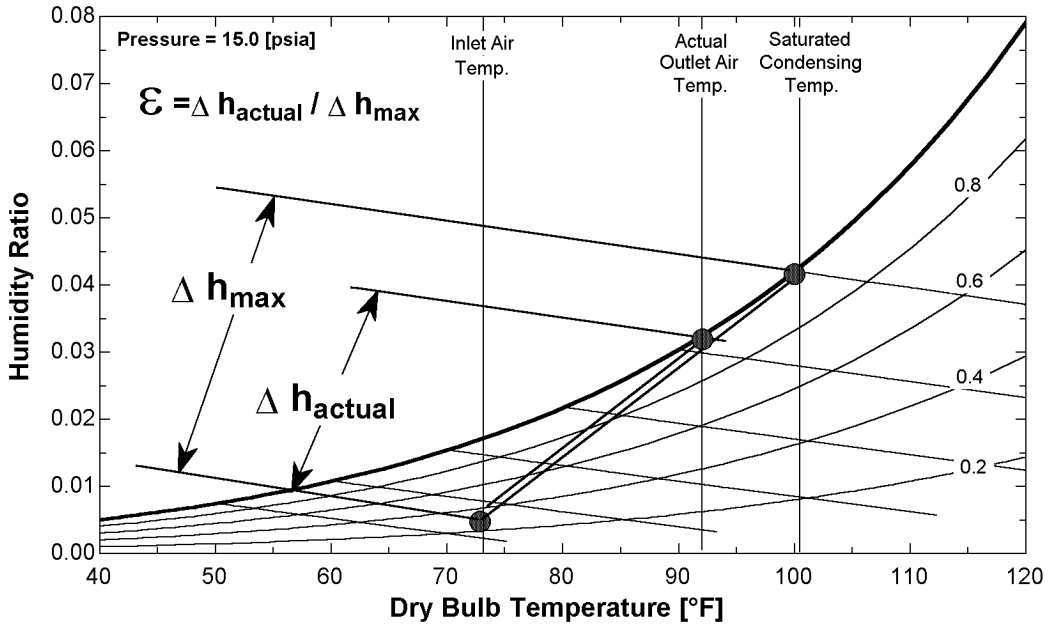


**Figure 2.9 Evaporative Condenser Psychrometrics**

Condenser capacity was calculated by Equation (2.7) for each of the HRF conditions given in the manufacturer's catalog. These ratings are given for full load or maximum volumetric airflow rate. Maximum condenser capacity, the denominator of Equation (2.8) , was calculated as the difference between the maximum possible outlet specific enthalpy minus the specific enthalpy of the inlet air times the mass flow of air. The maximum possible specific enthalpy would occur if air left the unit saturated at a dry bulb temperature equal to the refrigerant's saturated condensing temperature. The results of the effectiveness calculations are shown in Figure 2.10.

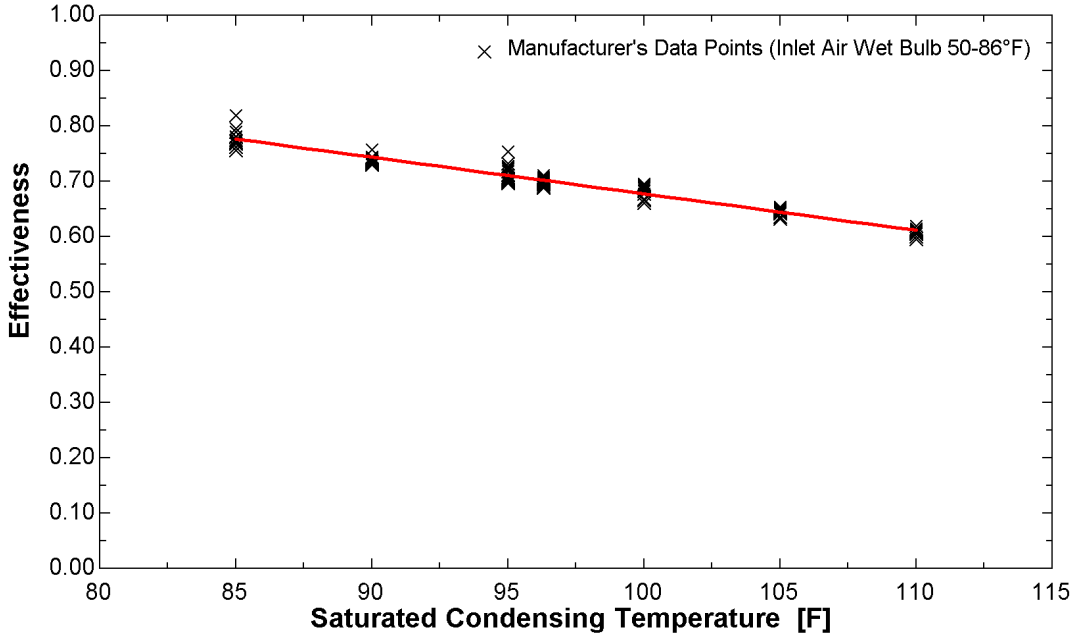


**Figure 2.10 Evaporative Condenser Effectiveness (Evapco model# PMCB-885)**

It can be seen in Figure 2.10 that inlet air wet bulb temperature does not have a significant effect on effectiveness. At the risk of sounding counter intuitive, this is because an evaporative condenser is a wet bulb driven device. As inlet air wet bulb temperature changes, the heat and mass transfer mechanisms driving the energy rejection to the air stream change inversely with wet bulb temperature. For example, in Figure 2.9 as the inlet air wet bulb temperature increases, the distance indicated as $\Delta h_{actual}$ would decrease maintaining a nearly constant ratio of $\Delta h_{actual} / \Delta h_{max}$ or value of effectiveness.

The effectiveness relation in Figure 2.10 was fit using a first order relation. The result is Equation (2.9) with a RMS = 1.0624e-2 and $R^2$ = 95.87%. (RMS = root mean square and R = residual are statistical analysis terms indicating how accurate a linear regression is.) This effectiveness curve was used to model the system's evaporative condenser.

$$Effectiveness = 1.34 - 6.608 \cdot 10^{-3} \cdot SCT \tag{2.9}$$

2.4.2.4 Evaporative Condenser Part-Load Operation

The main function of condensers in the system is to reject system energy to the environment. Condensing pressure/temperature (also referred to as head pressure) is

controlled with the fans to reject the required amount of energy to the environment. If the load on the system increases, the head pressure needs to increase. As the head pressure increases, the refrigerant condensing temperature increases which increases the condensers heat rejection capacity. If the condenser is operating in a mode where it is rejecting too much energy, the condensing pressure will decrease along with the condensing temperature of the refrigerant until a head pressure which balances the heat rejection needs of the system is reached. Allowing too low of condensing pressure can cause operational problems with other components in the system such as expansion valves, back pressure regulators, and hot gas defrost capacities. When the amount of energy that needs to be rejected from the system is less than the full load capacity of the evaporative condenser, which is most of the time, the capacity of the condenser must be reduced. An evaporative condenser's capacity can be reduced in two ways.

1. Head pressure control by altering the airflow through the unit with fan speed control or fan cycling.
2. Dry operation by shutting the cooling water off.

The capacity of a condenser can be changed by modulating the mass flow of air through the unit by controlling the speed or cycling the fans. Equation (2.10) is used to de-rate the performance of the evaporator using fan speed control.

$$Cap_{actual} = Cap_{rated} \cdot \left( \frac{FanSpeed_{actual}}{FanSpeed_{rated}} \right)^{N} \tag{2.10}$$

The coefficient N is expected to vary between 0.5 for laminar flow and 0.8 for turbulent flow[Mitchell and Braun, 1998]. A manufacturer's representative from Evapco suggested a value of 0.76 for their evaporative condenser units [Kollasch, 1999].

As air mass flow through the condenser is increased by increased fan run time or faster fan speeds, more energy is rejected from the warmer refrigerant and the SCT of the refrigerant is reduced. With a lower SCT to drive heat and mass transfer mechanisms, the capacity of the condenser will be reduced. With this capacity reduction scheme, the system sees an additional benefit in the reduction of the head pressure on the compressors which cuts down on the power consumption of the compressors.

The other method used to reduce the capacity of an evaporative condenser is to simply shut the cooling water off. Without a wetted exterior surface, the only mechanism of energy rejection is by sensible heat transfer between the refrigerant and outside air. With reduced loads and relatively cool outside air dry bulb temperatures, as commonly found during winter months in cooler climates, this is a perfectly acceptable method of capacity control. This type of control also has the advantage of reduced power consumption because the water circulating pumps are no longer energized. For outside air temperatures below 32°F, a manufacturer's representative suggested an evaporative condenser running dry operates between 30 and 35 percent of its wet capacity [Kollasch, 1999]. Thirty-five percent was used in the present model. Due to the drastic change in capacity between wetted and dry operation (100% to 35%), condenser water cycling should never be used for capacity control. Large fluctuations in head pressure will result as well as significant scaling on the water side. Instead, the water should only be allowed to turn off if it will remain off for the remainder of the winter or until the temperatures rise significantly.

Typically a combination of both capacity reduction schemes mentioned above are used to maintain the desired condensing pressure in the system throughout the year.

Dry operation of the system was included any time the outside air dry bulb temperature dropped below 31°F. This is consistent with the true operation of the system being modeled. This is more of a freeze safety issue that anything.

Mass flow of air through the condenser is controlled by the fan motors. Motors are usually controlled one of three ways.

- On\Off motor cycling. (current evaporator control strategy)
- Half-speed motor cycling. (high speed, low speed, off)
- Variable Frequency Drive (VFD) controllers on the motors.

With the on\off motor control strategy, the condenser fans are run at full speed until the condenser's pressure falls below an acceptable limit and then the motors are shut off.

Half-speed control first cycles the fans to half speed and then to full speed if the condenser's head pressure is still too high. VFD control runs the fans at a speed just fast enough to maintain a constant head pressure at a defined set point. The advantage of using the half-speed and VFD control can be explained by the fan laws. Fan power is related to the cube of fan speed. If the speed is cut in half, half the mass flow is achieved at only one-eighth of the design fan power. Depending on the size and arrangement of the condenser, there may be more than one motor driving any number of fans. Of course each individual motor can be sized differently. The evaporator modeled in this study has two motors. One 15 horsepower motor driving one fan and one 30 horsepower motor driving two fans. The condenser has an internal baffle that prevents internal recirculation of the air when only one of the motors is on. The internal baffle combined with two separate fan motors splits the large condenser into two smaller ones; one with 33.3 percent of the total capacity and the other with 66.7 percent. When one section is active the other will still reject approximately 10 percent of its nominal capacity due to natural convection effects. When this arrangement exists, there are several different control strategies to choose from. Each control strategy dictates a different order by which "parts" of the condenser are activated or deactivated to build up to its full capacity. When motors are purchased with a half-speed option, the number of possible control strategies increases even more. Several control schemes were selected and compared. Figure 2.11 shows what percent of the full load power each fan control scheme would use given the percent of full load that the condenser must operate at to satisfy the energy rejection requirements of the system. The fan power drops to zero at ten percent capacity because some natural convection effects were assumed.

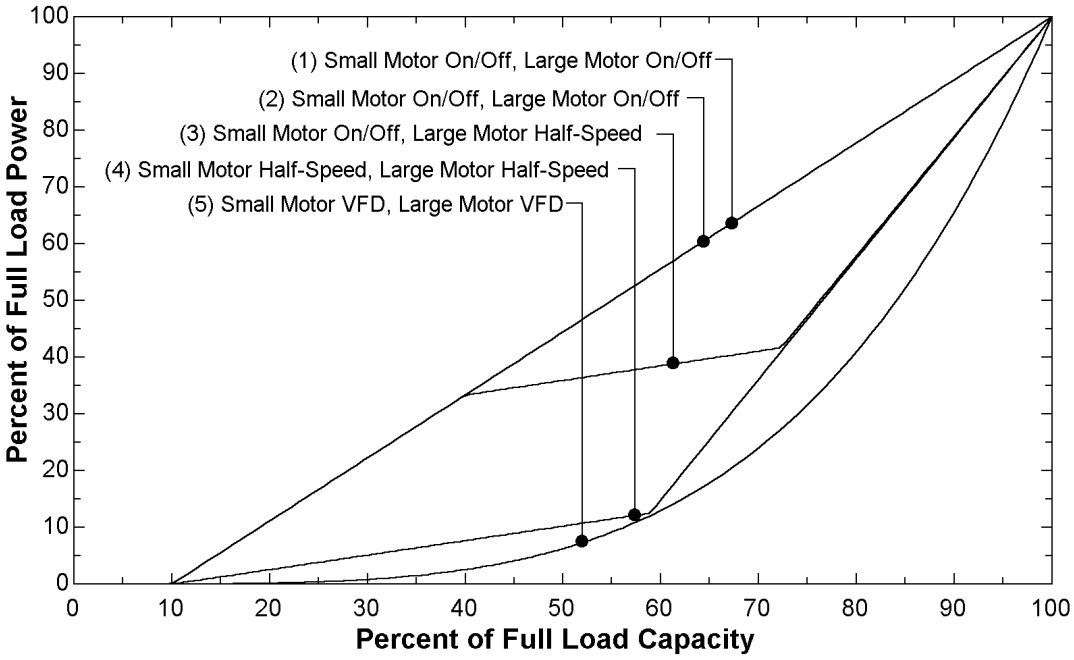


**Figure 2.11 Part Load Evaporative Condenser Operation**

The control strategies shown in Figure 2.11 are labeled 1-5 and are described below in Table 2.3. Each mode of operation sets the fan motors either on, off, half-speed, or at variable speed. If the condensing pressure is controlled to a near constant set point, each mode represents a specific amount of energy that can be rejected. For intermediate energy rejection requirements, fan settings are simply cycled between the nearest two modes. Control strategy 1 is the one currently being used at the actual facility.

| Strategy | | Mode 1 | Mode 2 | Mode 3 | Mode 4 | Mode 5 |
|---|---|---|---|---|---|---|
| 1 | Small Motor | off | on | off | on | |
| | Large Motor | off | off | on | on | |
| 2 | Small Motor | off | off | on | | |
| | Large Motor | off | on | on | | |
| 3 | Small Motor | off | on | on | on | |
| | Large Motor | off | off | half-speed | on | |
| 4 | Small Motor | off | half-speed | half-speed | on | on |
| | Large Motor | off | off | half-speed | half-speed | on |
| 5 | Small Motor | off | variable speed | | | |
| | Large Motor | off | variable speed | | | |

**Table 2.3 Condenser Fan Control Strategies**

Fan control for control strategy 1 would be as follows. Given a saturated condensing temperature and outdoor wet bulb temperature the nominal capacity of the condenser is 100 [MBH]. If the actual amount of heat that needed to be rejected was below 40 [MBH] (33.3 from the small fan side plus (0.1*66.6) = 6.7 from the natural convection of the large fan side), then only the small fan would have to be operated. For example if the load was 25 [MBH] the small fan would have to cycle on (25/40) = 62.5% of the time. The large fan would remain off. If the load was 50 [MBH] the large fan would cycle on (50/70) = 71.4% of the time.

The actual control of the evaporative condenser is considerably more complicated because the saturated condensing temperature does not remain fixed but rather floats as the heat rejection load on the condenser changes. The control schemes in this section will however make a good estimate of the total amount of energy used on average by the fan motors [Nicoulin et al, 1997].

## 2.4.3 Evaporators

### 2.4.3.1 Direct Expansion Evaporators

The two main types of evaporators modeled in this project include direct expansion (dx) and pumped liquid overfeed. Direct expansion evaporators are used in the banana/tomato ripening rooms. A piping schematic of a typical dx evaporator is shown in Figure 2.12. A piping legend can be found in Appendix D.

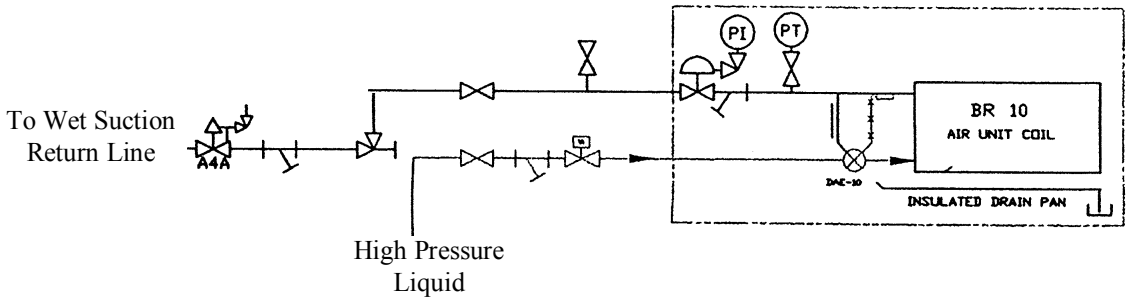


**Figure 2.12 Direct Expansion Evaporator Piping Schematic**

Direct expansion evaporators take a high pressure liquid and throttle it down a desired evaporator pressure, which is maintained by a back pressure regulator (A4A in Figure 2.12). Heat is absorbed by the two-phase refrigerant in the evaporator and the remaining liquid is converted to a superheated vapor. The degrees of superheat is controlled by a thermostatic expansion valve. In this particular system, the superheated vapor is then throttled down to the pressure in the intermediate pressure receiver wet suction return line. In this line, the superheated vapor from the dx evaporators combines with the two-phase flow from the cooler and dock evaporators. A small amount of liquid from the two-phase flow is converted to vapor as the superheated vapor from the dx evaporators comes into equilibrium with the wet suction return line refrigerant.

#### 2.4.3.2 Pumped Overfeed Evaporators

The evaporators in the freezer, cooler, and loading dock sections of the warehouse are all bottom fed, pumped liquid overfeed units. Figure 2.13 shows a piping schematic of a bottom fed evaporator. Defrost piping is also included in the schematic. Hot gas defrosting is discussed in Section 2.4.3.7.

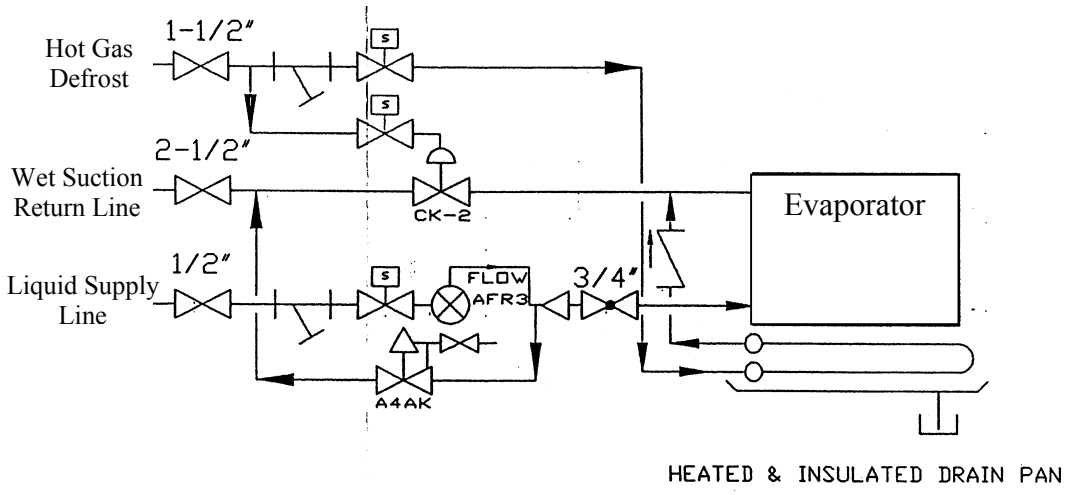


**Figure 2.13 Bottom Fed, Liquid Overfeed Evaporator with Defrost Piping Schematic**

In bottom fed evaporators, the refrigerant enters the bottom of the coil as a saturated low pressure liquid. As heat is absorbed by the refrigerant, vapor is generated. Refrigerant flow through the evaporators is metered by an AFR3 mass flow meter, which allows a

constant mass flow of refrigerant through the evaporator. Mass flow rates are typically set at three times the mass of vapor generated in the evaporator at full load to maintain a wetted surface and good heat transfer coefficient inside the evaporator coil. This is referred to as a liquid circulation rate of three. A two-phase mixture of quality 0.33 or less (depending on load) flows out of the top of the coil and is dumped into the wet suction return line.

Industrial refrigeration installations also use top fed, pumped liquid overfeed evaporators. A discussion on advantages and disadvantages of top and bottom fed evaporators can be found in the ASHRAE Refrigeration Handbook [ASHRAE Refrigeration Handbook, 1994].

#### 2.4.3.3 Manufacturer's Ratings

Manufacturers of industrial evaporators typically provide two rating parameters of relevance in modeling. The first is a unit load factor [Btu/hr-°F] and the second is its nominal volumetric airflow [cfm]. The unit load factor is based on coil size, coil circuiting, volumetric airflow, and whether the coil is frosted or wetted. Coil manufacturers state that coils will likely build frost when the saturated suction temperature of the coil is below 28 [°F]. The unit load factor is considered fixed for a particular coil and operating condition (frosted or wet and full airflow) by the manufacturers. The rating of a frosted coil is provided at a moderate amount of frost. As a coil continues to build frost, which impedes heat transfer and airflow, the unit load factor will decrease.

The capacity of the coil is then calculated from Equation (2.11). TD [°F] is defined as the temperature difference between the inlet air dry bulb temperature and the saturated refrigerant temperature.

$$Capacity = UnitLoadFactor \cdot TD \tag{2.11}$$

where:

$TD = T_{air,in} - T_{ref,sat}$

Evaporators are rated entirely on sensible heat loads as indicated in the fine print of most manufacturer's catalogs. Therefore, the capacity calculated by Equation (2.11) is a sensible heat transfer. The actual capacity of the evaporator is the sum of the capacity calculated in Equation (2.11) and the latent heat absorbed by the evaporator. Assume that the nominal volumetric airflow rate stays constant and the temperature of the exterior surface of the evaporator coil is the same temperature as the refrigerant. Then, the latent load depends on the inlet air humidity ratio, the temperature of the refrigerant and other physical characteristics of the evaporator such as blow-by factor [Mitchell and Braun, 1998]. If the temperature of the refrigerant is below that of the inlet air dew point temperature (which is the case in almost all air cooling applications) moisture will condense out of the air resulting in a latent load component of the total evaporator load. The larger the temperature difference, the higher the latent load will be. Figure 2.14 demonstrates the psychometric cooling process of an Evapco evaporator operating in a cool storage warehouse. The warehouse set temperature is 34°F and the refrigerant temperature is 25°F. Using the frosted coil unit load factor, TD, and the inlet air dry bulb temperature, we calculate an outlet air temperature of approximately 30°F.

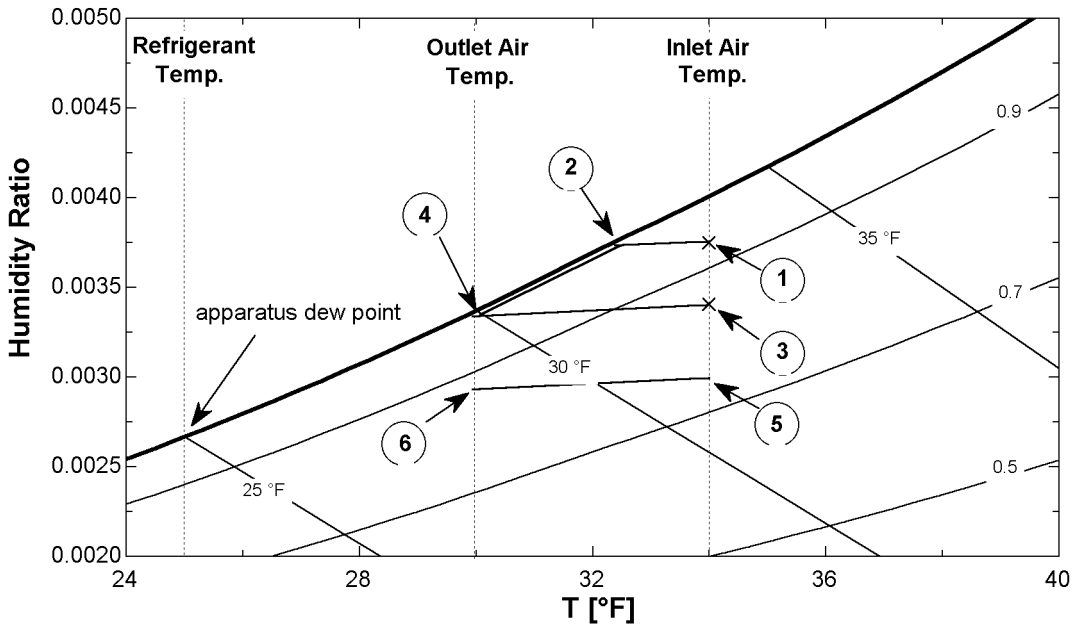


**Figure 2.14 Evaporator Psychrometrics**

#### 2.4.3.4 Conditioned Space Balance State

Three cooling processes are shown in Figure 2.14. The cooling process from one to four would be representative of a warehouse with high humidity and the evaporators would have a low sensible heat load ratio. Sensible heat load ratio is the ratio of sensible heat transfer to total heat transfer where total heat transfer includes both sensible and latent components. The cooling process from state three to four would have a medium sensible heat load ratio. The final cooling process from state five to six might be representative of a dry warehouse. It would have a sensible heat load ratio very close to that of the process from three to four except slightly larger. The process from one to four has a low sensible heat load ratio because as the air stream is cooled it becomes saturated. Once the air stream is saturated, water condenses out of the air stream very rapidly and the warehouse environment becomes dryer, assuming there is less water vapor infiltrating the space than being removed by the evaporators. This shifts the inlet air condition from state one towards state three. Conversely, if the warehouse environment is relatively dry like at state five, there is much less water condensing out of the air stream. If the quantity of water vapor infiltrating into the space is greater than the amount being removed by the evaporators, the warehouse environment will move from state five towards state three. The bottom line is that the warehouse environment will always tend to move towards state three. State three is established by the intersection of the warehouse dry bulb temperature and the horizontal sensible load line (horizontal line between state three and four) that originates at the saturation curve and has a length determined by the unit load factor and TD of the coil.

The balance state of the warehouse environment is somewhere close to state three because, as discussed above, the space humidity ratio will always tend to move toward the humidity ratio of state three. Dry bulb temperature is assumed to be maintained at its set point. Exactly where the balance state is depends on the sensible heat load ratio of the conditioned space. It also depends on the TD of the coil. Again, TD is defined as the difference between the inlet air dry bulb temperature and the saturated refrigerant

temperature. As the TD increases, the length of the sensible heat load line increases and the balance point will shift toward lower humidity ratios. Adjusting the TD of the coil is one way to control the humidity level in the conditioned space.

The balance state, which is somewhere near state three in Figure 2.14, is a dynamic equilibrium state dependent upon the absolute and relative magnitudes of the conditioned space's sensible and latent heat load components and the TD of the evaporator.

#### 2.4.3.5 Evaporator Effectiveness

The balance condition of state three in Figure 2.14 can be calculated given the refrigerant temperature, the conditioned space's dry bulb temperature, the unit load factor of the coil and the sensible and latent space loads. It was assumed that the evaporators operate near this condition most of the time. Evaporators are run long enough to take care of the sensible load in the space and the latent load automatically gets taken care of at the same time. This is not free cooling however; the refrigerant must absorb both the latent and sensible energy extracted from the air stream. In the same way that effectiveness was used to model the evaporative condenser in Section 2.4.2, an effectiveness approach can be used for evaporators as well. Effectiveness for an evaporator is defined in Equation (2.12) and shown in psychrometric coordinates in Figure 2.15.

$$Effectiveness = \frac{CoilCapacity}{MaxCoilCapacity} = \frac{\dot{m}_{air} \cdot \left( h_{air,in} - h_{air,out}\big|_{T_{air,out}} \right)}{\dot{m}_{air} \cdot \left( h_{air,in} - h_{air,out}\big|_{T_{refrigerant}} \right)} \tag{2.12}$$

Coil capacity and maximum coil capacity are illustrated in Figure 2.15.

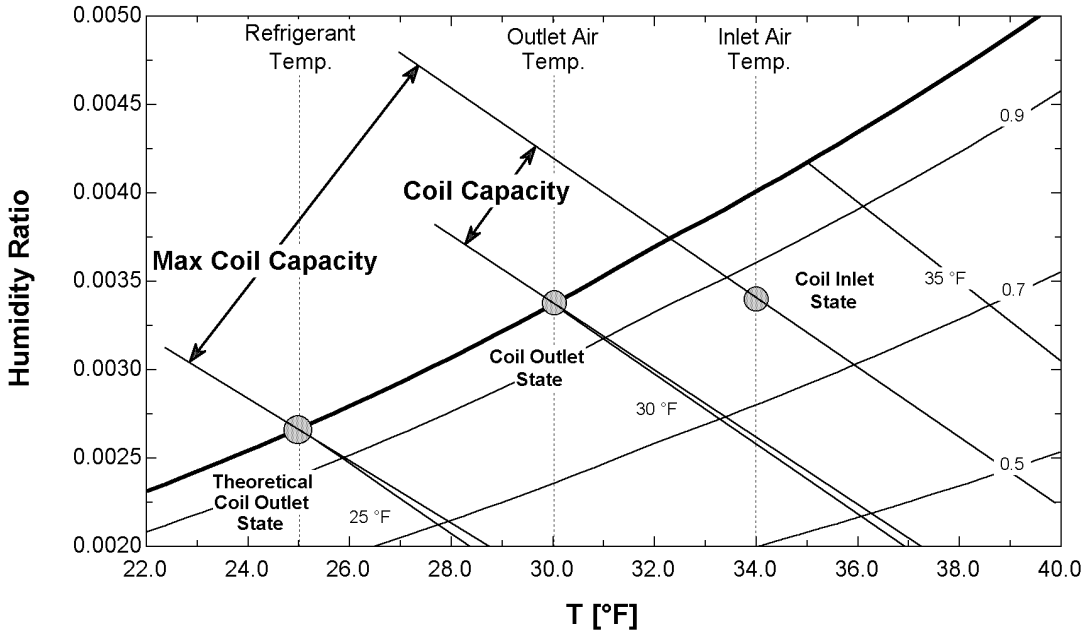


**Figure 2.15 Psychrometric Evaporator Effectiveness**

Figure 2.16 shows the behavior of the coil effectiveness as the conditioned space's relative humidity is varied. A relative humidity of 100% corresponds to the number 1 on the X axis of the Figure. When the relative humidity is high, there is a large latent component of the coil capacity and the effectiveness is slightly higher since the numerator in Equation (2.12) has increased. (This curve has not been adjusted to account for the effect of accelerated frost accumulation that will occur at high humidity conditions. If excess frost were allowed to accumulate on the coil, the effectiveness would actually decrease for conditions of higher humidity.) As the relative humidity decreases, the latent component decreases and we see a corresponding decrease in coil effectiveness until it reaches a minimum. This minimum corresponds to the near balance state, state three, shown in Figure 2.14 earlier in this discussion. As the conditioned space's relative humidity continues to decrease the specific enthalpy of the inlet air decreases which results in a decrease in the maximum coil capacity calculation or the denominator of the effectiveness calculation (Equation (2.12)). Since the coil capacity is now almost all sensible cooling, the numerator of Equation (2.12) remains nearly constant. This causes the effectiveness to increase again until it becomes a constant when the inlet air gets too dry and no condensate is formed on the coil. Figure 2.16 also shows

the effect of lowering the refrigerant temperature on the effectiveness trace as well. The TD of a coil has a small effect on the minimum effectiveness of a coil and a slightly larger effect on the conditioned space's equilibrium humidity.

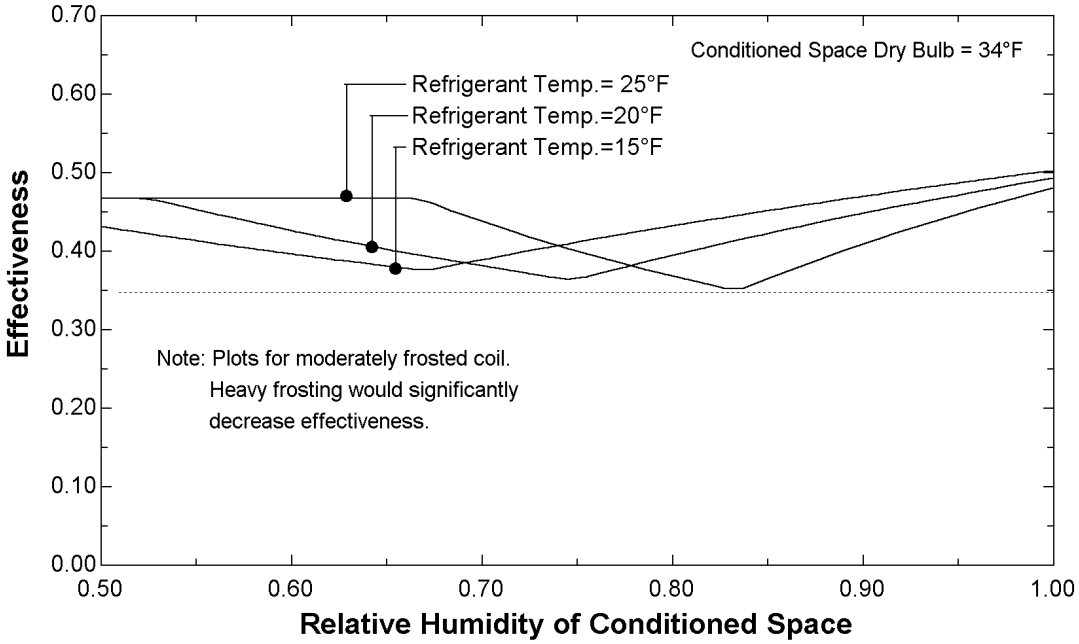


**Figure 2.16 Evaporator Effectiveness Trends**

2.4.3.6 Evaporator Part Load Operation

When the load on the conditioned space is less than its design value, which is most of the time, the refrigeration capacity delivered by the evaporators must be reduced. If a constant coil TD is desired, capacity can be reduced by either cycling the fans and/or refrigerant on and off or by reducing the mass flow of air through the coil. If the capacity is controlled by reducing the mass flow of air, Equation (2.13) is used to de-rate the performance of the evaporator.

$$Cap_{actual} = Cap_{rated} \cdot \left( \frac{FanSpeed_{actual}}{FanSpeed_{rated}} \right)^{N} \tag{2.13}$$

The coefficient N is expected to vary between 0.5 for laminar flow and 0.8 for turbulent flow. [Mitchell and Braun, 1998] A manufacturer's representative from Evapco suggested it is likely between 0.5 and 0.6 for their products [Struder, 1999]. Stamm, 1999

suggested his experimental measurements indicated a value of 0.65, consequently 0.65 was used in the model.

Five main schemes of part-load evaporator operation were examined.

- On/Off refrigerant control. (fan motors stay on)
- On/Off fan motor cycling. (current evaporator control strategy)
- Half-speed motor cycling.
- Variable Frequency Drive (VFD) controllers on the motors.
- Controlling refrigerant temperature.

On/off refrigerant control shuts off the flow of refrigerant to the evaporator, but the fans remain on for purposes of air circulation. With the on/off motor control strategy, the evaporator fans are run at full speed until the conditioned space's temperature requirements are met and then the motors are shut off. Half-speed control first cycles the fans to half speed and then to full speed if the evaporators still are not meeting the load. VFD control runs the fans at a speed needed to meet the load on the evaporator. The final way of reducing the capacity of a coil during part load operation is to change the refrigerant temperature being supplied to the coil. As the temperature difference (TD) of the coil decreases, so does the capacity.

The advantage of using the half-speed and VFD control can be explained by the fan laws. Fan power is related to the cube of fan speed. If the speed is cut in half, half the mass flow is achieved at only one-eighth of the design fan power. Figure 2.17 shows what percent of the full load power each fan control scheme would use given the percent of full load that the evaporators must operate at to satisfy the conditioned space's requirements. The power drops to zero at five percent capacity because some natural convection effects were assumed.

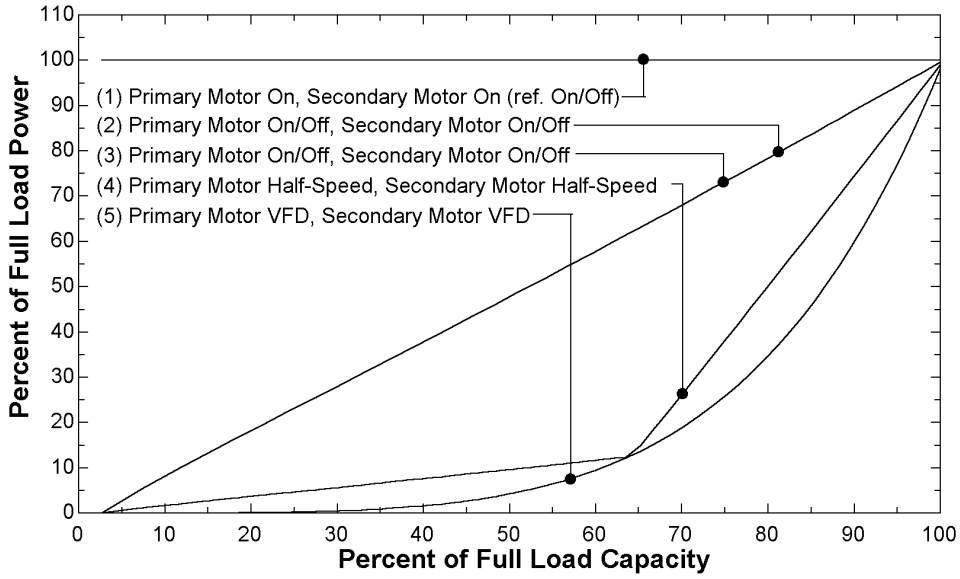


**Figure 2.17 Part Load Evaporator Operation**

The control strategies shown in Figure 2.17 are labeled 1-5 and are described below in Table 2.4. Each mode of operation sets the fan motors either on, off, half-speed, or at variable speed. If the evaporator pressure is controlled to a near constant set point, each mode corresponds to some amount of energy that is absorbed. For intermediate load requirements, fan settings are simply cycled between the nearest two modes. The evaporator would be forced between modes of operation depending upon the actual load on the evaporator. Actual load may be identified by the temperature trends in the conditioned space. A rapidly dropping temperature below the conditioned space's set point would indicate that the evaporator is absorbing too much energy and should be moved to a lower mode of operation. Control strategy 2 is currently being used at the actual facility.

| Strategy | | Mode 1 | Mode 2 | Mode 3 | Mode 4 | Mode 5 |
|---|---|---|---|---|---|---|
| 1 | Primary Motor | on | | | | |
| | Secondary Motor | on | | | | |
| 2 | Primary Motor | off | on | | | |
| | Secondary Motor | off | on | | | |
| 3 | Primary Motor | off | on | on | | |
| | Secondary Motor | off | off | on | | |
| 4 | Primary Motor | off | half-speed | half-speed | on | on |
| | Secondary Motor | off | off | half-speed | half-speed | on |
| 5 | Primary Motor | off | variable speed | | | |
| | Secondary Motor | off | variable speed | | | |

**Table 2.4 Evaporator Fan Control Strategies**

2.4.3.7 Evaporator Defrosting

All evaporators that operate with a refrigerant temperature below the freezing point of water and dew point of the conditioned space will build frost on the coils during operation. Frost accumulation degrades the performance of an evaporator by reducing the UA and impeding the airflow. Periodically the frost must be removed from the coil surface. Several defrosting methods are commonly used. Hot gas, hot water, electric heat, and warm air can all be used to melt the frost off of evaporator coils [Stamm, 1985].

This system uses hot gas for defrosting. The defrost requirements of the current system account for 13 percent of the total electrical energy used by the system. A schematic of defrost piping is shown in Figure 2.13. This type of piping arrangement is commonly found in industrial refrigeration applications. A hot gas defrost cycle typically proceeds in the following sequence. First the flow of cold liquid refrigerant is shut off to the evaporator while the evaporator fans continue to run boiling out most of the liquid refrigerant remaining in the coil. Then the fans are shut off and a portion of the hot gas from the compressor discharge is allowed to flow into the evaporator. The internal pressure of the evaporator is maintained at a desired level by a pressure regulating valve (A4AK). The temperature inside the evaporator must be warm enough to melt the ice. However, too high of evaporator defrost set pressure will result in excess flash gas in the wet suction return line and will unnecessarily load the compressors. After the frost is melted off the coil, the flow of hot gas is stopped and the coil is allowed to fill back up

with low temperature liquid before the fans are restarted in order to re-freeze any water left on the coil surface so it doesn't get blown out into the conditioned space when the fans cycle on.

Defrost cycles are time initiated and time terminated in this system. Regardless of how much frost has actually accumulated, units are preset to go into defrost twice or three times a day for a specified length of time. Due to the design of the pressure regulating valves used in this system, a certain amount of hot gas passes through the coil without condensing. This hot gas is commonly termed blow-by. It is important to time defrost cycles properly. Defrost cycles that are too long, meaning hot gas is still flowing through the coil after the ice has melted, produce excessive amounts of blow-by and place an unnecessary load on the system.

As an alternative to time-clock-initiated, defrost cycles can also be demand-initiated. Sensors that measure static pressure drop of the airflow across the evaporator coil or time clocks on solenoid valves can be used to gauge how long the evaporator has been "on". The "time on" can then be used to estimate whether the coil needs defrosting yet or not. This type of control strategy will reduce the amount of blow-by in the system.

### 2.4.4 Refrigerant Piping

#### 2.4.4.1 Critical Piping Sections

Piping connects all the components together in a system. Pressure losses in the piping affect the refrigerant conditions that each component operates at relative to each other. The three main types of lines are discharge lines, liquid supply lines, and suction lines. In general, discharge lines carry hot gas, liquid supply lines carry saturated liquid, and suction lines carry mixtures of liquid and vapor.

The most critical piping sections in refrigeration systems are the suction lines because they operate at the coldest temperatures, carry mostly vapor refrigerant with a high specific volume, and directly influence the operating conditions of the compressors and evaporators. A system with pumped liquid overfeed evaporators has two major suction

lines. The first is between the evaporators and the low pressure receiver. This is called the wet suction return (WSR) line. The second is between the low pressure receiver and the compressor suction port called the dry suction return (DSR) line. Figure 2.18 shows the saturation temperature drop that corresponds with 1 psia of pressure loss over a range of refrigerant temperatures. For instance, if a low pressure receiver has 20°F refrigerant, the evaporator refrigerant will be approximately 1°F above the receiver temperature for each pound per square inch of pressure drop in the WSR line.

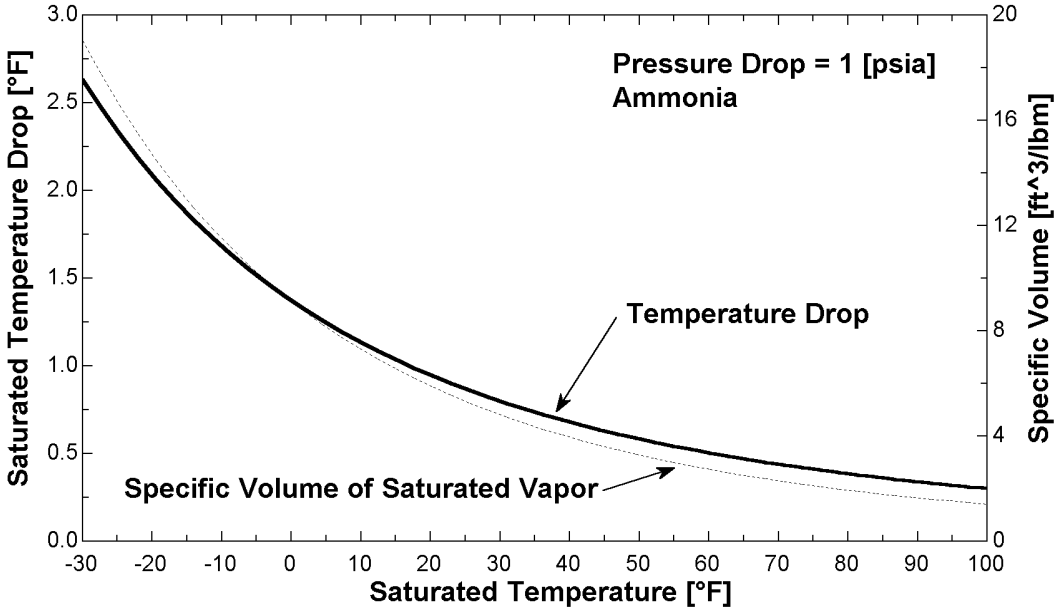


**Figure 2.18 Saturated Temperature Drop [°F] Corresponding to a 1 [psia] Pressure Drop for Ammonia and Specific Volume [ft$^3$/lbm]**

Figure 2.18 also illustrates why pressure drops in colder suction lines are more important. For each increment of pressure drop at lower temperatures there is a larger change in saturation temperature. A larger temperature change results in more superheat which results in an increased specific volume at the compressor suction. A larger specific volume at the compressor suction results in less compressor mass flow and less available capacity.

Liquid supply lines are not as critical because they carry mostly liquid where the specific volume changes very little with temperature drop. Also, pressure drop in liquid lines supplying the evaporators is recovered with a liquid refrigerant pump.

Compared to suction lines, pressure drops in discharge lines do not degrade system performance as much. The fan control scheme for the condenser controls the discharge pressure of the compressors. If the load on the system increases, the head pressure will start to rise. As the controls sense the excess head pressure, the condenser will cycle on more fans which rejects more energy and reduces the refrigerant pressure in the condenser resulting in lower head pressure at the compressors. Any pressure drop in the discharge line will have to be accounted for by increased condenser fan operation time. Since the energy consumed by the condenser fans is generally much less than consumed by the compressors, the effect of prolonged condenser fan run time on system performance is small.

Another comparison between the importance of pressure drop in suction lines, relative to discharge lines, can be demonstrated by using the actual compressor maps discussed in Section 2.4.1. Figure 2.19 shows the increase in compressor horsepower and decrease in compressor capacity for pressure losses in the suction and discharge lines. Evaporator capacity, evaporator suction temperature, and condensing pressure are all kept constant. (An increase in suction line pressure drop will result in a lower compressor suction pressure.) A three psi pressure loss in the discharge line would result in a two percent increase in power. The same pressure drop in a suction line results in an increase in power nearly five times that. Figure 2.19 also illustrates the drastic reduction in available compressor capacity with suction line pressure drop due to the specific volume effects mentioned Section 2.4.1.

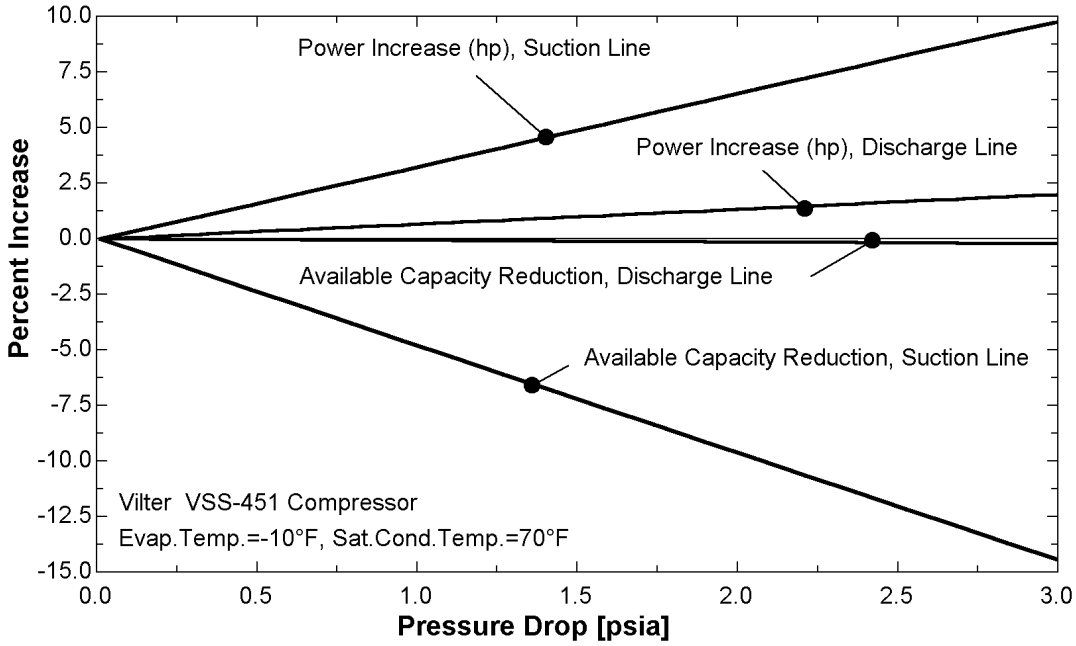


**Figure 2.19 ΔP Effects in Suction and Discharge Lines**

2.4.4.2 Pressure Drop Calculations

Pressure drop through a pipe with single phase flow can be calculated from a simplified version the Bernoulli's equation shown in Equation (2.14).

$$\Delta P = \rho \cdot g \cdot \left( \Delta Z + h_{1f2} \right) \tag{2.14}$$

where:

ρ = density; g = acceleration of gravity;

ΔZ = change in elevation; $h_{1f2}$ = static frictional head

The static frictional head is calculated with the Darcy equation shown by Equation (2.15). The Darcy equation is a function of the resistance coefficient and the velocity of the fluid [Crane, 1988].

$$h_{1f2} = K_{tot} \cdot \frac{Vel^2}{2 \cdot g} \tag{2.15}$$

The total resistance coefficient, $K_{tot}$, is calculated by summing the individual coefficients from each length of pipe and fitting in the total pipe run as indicated in Equation (2.16).

In this equation the indices i and j represent the number of different kinds of fittings and pipe sizes respectively. N is the number of similar fittings or pipe segments. The individual coefficients ($K_i$ and $K_j$) are calculated by multiplying the friction factor of the pipe by an equivalent length over diameter ratio that is specific to each fitting or pipe length.(Equations (2.17)) [Avallone, 1987]

$$K_{tot} = \sum_{1}^{i} K_{i,fittings} \cdot N_{i,fittings} + \sum_{1}^{j} K_{j,pipe} \cdot N_{j,pipe} \tag{2.16}$$

$$\begin{aligned} K_{Tee,through} &= 20 \cdot f & K_{AngleValve} &= 200 \cdot f \\ K_{Tee,branch} &= 60 \cdot f & K_{CheckValve} &= 135 \cdot f \\ K_{Piping} &= \frac{length}{diameter} \cdot f & K_{90° Elbow} &= 30 \cdot f \end{aligned} \tag{2.17}$$

The friction factor of the pipe (*f*) is found by using the Colebrook equation which is displayed in Equation (2.18) [Marks, 1996]. A value of $180 \times 10^{-6}$[ft] was used for ε.

$$\frac{1}{\sqrt{f}} = -2\log_{10}\left(\frac{\varepsilon/Dia}{3.7} + \frac{2.51}{\mathrm{Re}\sqrt{f}}\right) \tag{2.18}$$

The Colebrook equation is valid only for turbulent flow. Internal pipe flow transitions to turbulent flow at Reynold's numbers between 2,000-4,000. Some preliminary calculations done on the system gave Reynold's numbers in the 50,000 to 500,000 range depending upon part load conditions. Flow is clearly in the turbulent regime.

The equivalent lengths of piping and valves used for pressure drop calculations in each dry suction return segment are given in Table 2.5. Equivalent lengths can be converted into the length/diameter ratios used in Equations (2.17)) by dividing by the diameter and allocating the correct proportion to each fitting. Also included in Table 2.5 is the change in height between the section inlet and outlet. A negative number indicates a decrease in elevation.

| Piping Segment | Change in Height [ft] | Diameter [inch] | Fitting Equivalent Length [ft] | Lenth of Straight Pipe [ft] |
|---|---|---|---|---|
| -12°F Dry Suction Line, Segment 1 | +1 | 8 | 510 | 15 |
| -12°F Dry Suction Line, Segment 2 | -19 | 5 | 410 | 30 |
| 23°F Dry Suction Line, Segment 1 | +1 | 8 | 510 | 20 |
| 23°F Dry Suction Line, Segment 2 | -19 | 4 | 710 | 25 |

**Table 2.5 Piping Pressure Drop Calculation Parameters**

2.4.4.3 Pressure Drop – Model Implementation

Due to the non-linearities introduced by the Darcy and Colebrook equations, the model had convergence difficulties when these equations were used directly. Alternatively, a correlation for pressure drop in the form of a second-order polynomial with mass flow and inlet temperature as the independent variables was developed (Equation (2.19)). A separate correlation was developed for each dry suction return line given the physical dimensions and number of fittings. The pressure loss (PL) coefficients along with other relevant statistical data from the regression (rms and $r^2$ values) for each piping section is located in Appendix C.

$$\Delta P = PL_1 + PL_2 \cdot \dot{m} + PL_3 \cdot \dot{m}^2 + PL_4 \cdot T + PL_5 \cdot T^2 + PL_6 \cdot m \cdot T \tag{2.19}$$

The second-order polynomial with cross-term fits the calculated points quite well as shown in Figure 2.20.

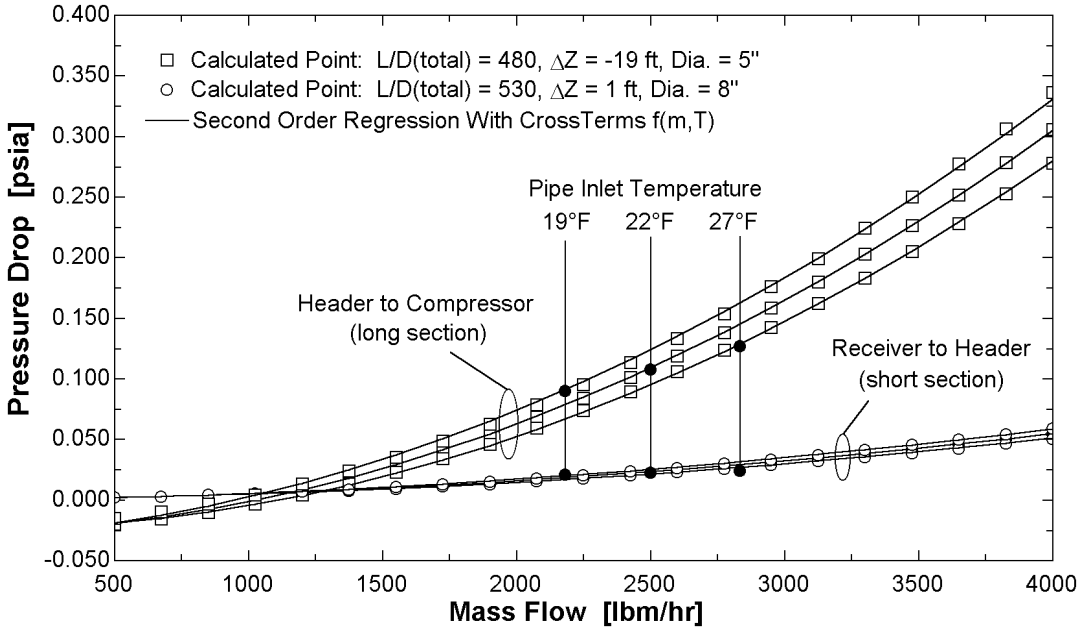


**Figure 2.20 Piping Pressure Drop Correlations**

As mentioned before, pressure drops in hot gas discharge lines or liquid supply lines have very little effect on system performance if the pipes are designed to typical design standards. Therefore, the model assumes a constant estimated value for pressure drop in the discharge line of four [psi]. Four [psi] includes pressure losses in discharge valve train, oil separator, piping, and piping fittings. Pressure drops in all other liquid supply lines, except the lines serving the evaporators, are assumed to be negligible. A constant pressure drop equal to 3°F is assumed for the evaporator supply and WSR lines to the cooler and loading dock. A value of 2°F was used for the freezer WSR lines. These assumptions were based on the common ammonia pipe sizing design practice of 0.5 to 1°F per 100 [ft] of equivalent piping length [ASHRAE Refrigeration Handbook, 1990]. This leaves the suction lines between the low pressure receivers and compressors to be examined. The physical parameters of these lines were fed into the Darcy and Colebrook equations. (See Table 2.5 for physical parameters.) Equations in the form of Equation (2.19) are used to approximate the pressure drop in these lines.

### 2.4.5 Vessels

#### 2.4.5.1 Vessels as Mass Flow Accounting Devices

The practical need for vessels in refrigeration systems is discussed in Section 1.4. The modeling scheme detailed in Section 2.2 explained that this system was modeled based on each component contributing a certain mass flow of vapor and liquid to and/or from the vessels. This model assumes no liquid level fluctuations in any of the vessels, which essentially make them separation devices used to separate the vapor from the liquid refrigerant with no storage capability. This assumption provides a close approximation to actual operation because the level in each low pressure vessel is closely controlled by a Phillips float switch which works in combination with a modulating expansion valve. Occasionally, as evaporators cycle in and out of defrost, a large surge volume of liquid may temporarily increase the liquid level in the vessels. This type of effect is not accounted for in the model. When averaged into the hourly operation of the system, small surge volumes have very little effect in the overall performance of the system because the pressure/temperature of each vessel is still controlled. Pressure/temperature fluctuations in the vessels would have an impact on system performance.

Vessels are not modeled as individual components in the system but rather as mass flow accounting devices. The mass balances that result link each component to one another. The model also does not account for any heat gains or losses in any of the vessels.

### 2.4.6 Expansion Valves

#### 2.4.6.1 Isenthalpic Throttling Devices

The two main expansion valves are located between the high pressure receiver and intermediate pressure receiver and between the intermediate pressure receiver and low pressure receiver. Their function is to throttle a high pressure liquid to a lower pressure and temperature. They are Phillips series 701S pilot-operated expansion valves which modulate the flow of refrigerant through them based on the amount of make up

refrigerant required in the intermediate and low pressure receivers to maintain a set liquid level. There are also expansion valves located on each of the direct expansion coils in the banana rooms. All expansion valves are assumed adiabatic which dictates that the expansion process is isenthalpic.

### 2.4.7 Subcooler

#### 2.4.7.1 Construction

The two subcoolers are located in the liquid supply lines of the intermediate and low pressure receivers just ahead of the mass flow meters. Their purpose is to assure that there are no vapor bubbles in the refrigerant stream. A subcooled liquid is required for accurate measurements in the mass flow meters. Both subcoolers are shell and tube heat exchangers. The tube-side contains the high pressure and high temperature liquid before it is sent through the mass flow meter and then throttled to the lower pressure receiver. The shell-side of the heat exchanger is feed with liquid from the lower pressure receiver.

#### 2.4.7.2 Purpose

In some refrigeration systems, refrigerant in liquid supply lines is subcooled in order to reduce the amount of flash gas produced when the refrigerant is throttled. The portion of refrigerant that is flashed in the throttling process produces almost no useful cooling. In this system, since the subcooling is provided by refrigerant at the same pressure that the refrigerant is throttled to, the subcoolers provide no performance benefit to the system. The volume of flash gas saved by throttling subcooled liquid is essentially the same volume produced in the shell part of heat exchanger. The subcooler’s only function is to ensure a single-phase fluid is flowing through the mass flow meters.

2.4.7.3 Model Implementation

Experimental temperature data were available for one of the subcoolers. A temperature-based effectiveness approach was used to model the subcoolers. Subcooler effectiveness was calculated using Equation (2.20).

$$\varepsilon = \frac{T_{HighPressureLiquid,In} - T_{HighPressureLiquid,Out}}{T_{HighPressureLiquid,In} - T_{shell,refrigerant}} \tag{2.20}$$

For very small mass flow rates the temperature of the high pressure refrigerant stream out would be very close to the temperature of the refrigerant in the shell and the effectiveness would be nearly 1. As mass flow rate increases the temperature of the high pressure outlet fluid starts to increase and effectiveness will decrease. Figure 2.21 shows some experimental data for one day.

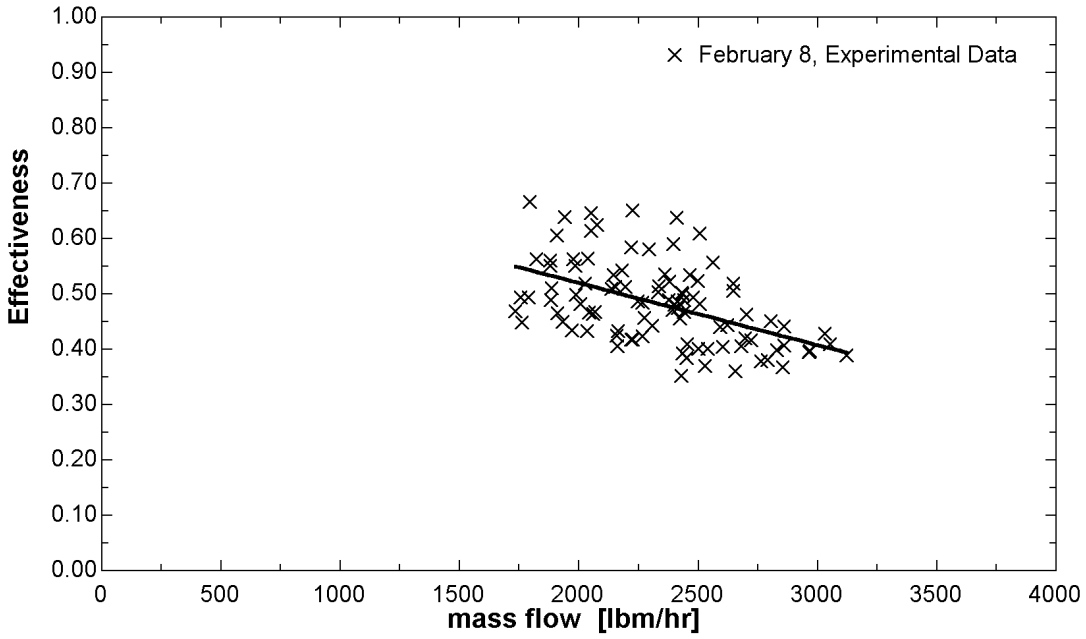


**Figure 2.21 Subcooler Experimental Effectiveness Data**

In terms of the overall system performance, heat exchanger effectiveness has no effect. Therefore, it was decided that a simple modeling approach would be used. A linear regression to a first order polynomial was done on this data which resulted in Equation (2.21). Equation (2.21) is shown in Figure 2.21 as the solid line. Although the fit is very

rough it serves the purpose of modeling the subcooler component in this system for sake of completeness.

$$\varepsilon = 0.75 - 1.12 \cdot 10^{-4} \cdot \dot{m} \tag{2.21}$$

### 2.4.8 Liquid Recirculating Pumps

Two five horsepower pumps are used in separate liquid supply lines to circulate the liquid refrigerant from the intermediate and low pressure receivers to two the cooler and freezer evaporators respectively. The pumps must be selected in order to overcome the pressure loss from the receiver vessel to the evaporator that is located the farthest away. The energy added to the refrigerant stream by the pump impeller is added to the appropriate space load in the model.

## 2.5 Warehouse

The purpose of modeling the actual cold storage space is to predict the refrigeration load on the evaporators. The evaporator load usually consists of both sensible and latent components. The sensible component of the load is related to the change in temperature of the air. The latent component is related to the change in moisture content. Figure 2.22 shows the sensible and latent components of warm moist air being cooled and dehumidified to a desired condition.

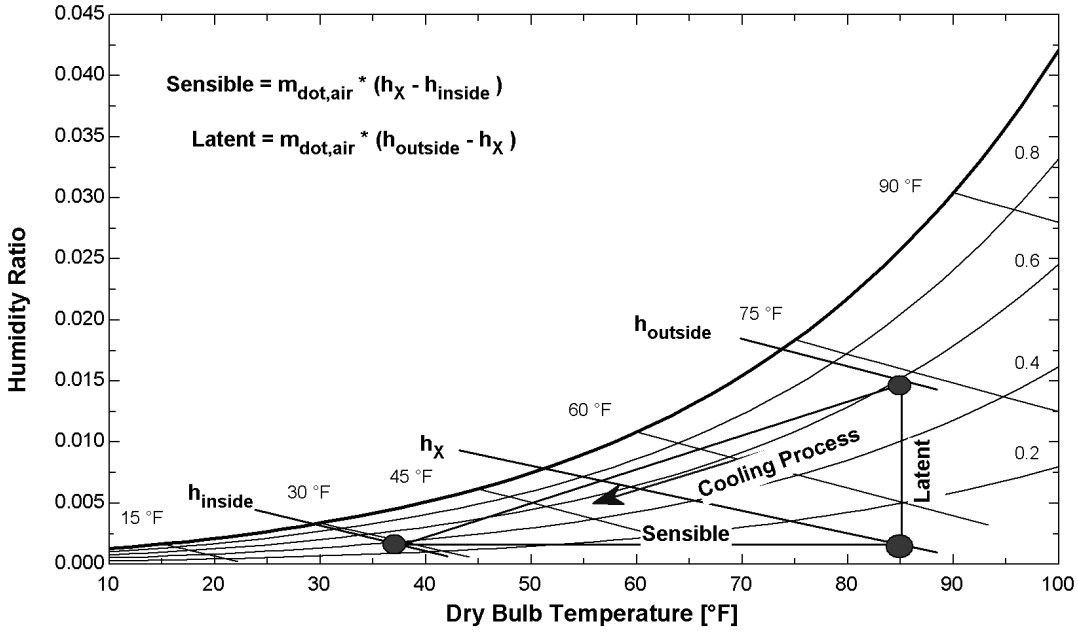


**Figure 2.22 Psychrometrics of the Cooling Process**

A cold space's load (sensible and latent components) is generated by three main sources: wall transmission load, infiltration load, and internal space loads.

### 2.5.1 Wall Transmission Gains

Heat transmission through walls, roofs, and floors adds sensible energy to the cold space. The transmission heat flux driving potential is the temperature difference between the inside and outside wall surface. The inside surface is always at a temperature slightly above the cold space temperature. The outside surface temperature is slightly below that of the sol-air temperature [Mitchell and Braun, 1998]. The sol-air temperature of a wall is always changing due to fluctuations in outside air dry bulb temperature and the amount of solar radiation that is absorbed by the outside surface. Therefore, heat gain through walls is a transient process. The amount of heat gain depends upon the resistance of the wall to heat transfer. The specific heat and density of the wall material determine the transient behavior of the heat gain.

Wall and roof U values [Btu/hr-ft²-F] as well as wall orientations were obtained from the design load calculations performed by the design-build mechanical contractor who installed the refrigeration system. One dimensional, finite difference equations employing

the Crank-Nicholson method solving a four-node system are used to calculate the transient behavior of the heat flux through the roofs and walls [Altweis, 1998]. After the heat flux is calculated for each section of wall or roof, the flux is multiplied by the area of that section and summed over the entire building surface. A constant value of 2.5 [Btu/hr-ft²] was recommended by the mechanical system designer for calculating the heat gain through the heated floor of the freezer for this system [Kastello, 1999].

### 2.5.2 Infiltration

Infiltration load is due to warm, moist outside air leaking in through cracks in the walls and roofs and from open doors that separate a cold space from a warmer, moister spaces. Infiltration adds both sensible and latent load components to a cold space. This model ignores infiltration due to air leaking in through cracks in the walls and roof. Instead, each cold space has a door that leads directly to the outside that can account for any extra outdoor air leakage. Infiltration through an open door was calculated using an air velocity technique that is detailed in the Krack refrigeration load estimating manual [Krack,1992]. When a door separating a cold space from a warmer space is opened, cold air from the colder space rushes out the bottom half of the door and warm air gets pulled in through the top half of the door. The average air velocity at either the bottom or top half of an open door depends upon the height of the door and the temperature difference between the two spaces. Air velocity in feet per minute is calculated by Equation (2.22).

$$Velocity_{fpm} = 4.88 \cdot \sqrt{Height_{ft}} \cdot \sqrt{\Delta Temp._{\circ F}} \tag{2.22}$$

This velocity is then multiplied by half the door area and the actual time the door is open to find the total volume of air that infiltrated the cold space (Equation (2.23)).

$$Cu\ ft = Vel_{fpm} \cdot \frac{Door\ Area_{ft^2}}{2} \cdot Time\ Open_{min} \tag{2.23}$$

The sensible and latent components of the infiltration load are calculated as demonstrated earlier in Figure 2.22. The door open time is, in most instances, is highly variable as door traffic changes widely. For purposes of this model, door open fractions were adjusted to constant values on the peak load hour (the 17$^{th}$ hour of July 16$^{th}$) until the sensible heat load ratio matched that of the design load calculations used by the installing mechanical contractor.

### 2.5.3 Internal Space Loads

Internal space loads in a typical warehouse include heat and/or moisture gains from people, warehouse product, evaporator defrosting, machinery, interior heated spaces, and lights. These loads were estimated from the design load calculations from the mechanical contractor who installed the system. They are itemized for each space (freezer, cooler, loading dock, and banana/tomato rooms) in Appendix E.

# *Chapter 3 -Model Verification*

After all components were modeled it was then necessary to validate the model with experimental data.

## 3.1 Experimental Data Sources

Experimental data from three sources is available for two one-week periods. The first one-week period extends from January 9$^{th}$ to the 16$^{th}$ and the second from February 7$^{th}$ to the 14$^{th}$. The three data sources are identified as the data acquisition database, the mass flow meter database, and the WEPCO power demand database. A fourth source of data is also available. This source provides monthly summary information about the total amount of refrigeration [ton-hrs] produced for the months between March and September, 1998.

The first source of available experimental data is the data acquisition database. The data acquisition database includes 15-minute averaged data from several main system parameters which are listed below.

**Pressures**
- Banana room evaporator pressure.
- Tomato room evaporator pressure.
- Compressor discharge header.
- High and low temperature compressor suction header.

**Temperatures**
- Freezer, cooler, and loading dock space temperatures.
- Outside air dry bulb.
- Intermediate and low pressure receiver temperatures.
- High temperature subcooler refrigerant outlet temperature.

**Compressors**
- Percent of full load capacity for all compressors

A second source of experimental data is the mass flow meter database. The mass flow meters in the system keep a running total of the mass of refrigerant that has passed through. After a predetermined amount of mass has passed, the meters will send a pulse to another data acquisition system. This system records the time the pulse occurred and also is set up to calculate the total amount of refrigeration capacity (ton-hr) that has

passed through the flow meter. The meter between the high and intermediate pressure receiver pulses every 60 [lbm] of refrigerant. The meter between the intermediate and low pressure receiver pulses every 30 [lbm] of refrigerant. The mass flow of refrigerant through the system at these specific locations can be calculated by taking the mass of refrigerant per pulse for the particular mass flow meter and dividing by the time between the pulses.

The third source of experimental data comes from the Wisconsin Electric Power Company. Electric demand data [kW] is available in 15-minute time intervals for two submeters serving the entire warehouse. One submeter distributes power to the entire mechanical room of the refrigeration system. This includes the compressors, condenser fans, cooling water pumps, and lights. Also, a relatively constant electric load arising from devices such as recirculating pumps, control panels, and computers, needs to be accounted for. The other submeter distributed power to the entire warehouse, which would include evaporator fans, lights, forklift recharging stations, and electric heating coils.

The final source of data was extracted from a system performance tracking spreadsheet made available by a WEPCO associate. This spreadsheet contains a monthly summary of the total amount of refrigeration [ton-hrs] produced by the system for the months of March through September, 1998. Refrigeration totals are calculated with the mass flow meters and temperature sensors in the high, intermediate, and low pressure receivers. The total amount of refrigeration is separated into two values, one that is representative of the load on the low temperature (screw) compressor and one for the high temperature (recip.) compressor. The instantaneous low temperature load is calculated by multiplying the mass flow through the low temperature mass flow meter times the change in specific enthalpy of saturated liquid from the intermediate pressure receiver and saturated vapor from the low pressure receiver. This load is then integrated over the month by summing the calculation each time the flow meter pulses during the month. (Equation (3.1))

$$Refrigeration = \int_{month} \dot{m}_{ref} \cdot \left( h_{sat,vap} - h_{sat,liq} \right) \tag{3.1}$$

The high temperature compressor refrigeration effect is calculated by multiplying the mass flow through the high temperature mass flow meter times the change in specific enthalpy between saturated liquid in the high pressure receiver and the saturated vapor in the intermediate pressure receiver. The low temperature refrigeration calculation (Equation (3.1)) is subtracted from this value to get the total refrigeration effect produced by the high temperature compressor. The low temperature refrigeration effect must be subtracted because the refrigerant that flows through the low temperature mass flow meter first passed through the high temperature flow meter. Again this is integrated over the month by summing this calculation each time the flow meter pulses.

Also included in this performance tracking spreadsheet was the total electrical energy [kWh] used by the mechanical room and warehouse for the months of March through September 1998.

## 3.2 Model Verification

Model verification was done in two parts. First, the refrigerant or “wet” side of the system was verified. Second, the air or “dry” side of the system was verified.
Table 3.1 lists the main parameters that were used and calibrated for each part.

| Component Calibration Model Input Parameters | Known | Assumed | Calibration Parameter |
|---|---|---|---|
| Compressor(s) Suction Pressure | X | | |
| Compressor(s) Discharge Pressure | X | | |
| Compressor(s) Part Load Ratio | X | | |
| Intermediate Pressure Receiver Temperature | X | | |
| Low Pressure Receiver Temperature | X | | |
| Outside Dry Bulb Temperature | X | | |
| Outside Wet Bulb Temperatue | X | | |
| DX Evaporator Pressure | X | | |
| Mechanical Room Power Consumption | X | | |
| Refrigerant Mass Flow (meters 1 and 2) | X | | |
| Defrost Load | | X | |
| Blow-by Fraction | | | X |
| Other Equipment Power in Mechanical Room | | | X |

| Load Calibration Model Input Paramenters | Known | Assumed | Calibration Parameter |
|---|---|---|---|
| Outside Dry Bulb Temperature | X | | |
| Outside Wet Bulb Temperature | X | | |
| Warehouse Transmission Heat Gain | X | | |
| Monthly Refrigeration Totals | X | | |
| Blow-By and Other Equipment in Mechanical Room Calibration Parameters | | X | |
| Building Activity Schedule | | X | |
| Defrost Heat Gains | | X | |
| Sub-floor Heating Hot Gas Demand | | X | |
| Warehouse Door Open Time Fractions | | X | |
| Interior Heat Gains | | | X |
| Banana/Tomato Room Loads | | | X |

**Table 3.1 Model Validation Parameters**

### 3.2.1 Component Verification

Input parameters from the data acquisition database were used to predict mass flow and system power consumption. The mass flow and power outputs from the model were compared to the information obtained from the remaining two databases. Upon detailed examination of the acquired data, not every day of the 14 available had continuous data. From the trends in the recorded data, it was apparent that the system experienced some abnormal operation during some of the days in the data set. Some abnormalities observed were suspected to be attributed to compressor maintenance, which resulted in uncontrolled warehouse temperatures. No maintenance or operation logs were available

to verify these suspicions. Four “good” days were selected for model validation; January 12,13 and February 8, 12.

A 24 hour sequence was simulated for each of the selected days. To be consistent with the time resolution of the experimental databases, 15-minute time intervals were used for the simulation. Refrigerant mass flow rates at the flow meter locations and compressor power were recorded into a table for comparison to the mass flow and demand data obtained from the mass flow and demand power databases. A simplified explanation of the verification process is listed below:

1. With some assumptions of pressure drop (See Section 2.4.4), the suction and discharge header line pressure losses along with the percent of full load capacity of each compressor were used to calculate the power draw and mass flow through the compressors.
2. The cumulative mass flow through the low temperature compressor should be equal to the cumulative mass flow through the low temperature flow meter after some time has passed. (Enough time must pass to allow the transients of the evaporator operation to average out.)
3. The total mass flow through both high and low temperature compressors, minus the amount of refrigerant used to defrost, should equal the amount of refrigerant that flows through the high temperature flow meter. (Again, after some time has passed to average out the transients.)
4. Finally, the power required by the compressors was also calculated based on the suction and discharge header line pressure along with the percent of full load capacity. This power plus a constant value from the electric machinery in the engine room can be compared to the power recorded in the WEPCO electrical demand power database. The outdoor air dry and wet bulb are cold (January and February days) and the condenser is over-sized so we can expect very little activity from the condenser fans and pumps. Therefore, little of the power demand recorded at the submeter can be expected from the evaporative condenser unit.

Due to the limited amount of data available in the data acquisition database, two calibration variables have to be assumed. The first has to do with estimating how much hot gas is used in defrosting the evaporators and in the heat exchanger used to heat glycol for subfloor heating in the freezer. This defrost/glycol heater mass flow represents the total refrigerant mass flow from the compressors that short circuits the high temperature mass flow meter. The installing mechanical contractor estimated a glycol heater load of 132 MBH. Also, a design defrost vapor load of 42.6 MBH was estimated by the contractor. The defrost vapor load is defined as the load that the high temperature compressor sees as a result of the blow-by gas from the evaporators. Evaporator blow-by is defined in Section 2.4.3.7. The required amount of defrost needed during January and February is assumed to be 60 percent of design due to the low humidity ratio of the ambient air. This assumption is consistent with the operation of the facility. The number of defrost cycles initiated during the winter is less than during the summer. With estimates of the defrost and heat exchanger loads, the calibration parameter of hot gas blow-by can be adjusted until the predicted amount of mass flow through the high temperature mass flow meter matches the recorded amount.

The second calibration variable that must be selected to compare the model results with the other databases is the amount of power distributed by the mechanical room submeter that does not include the compressor power. Given that the simulation periods are in winter months, we would not expect the condenser fans to be cycled on very frequently. The mechanical room constant power calibration variable value should stay nearly constant throughout the 24-hour period.

Figure 3.1 and Figure 3.2 show the high and low temperature mass flow meter comparisons for February 8 after adjusting the blow-by parameter. Calibration suggests that, on average, ten percent of the refrigerant mass flowing to the evaporators during defrost does not condense. The bold lines indicate the data obtained from the mass flow meter database. Linear interpolation was used to adjust the mass flow data to 15 minute time steps to match the simulation results. The thin lines indicate a plus or minus five percent range on the predicted results. Actual predicted results are not plotted so the plot

would be less cluttered. Actual predicted results would lie exactly halfway between the plus and minus five percent boundary lines. No more than five percent accuracy can be expected due to the error of the compressor maps. Although the instantaneous mass flow results generally follow the same trends, they do not match exactly due to the inherent transient behavior of the real system. However the integrated results, which average out the transient behavior, agree quite nicely.

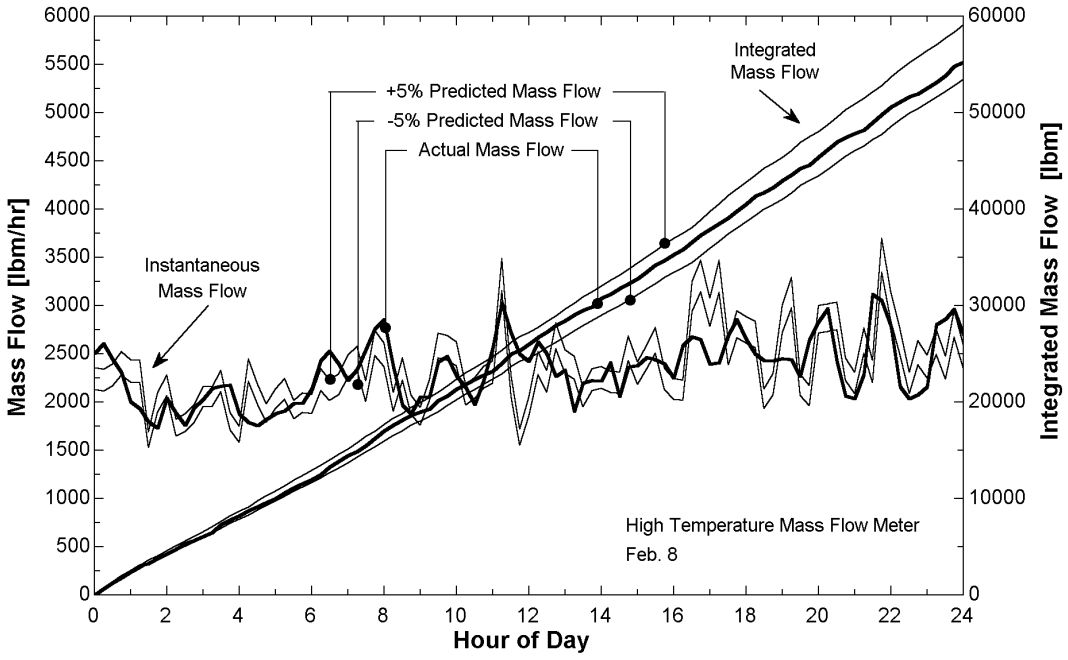


**Figure 3.1 High Temperature Mass Flow Meter Verification**

It is important to point out that the blow-by calibration variable only effects the mass flow through the high temperature flow meter as demonstrated in Figure 3.1. No such calibration variable exists to calibrate mass flow through the low temperature flow meter. Figure 3.2 displays the results of the February 8$^{th}$ simulation for the low temperature flow meter. The measured data are well within the allowable error of the model.

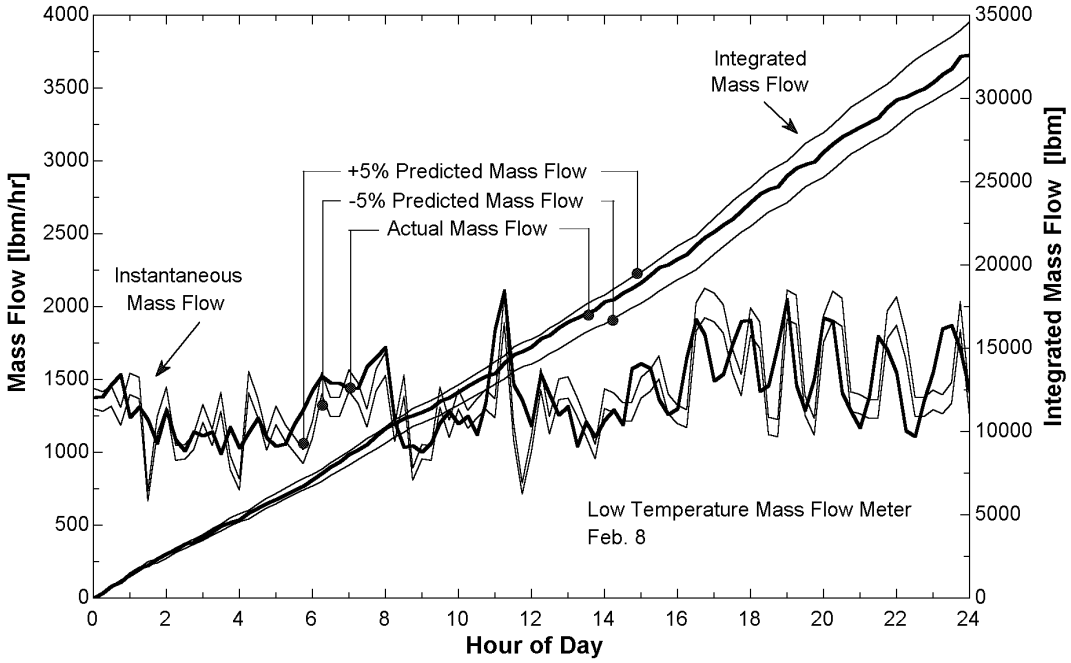


**Figure 3.2 Low Temperature Mass Flow Meter Verification**

Calibration of the mechanical room power for February 8th suggests an average value of 56 [kW] for the constant power draw from all devices except the compressors. This value includes all circulating pumps, lighting, computers, data acquisition equipment, and control panels. The calibration also averages the power required by the condenser fans over the day. The results of the simulation are displayed in Figure 3.3 in a format similar to that described in the previous mass flow plots.

An additional calculation was also plotted in Figure 3.3. The lower line is in fact the calibration variable, which is estimated by subtracting the calculated compressor power from the mechanical room total power recorded in the WEPCO demand power database. This plot shows a clear "bump" in the afternoon where due to the increasing load on the system, the condensing pressure started climbing and the condenser fans cycled on. The step increases in power are consistent with the size of the motors on the fans. This plot is a good indication that the compressor models are estimating power consumption accurately. It also suggests that the actual "constant" load calibration variable in the mechanical room might be better estimated below 50 [kW] for February 8th. This would

include the power draw from all the circulating pumps, and control panels etc… except the compressors and condenser fans.

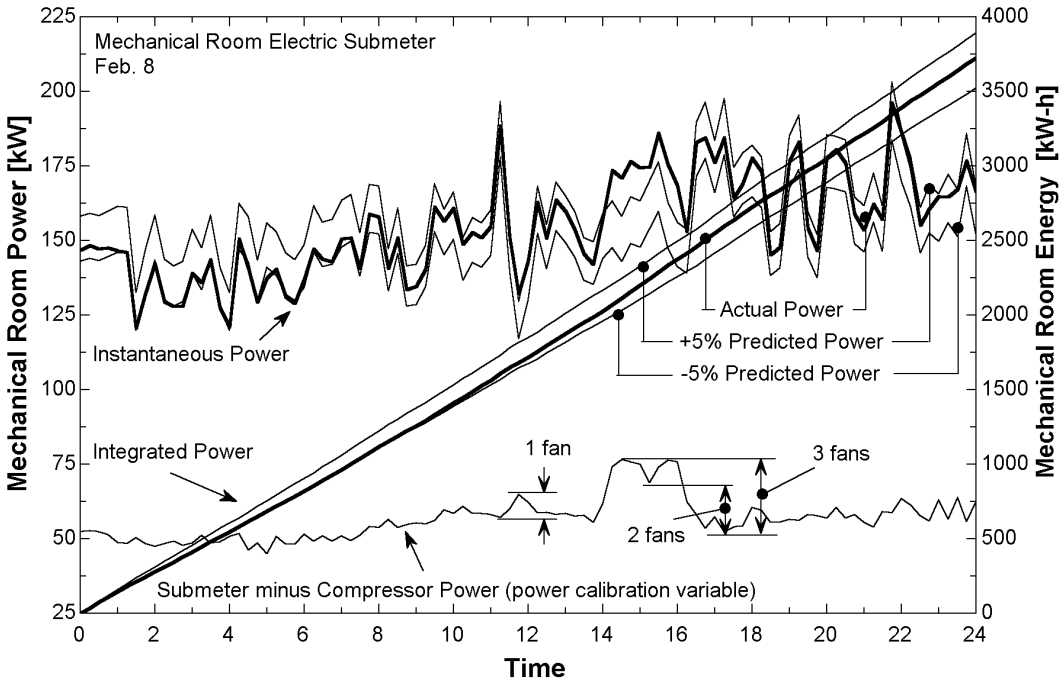


**Figure 3.3 Mechanical Room Electric Submeter Verification**

Figure 3.3 was re-plotted for January 12 in Figure 3.4 below. It is apparent from the nearly constant value of the power calibration variable curve at the bottom of the plot that the condenser fans did not have to cycle on much this day. The simulation of January 12 suggests that the power calibration variable is closer to 45[kW].

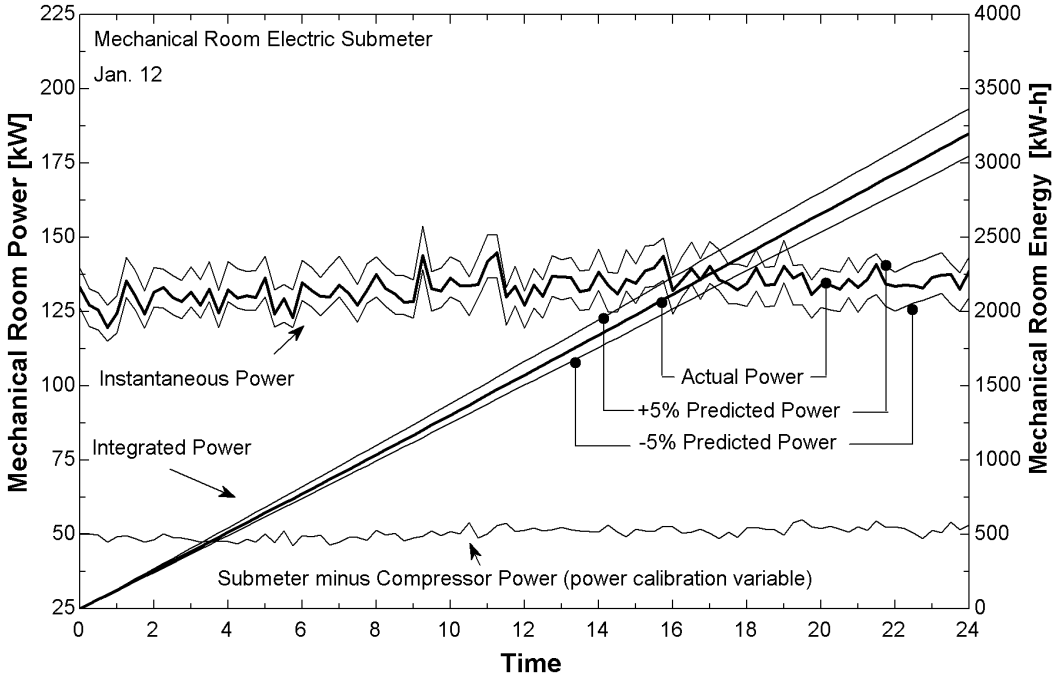


**Figure 3.4 January 12 Mechanical Room Electric Submeter**

Values for the calibration variables were calculated for January 12th, January 13th, February 8th, and February 12th and are displayed in Table 3.2.

| Day | Calibration Variable | |
|---|---|---|
| | Blow-By | Other Equip. Mech.Rm.Power |
| Tues, Jan. 12 | 6.5% | 45 [kW] |
| Wed, Jan. 13 | 6.5% | 46 [kW] |
| Mon, Feb. 8 | 10% | less than 50 [kW] |
| Fri, Feb. 12 | 20% | 37 [kW] |
| Mean | 10.8% | 43 [kW] |
| Std.Dev. | 6.4% | 4.9 [kW] |

**Table 3.2 Calibration Variables**

A good estimate of the system's mechanical room power calibration variable seems to be near 43 [kW] from January 12th and 13th and February 12th. February 8th was not used in the average calibration variable calculation because it was apparent in Figure 3.3 that the condenser fans were cycling on that day. Similar power plots showed that the fans did not cycle much on the other days. On the other hand, there is a large variance in the blow-by variable. This variability could be due to the fact that defrost for this system is on a time-

initiated and time-terminated schedule. Evaporator units are defrosted for the same amount of time each day. If, on a particular day the evaporator coils had less frost build up for whatever reason, perhaps there was not much infiltration from the loading dock doors that day, less hot gas would condense and the blow-by from the evaporator would increase.

One additional comparison was available to verify estimation of the mechanical room other equipment power calibration variable. The yearly simulation results of the entire mechanical room electrical energy [kWh] with the mechanical room other equipment power calibration variable set at a constant 43 [kW] can be compared with the actual mechanical room electrical energy [kWh] that was reported on the utilities performance tracking spreadsheet. Figure 3.5 below shows this comparison.

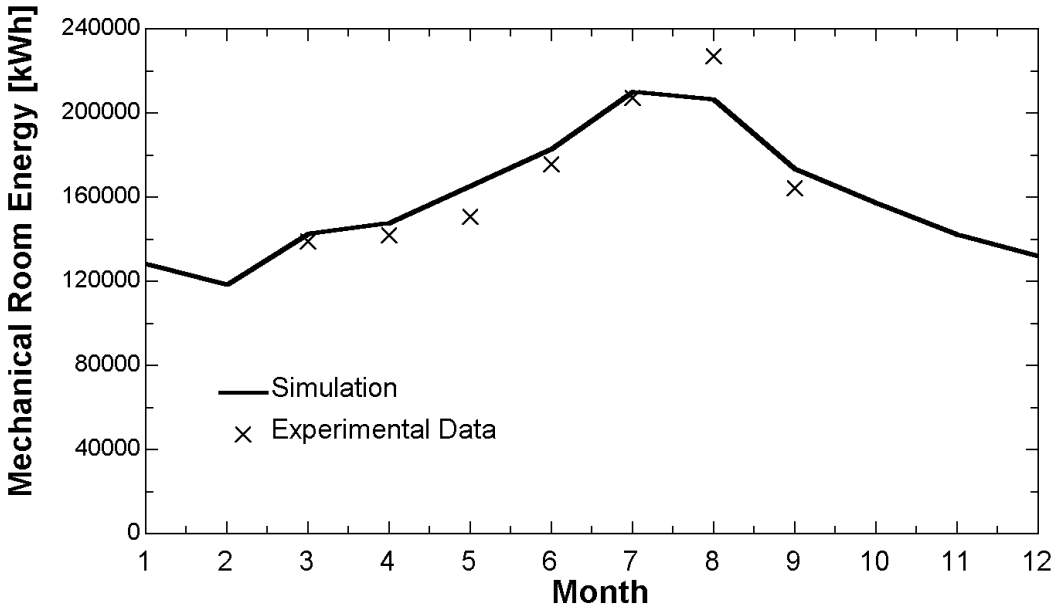


**Figure 3.5 Mechanical Room Power Comparison**

Table 3.3 below shows the results of the simulations from the four days when the blow-by and power calibration variables are held constant at 10.8% and 43[kW] respectively.

| | Mechanical Room Submeter | | | High Temp Flow Meter | | | Low Temp. Flow Meter | | |
|---|---|---|---|---|---|---|---|---|---|
| | kW-hr | | % diff. | lbm | | % diff. | lbm | | % diff. |
| | Observed | Calc | | Observed | Calc | | Observed | Calc | |
| Jan.12 | 3200 | 3265 | 2.0 | 48193 | 55059 | 14.2 | 29433 | 32036 | 8.8 |
| Jan.13 | 3242 | 3271 | 0.9 | 48660 | 55122 | 13.3 | 29400 | 31315 | 6.5 |
| Feb.8 | 3727 | 3459 | -7.2 | 55260 | 56808 | 2.8 | 32653 | 32959 | 0.9 |
| Feb.12 | 3308 | 3479 | 5.2 | 59037 | 55837 | -5.4 | 30561 | 31303 | 2.4 |

**Table 3.3 Simulation Comparison**

The results obtained from the electrical submeter comparison are in agreement with the assumption of a 43 kW fixed mechanical room electrical load. This is expected since the power required by the compressors is a function of pressure lift and can be directly calculated from the compressor maps. Direct measurements of suction and discharge pressure were available in the data acquisition database. Also, because of cold ambient outdoor conditions in January and February, the condenser fans do not run as often. This would support the hypothesis that the power draw from the mechanical room submeter is nearly constant except for the power required by the compressors. The only day with an error significantly over five percent is February 8$^{th}$. This is likely due to the fact that the condenser fans were indeed cycling on and off that day (See Figure 3.3). The fans would tend to increase the mechanical room power calibration coefficient, which explains the negative error shown in Table 3.3.

There were no calibration variables available to calibrate the refrigerant flow through the low temperature flow meter. A comparison between the calculated mass flow and the mass flow database showed the simulations agreed to within 10% of the calculated values. The main model parameter governing this low temperature flow meter comparison is the percent of full load capacity available from the compressor. This parameter is related to the position of the slide valve on the Vilter screw compressor. Assuming this reading has an error of ± 5% the results are well within an acceptable tolerance.

The final comparison to help validate the model components relates to the high temperature flow meter. Here the difference between the observed value and the calculated value varies as much as 14 percent. The flow through the high temperature flow meter changes as the defrost characteristics of the system change. More or less frost build up on the evaporator coils will change the amount of refrigerant that blows by coils in defrost. If there is more ice to melt on the coil, more of the hot gas will condense resulting in less blow-by. Defrost load changes the amount of refrigerant vapor that short circuits the high temperature flow meter and causes a large error in the comparison. The estimated range of the blow-by variable for the four days can be extracted from Table 3.2.

### 3.2.2 Load Calculation Verification

The average blow-by and power calibration variables discussed in the previous section were used to calibrate and verify the wet side of the refrigeration system. Those calibration variables were set to their constant average value shown in Table 3.2. To verify the load calculations or dry side of the refrigeration system, several more variables had to be estimated. The only experimental data available that involves the annual load on the system was the refrigeration effect data recorded in the performance tracking spreadsheet. The total amount of refrigeration [ton-hrs] produced by each compressor was available for the 1998 months March through September. The methodology to simulate the yearly performance of the system is discussed in Section 4.1.1. No experimental data is available for determining how the total load was split between the freezer, cooler, loading dock, banana/tomato rooms, and defrost. The following calibration variables have to be estimated for the load calculation verification:

- Interior Load Time Schedule
- Door Open Fractions
- Tomato Room Load
- Banana Room Load
- Freezer Interior Warming Room Load
- Freezer Hot Gas Defrost Space Load
- Loading Dock Air Defrost Space Load
- Cooler Hot Gas and Electric Defrost Space Load

Design interior loads are discussed in Section 2.5.3. All interior loads except the lights and warming room loads were assumed to be at design during second shift and at half design all other times. Second shift was defined as the hours between 3pm and midnight. The lighting load remained constant throughout the day at design levels. Door open fractions were determined by the method discussed in Section 2.5.2 and are listed in Table 3.4.

| Door Location | No. of 8'X10' Doors | Door Open Fraction |
|---|---|---|
| Freezer/Outside | 4 | 4/60 |
| Freezer/Cooler | 1 | 10/60 |
| Cooler/Outside | 1 | 10/60 |
| Cooler/Dock | 2 | 15/60 |
| Cooler/Warehouse | 2 | 12/60 |
| Dock/Outside | 4 | 5/60 |

**Table 3.4 Door Open Fractions**

Defrost thermal energy loads on the spaces were estimated from the load calculations performed by the mechanical contractor. Table 3.5 lists the estimated thermal energy that defrosting adds to the cold space. Values listed are design values. An operator of the system revealed that the evaporator units near the loading docks needed to be defrosted more frequently during the summer; consequently, the design load values are lowered slightly for months where the latent load from infiltration is small. The actual defrost load for each month was adjusted so the general trend of the recorded data was matched. Exact annual defrost load profiles are displayed in Appendix E.

| Cold Space Defrost Load | Design Value [MBH] |
|---|---|
| Hot Gas, Freezer | 72 |
| Hot Gas, Cooler | 180 |
| Electric, Cooler | 60 |
| Air, Loading Dock | 120 |

**Table 3.5 Estimated Space Loads as a Result of Defrosting**

The ASHRAE refrigeration handbook [ASHRAE Refrigeration Handbook, 1994] predicts that 50 percent or more of the total energy consumed during defrost is lost to the space. The rest goes to melting ice and warming the internal mass of the evaporator. This 50 percent ratio, along with the cold space defrost load estimates in Table 3.5, is used to determine the total amount of hot gas required for defrosting.

Once the defrost load on the freezer is estimated, the amount of energy added to the freezer space from the warming rooms is adjusted until the annual load profile looks reasonable and matches with the experimental data. The calibration results in a warming room load of 120 MBH throughout most of the year with it increasing to 156 MBH during the summer months of June, July, and August. This calibration load might also account for any extra internal loads not accounted for in the design load calculations. This high of a warming room load might be expected since often times the thermostats in these room are set very high for a "quick thaw at break". Also, as an operator of the system observed, sometimes the doors between the warming rooms and the cold space are left wide open when the workers return to their jobs after break.

The load from the banana and tomato rooms is determined in the same manner as the warming room load. After the cooler defrost load was estimated, the loads on the banana and tomato rooms are adjusted until the annual load profile matches the experimental results. The resulting loads for the banana and tomato rooms was 40.5 [tons]. This value might also account for any discrepancies between the design internal loads estimated by the mechanical contractor and the actual operation of the warehouse. The design load for the banana and tomato rooms which was estimated in the load calculations of the mechanical contractor is 90.3 [tons]. An average annual load of 40.5 [tons] is not unreasonable since the fruit is ripened in individual batches and there is usually only 10-15 percent of the fruit peaking at any given time. Occasionally, when demand for bananas is high as during sale promotions, the load could increase to near design conditions.

### 3.2.3 Load Verification Results

The model simulated an average day from each month of the year and the high and low temperature refrigeration loads [ton-hrs] were compared to the average daily refrigeration load from the experimental data for the months between March and September, 1998. The results are shown in Figure 3.6 and Figure 3.7.

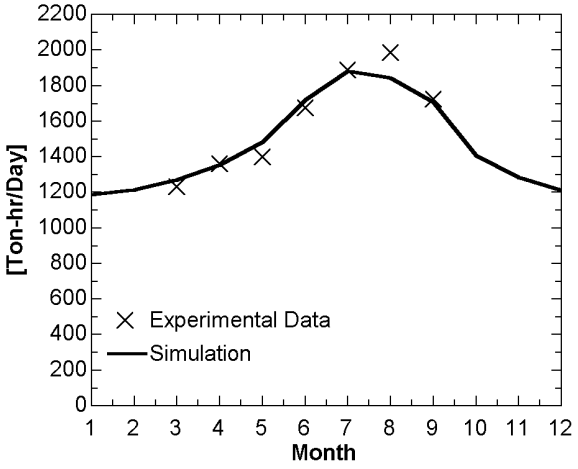


**Figure 3.6 High Temperature Load**

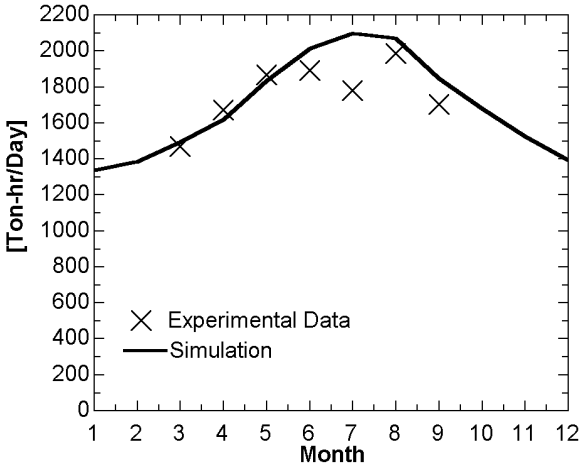


**Figure 3.7 Low Temperature Load**

In general, the profile of the simulation curve matches the trend of the experimental data points. The two notable exceptions are the month of August for the high temperature load and the month of July for low temperature load. The discrepancy of the high temperature August load equates to an underestimation of the banana and tomato room loads of six tons. This could easily be explained by a simple 15% increase in the demand for bananas and/or tomatoes that month. The difference between the simulated and experimental data for the low temperature load in the month of July is a little larger at 13 [tons]. No reasonable explanation for the rather odd dip in the July load could be recalled by an associate of WEPCO. One possible explanation could be that the warming room heaters were shut off at the very end of June and then turned back on at the beginning of August. In these months, it would be warm enough outside for workers to spend their "quick thaw" break outdoors. This would account for the 13 [ton] discrepancy in July as well as the small discrepancies in June and August.

## 3.3 Modeling Conclusions

### 3.3.1 Temperature / Pressure Measurement Disagreement

Discrepancies in experimental data were noticed in the process of developing the model. The data acquisition system database contains experimental data from thermocouples in both the intermediate and low pressure receivers as well as pressure measurements in the

compressor suction header lines. The calculated saturation temperature corresponding with the pressure measurement should be very close to the temperature measured by the thermocouples since the piping section between the receivers and header lines is oversized and has very little pressure drop. Figure 3.8 plots the temperature recorded with the thermocouples with the temperature in the receiver calculated by the saturation temperature of the refrigerant at the pressure of the suction header minus the small calculated pressure drop in the piping between the receiver and suction header.

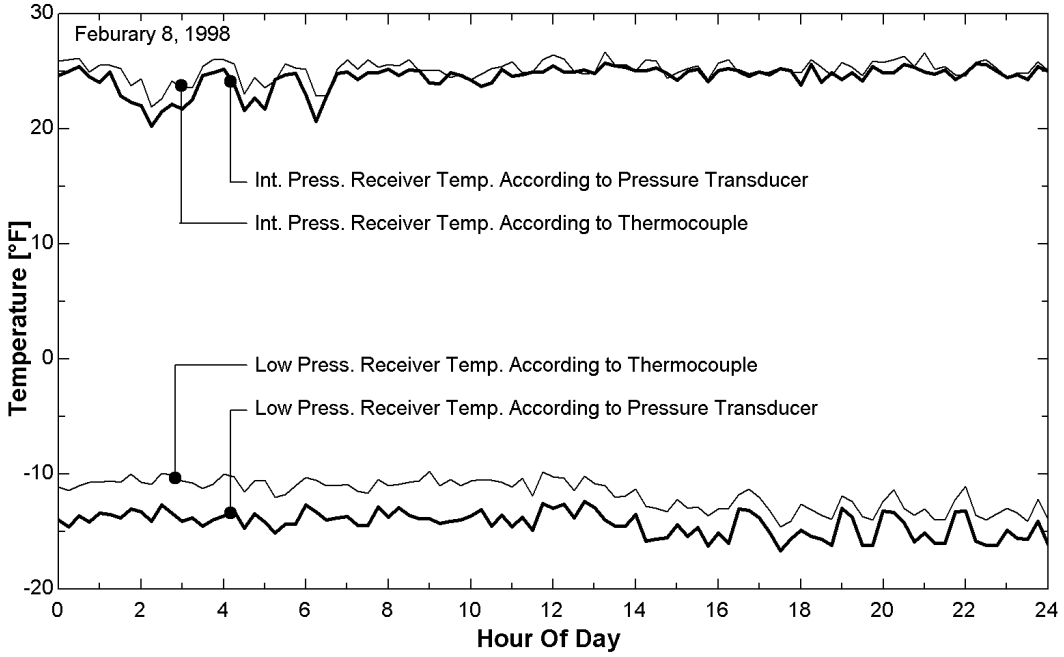


**Figure 3.8 Pressure/Temperature Discrepancy**

The typical precision at 25°F saturated ammonia conditions for thermocouples and pressure transducers is ±0.1-5°F and ±0.03-0.15 psi respectively [ASHRAE Fundamentals, 1989]. At typical operating conditions, pressure transducers give more precise measurements. The intermediate pressure receiver's thermocouple is generally within the typical ±1°F accuracy of a thermocouple. The low pressure receiver's thermocouple always recorded temperatures three to four [°F] above what the pressure transducer was reading and obviously needs to be re-calibrated.

### 3.3.2 Error Analysis

An uncertainty analysis was performed for several "design" parameters of the system to identify critical spots in the refrigeration system. The method for determining this

uncertainty propagation is described in NIST Technical Note 1297 [Taylor B.N. and Kuyatt, C.E., Guidelines for Evaluating and Expressing the Uncertainty of NIST Measurement Results, National Institute of Standards and Technology Technical Note 1297, 1994]. The parameter subjected to the uncertainty analysis was the overall power demand of the system [kW] since this system indicator parameter gives a good bottom line look at cost of operating the overall system. The uncertainty analysis was done twice. Once for the system's design loads which occur in July and once for the average day in January to give an idea of the effect of each parameter has on the system given the time of year. Table 3.6 is a summary of the partial derivatives of the system indicator parameter (Total System Power [kW]) with respect to the selected "design" parameters. For instance, the partial derivative of the *total power* with respect to the *blow-by* fraction of hot gas in the cooler evaporator is 22.6 for the design load calculations. Equation (3.2)

$$22.6 = \partial_{total\ power} \Big/ \partial_{blow-by,cooler} \tag{3.2}$$

| Partial Derivative Denominator Parameter | Design Day | | January Day | |
|---|---|---|---|---|
| | Model Setting | Total System Power [kW] | Model Setting | Total System Power [kW] |
| Blow-By Fraction Cooler | 0.1075 | 22.6 | 0.1075 | 15.1 |
| Blow-By Fraction Freezer | 0.1075 | 9.1 | 0.1075 | 6.3 |
| Discharge Pressure Drop [psia] | 4 | 1.3 | 4 | 0.8 |
| High Temp Suction Pressure Drop [psia] | 0.41 | 2.7 | 0.11 | 1.3 |
| Low Temp Suction Pressure Drop [psia] | 1.12 | 5.2 | 0.28 | 1.7 |
| Cooler WSR Temp. Drop [°F] | 3 | 4.1 | 3 | 1.9 |
| Dock WSR Temp. Drop [°F] | 3 | 0.2 | 3 | 0.1 |
| Freezer WSR Temp. Drop [°F] | 2 | 4.7 | 2 | 2.3 |
| Outside/Freezer Door Open Fraction | 4/60 | 597.5 | 4/60 | 43.6 |
| Cooler/Freezer Door Open Fraction | 10/60 | 5.8 | 10/60 | 5.2 |
| Outside/Cooler Door Open Fraction | 10/60 | 56.7 | 10/60 | 0 |
| Loading Dock/Cooler Door Open Fraction | 15/60 | 2 | 15/60 | 1.8 |
| Warehouse/Cooler Door Open Fraction | 12/60 | 42.6 | 12/60 | 15.4 |
| Outside/Loading Dock Door Open Fraction | 5/60 | 150.8 | 5/60 | 0 |
| Condensing Pressure [psia] | 165 | -0.42 | 134 | 0.8 |
| Int. Press. Receiver Temp. [°F] | 23 | 1.1 | 23 | 0.5 |
| Low Press. Receiver Temp. [°F] | -12 | 1.9 | -12 | 1.6 |

**Table 3.6 Partial Derivatives from Uncertainty Propagation Analysis**

The relative size of these partial derivatives gives an indication of the parameter's influence on system performance. A high positive partial derivative indicates that increasing that particular "design" parameter value will increase the overall power consumption of the system. A high negative number would decrease the overall power consumption.

Caution should be used when utilizing the values presented in Table 3.6. All the set values for the "design" parameters except for the condensing pressure are about an order of magnitude smaller than the total system power [kW] value. Even if the partial derivative value is large, a large change in the design parameter must be made in order to affect the total system power significantly. For instance, a 50 percent change in the blow-

by parameter results in only a 0.3 and 0.4 percent change in the total system power for the design load and January load respectively.

Further analysis of Table 3.6 leads to several conclusions:

- The infiltration from doors that lead to the outside has the highest impact on the overall power requirements of the system of the "design parameters" looked at. The colder the space the higher the impact.
- Improperly controlled or installed hot gas defrost that increases the amount of vapor refrigerant passing through the evaporator coil increases the power demand of the system by falsely loading the compressor.
- Pressure drops in suction and discharge lines all contribute to higher power requirements. Pressure drops in suction lines have more of an impact than in discharge lines.
- Proper control of refrigerant temperature and head pressure can also have a significant effect on the power consumption of the system.

# *Chapter 4 -System Baseline Operation*

## 4.1 12-Month Simulation

In order to investigate the performance characteristics of a system, a baseline of operation first needs to be established. Also, it is important explore the behavior of the system at maximum load as well as part load conditions which it operates at most of the year. An appropriate way to do this is to simulate the system for an entire year. The baseline simulation attempts to emulate the operating strategies used in the actual system between the months of January 1998 and January 1999.

### 4.1.1 Methodology

#### 4.1.1.1 Unsuccessful Attempts

The first attempt to do a 12-month simulation of the system was to force the model with hourly outdoor weather data for each of the 8,760 hours. Unfortunately, as loads increased beyond the capacity of a single compressor, the model experienced convergence problems as control logic was introduced to cycle on an additional compressor. This every-hour approach also demanded significant computational time.

A second attempt at simulating a full years worth of outdoor weather conditions used a bin approach. Similar outdoor conditions could be placed in a bin identified by the average conditions and the yearly data could be summarized in several individual calculations. However, this quickly proved to be a fruitless effort. The load and performance of a refrigerated warehouse with evaporative condenser depends upon three outdoor air conditions; dry bulb temperature, wet bulb temperature, and solar irradiation. Dry bulb and irradiation have the most significant impact on the warehouse load where as the wet bulb is a strong factor in determining the performance of the system because of the evaporative condenser's performance dependence on the outdoor wet bulb. Unfortunately, due to the thermal capacitance of the warehouse construction, there is a time lag between the effects of the current wet bulb temperature and the dry bulb/solar irradiation effects which can not be captured with binned weather data.

#### 4.1.1.2 Successful Attempt

The final and successful approach to model the system for 12 months employed the use of a weather generating software package called Extremes [Schmidt]. With this software hourly dry bulb, wet bulb, and irradiation data for an average day of each month of the year could be generated. Also, to capture the peak load of each month, which would help in quantifying electrical demand charges for the system, the Extremes software was used to generate the maximum day for each month.

After hourly data of average and maximum weather conditions were identified for each month, the warehouse wall transmission load was simulated using the techniques described in Section 2.5.1. The simulation for each weather profile was carried out until a quasi-steady state heat flux through the walls could be matched with the appropriate outdoor wet bulb condition. This matching allowed the model to incorporate the time lag between the dry bulb/irradiation, and wet bulb effects.

The entire year can be simulated with 24 separate weather profiles; one average and one maximum profile per month. To find the total load for the entire year, the results for the average day are multiplied by the number of days in the month and then the months are summed to give the yearly total. The maximum system demand for each month can be quantified by simply simulating all 12 of the maximum weather profiles and picking the maximum hour from each.

In the actual operation of the system, the VSS 451 single screw compressor meets the low temperature load and the VMC 4412 reciprocating compressor meets the high temperature loads most of the year. During the very warm and humid weeks of July and August the low temperature system load frequently exceeds the capacity of the VSS 451 compressor. In this case a larger VSS 751 is available and it is used instead of the VSS 451. According to an associate from WEPCO, the 751 sees less than 2000 hours of operation per year. In the simulation using the model, the 751 compressor model was

used in place of the 451 when the capacity of the 451 was exceeded. This happened between noon and midnight in July and August when the average days were being simulated and for the entire day during the months of June through September when the maximum days for each month were being simulated.

## 4.2 Baseline Operation

### 4.2.1 System Layout

The system components in the model used to calculate the baseline operation are configured in the same way as the actual warehouse facility. This includes the use of liquid overfeed evaporators for the freezer, cooler, and loading dock, and direct expansion evaporators in the banana and tomato rooms. Vapor from the low and intermediate pressure receiver vessels is compressed by a single-stage compression process to a common evaporative condenser. A detailed description of the system is provided in Section 1.4.

### 4.2.2 Control Strategies

Control strategies to obtain the baseline were also selected to closely emulate the control of the system as it was operated in 1998.

- The condenser water pump is shut off when the outdoor dry bulb temperature is below 31°F.
- Head pressure is set at a minimum of 130 psia and allowed to float up as the load increases during the summer months. Condenser fans are cycled on one at a time in increments of four psi above the minimum to maintain the head pressure as close to the minimum as possible. The condenser was oversized for the system and consequently the head pressure remains at its first fan cycling set point of 134 psia most of the year. 130 psia was selected as the minimum head pressure because the back-pressure regulators for the direct expansion evaporators have control problems if the head pressure is set any lower.
- Constant set point temperatures of 23°F and –12°F were maintained in the intermediate and low pressure receiver vessels respectively. A fluctuation of 2 or 3 degrees in the intermediate and low pressure receivers is not uncommon due to the

dead bands associated with the actual control strategies of the compressors (See Figure 3.8).

- Evaporators are assumed to have two fans each. Both fans are cycled on and off together as the load on the space warrants. The load is assumed to be equally distributed among all evaporator units in the space.
- Defrost loads are kept nearly constant though out the year with a small increase in the summer to reflect the time clock control strategy currently in place. Defrost loads are estimated using the reasoning detailed in Section 3.2.2.
- The calibration variables of defrost blow-by, mechanical room power, warming room load, and banana/tomato room load are discussed in Section 3.2. They are set at their average values also discussed in that section.

### 4.2.3 Characteristic Performance Indicators

Two useful parameters of a refrigeration system that help indicate the performance are the quantity of useful cooling [ton-hrs] and the amount energy consumed in order to produce the cooling [kWh]. It is also useful to itemize these quantities for each conditioned space or load. The performance of a system transferring heat at a very low temperature/pressure is different from that of one operating at a higher suction pressure. One way of characterizing a cold storage warehouse facility is to list the entire load on a square foot basis. This number characterizes the use of the facility. High loads per square foot could indicate poor wall and roof insulation, heavy traffic or activity in and out of the cold space, or high product loads. Another useful indicator of system performance is to track how much power is required to deliver a certain amount of cooling. This number will change drastically based upon the temperature the heat is transferred at and how the system is configured. It is interesting to analyze how much energy [kWh] it takes to produce one ton-hr of cooling at 0°F and compare it to how much it takes for one ton-hr at 34°F. The coefficient of performance (COP) is defined as the dimensionless ratio of cooling capacity to power. This ratio is another parameter used to compare system performance. Finally, systems can be characterized on a monetary basis. The cost per square foot to operate the facility and cost per ton-hr of cooling are bottom-line dollar figures that can be used to gauge system performance.

### 4.2.4 Results

Table 4.1 lists some baseline performance parameters of the system. The table reports performance for both the high and low temperature loads of the system. High temperature loads include the cooler, loading dock, and the banana/tomato rooms since the vapor generated by these loads is sent to the intermediate pressure receiver. The only low temperature load is the freezer load.

| Performance Measures | High Temperature | Low Temperature | Combined |
|---|---|---|---|
| ton-hr / ft²-yr | 19.4 | 11.6 | 15.2 |
| kWh / ton-hr | 1.2 | 1.8 | 1.4 |
| COP | 3.0 | 1.9 | 2.4 |
| hp/ton | 1.6 | 2.5 | 1.9 |
| hp(comp.)/ton | 0.9 | 1.6 | 1.2 |
| hp(cond.)/ton | 0.1 | 0.2 | 0.2 |
| hp(evap.)/ton | 0.2 | 0.3 | 0.2 |
| OnPeak kWh / yr | 379107 | 426176 | 805271 |
| OffPeak kWh / yr | 655582 | 736493 | 1392118 |
| Peak kW | 194.4 | 218.4 | 412.8 |
| $ / ft² -yr | $0.92 | $0.88 | $0.90 |
| $ / cu.ft -yr | $0.05 | $0.04 | $0.04 |
| $ / ton-hr -yr | $0.05 | $0.08 | $0.06 |
| $ / yr | $42,158 | $47,402 | $89,667 |

**Table 4.1 Baseline System Performance Statistics**

The performance parameters are defined in the following way.

**ton-hr / ft²-yr:** The ratio of actual cooling delivered by the system in a year over the floor area of the cold space. High temperature loads include cooler, loading dock, and banana/tomato room loads. The low temperature load is the freezer load.

**kWh / ton-hr:** The ratio of electrical energy consumed in a year over the total amount of cooling produced by the system. High temperature energy includes fan energy from the cooler, dock, and banana/tomato rooms, a fraction of condenser fan and pump energy proportional to the heat rejected from the high temperature compressor, half of the "other" equipment in the mechanical room energy, and the fraction of the high temperature compressor electrical energy due to the high temperature loads, the vapor load from defrosting the cooler, and the recip. compressor oil cooling load. The low temperature energy includes freezer fan energy, the other half of the "other" equipment

energy in the mechanical room, the low temperature compressor energy, and a fraction of the high temperature compressor energy proportional to the amount of load placed on that compressor by the flash gas generated as the low temperature refrigerant is throttled to the intermediate pressure and the defrost vapor load introduced by defrosting the freezer evaporators.

**COP:** A dimensionless ratio of delivered system capacity [ton-hr] per year over electrical energy [kWh] used. Also referred to as the first law efficiency of the system.

**hp/ton:** The average of the instantaneous ratio of total system power over cooling load for each hour of the simulation. High temperature total system power includes power from all cooler, dock, and banana/tomato room evaporator fans, a fraction of condenser fan and pump energy proportional to the heat rejected from the high temperature loads, high temperature compressor power, and half of the "other" mechanical room power. The cooling load for the high temperature calculation is the sum of cooler, dock, and banana/tomato room loads. Low temperature total system power includes power from the freezer evaporator fans, a fraction of condenser fan and pump energy proportional to the heat rejected from the low temperature load, low temperature compressor power, and half of the "other" mechanical room power. The cooling load for the low temperature calculation is the freezer load.

**hp(comp.)/ton:** This ratio is calculated in the same manner as the hp/ton ratio above. However, it separates the compressor power of the system out from the rest of the energy consumed allowing the direct examination of system compressor performance. The denominator of this ratio is defined the same as in the hp/ton ratio above. The high temperature compressor power also incorporates the compression of the flash gas generated by the low temperature refrigerant stream as it is throttled to the intermediate pressure.

**hp(cond.)/ton:** This ratio is like the hp(comp.)/ton ratio above except now a direct examination of the condenser power is made. Condenser power is proportioned between the high and low temperature loads in the same proportion of the high and low temperature loads.

**hp(evap.)/ton:** This ratio is like the hp(comp.)/ton ratio above except now a direct examination of the evaporator power is made.

**OnPeak kWh / yr:** The total number of kWh required throughout the year during the OnPeak hours of 8am to 8pm Monday through Friday. Electrical energy [kWh] is divided into the high and low temperature columns similar to the way it is done in the kWh / ton-hr ratio.

**OffPeak kWh / yr:** The total number of kWh required throughout the year during the OffPeak hours of 8pm to 8am Monday through Friday and all day on the weekends. Electrical energy [kWh] is divided into the high and low temperature columns similar to the way it is done in the kWh / ton-hr ratio.

**Peak kW:** This is the highest electrical demand during on-peak hours for the entire year. This would typically happen in the late afternoon some time in July or August for most systems.

**$ / ft² -yr:** This ratio is the cost of electrical energy over the gross floor area of the cold space for the entire year. Electrical energy [kWh] and demand [kW] is divided into the high and low temperature columns similar to the way it is done in the kWh / ton-hr ratio.

**$ / cu.ft -yr:** This ratio is the cost of electrical energy over the gross interior volume of the cold space for the entire year. Electrical energy [kWh] and demand [kW] is divided into the high and low temperature columns similar to the way it is done in the kWh / ton-hr ratio.

**$ / ton-hr –yr:** This ratio is the same as the $/ft²-yr ratio except the total cost to operate the equipment for the cold space is divided by the total cooling load met for the year in that space.

**$ / yr:** This is the electrical energy cost associated with running the refrigeration equipment in the warehouse.

Electrical cost is calculated on a monthly schedule from four parameters dealing with electrical usage. The first two parameters are the on-peak and off-peak energy charges. This is the total amount of electricity [kWh] consumed during on or off-peak hours. The charge is $0.0327 and $0.0203 per kWh for on and off-peak respectively. The third charge is referred to as the billing demand charge. This is the peak demand electrical load [kW] in the month that occurs during the on-peak hours Monday through Friday. The cost for billing demand is $8.24 per kW. The final electrical charge is referred to as the

customer demand charge. This is a monthly charge based on the highest electrical demand reached in the last 12 months of operation. The customer demand charge is $0.65 per kW. These electric rates are assumed constant for the whole year.

# *Chapter 5 -Alternative System Designs*

## 5.1 Design Alternatives

### 5.1.1 Condenser Selection

The two main types of condensers used in refrigeration systems are air-cooled and water-cooled. The saturated condensing temperature/pressure of the system must be maintained at a temperature above the outside air dry bulb when using air-cooled condensers. This generally leads to high system head pressures and increased compressor horsepower to provide the higher pressure lift. Systems that utilize water cooled condensers can typically operate at much lower saturated condensing temperature/pressures because the evaporative processes occurring with the cooling water are closer to the outside air wet bulb temperature. However, additional system capital investments such as water conditioning equipment and cooling water pumps are needed to operate the cooling water part of the system. Industrial refrigeration systems typically need to reject a very large amount of heat and the significant amounts of compressor horsepower saved by operating at lower head pressures justifies the extra cost for cooling water equipment. Also, water-cooled condensers need much less heat transfer area due to the increase in convection heat transfer coefficient by using a wetted surfaces instead of a dry one. Cooling water condensers should be used in industrial refrigeration applications.

There are two main types of water cooled condensers, evaporative and shell-and-tube. Evaporative condensers are described in Section 2.4.2. They are most commonly used when a stand-alone refrigeration system is needed. Evaporative condensers have the advantage of being able to operate dry when the outside air dry bulb temperature is sufficiently low (generally below the freezing point of water). Shell-and-tube water cooled condensers are used when a facility has a large quantity of cooling water already available such as from a river, lake, or cooling tower. Extremely large refrigeration plants (>5,000 tons) with many compressors may also warrant the use of cooling towers with

shell-and-tube condensers in order to reduce the number of individual evaporative condensers needed to reject the total heat load.

### 5.1.2 Liquid-Suction Heat Exchangers

Liquid suction heat exchangers are generally installed in halocarbon refrigeration systems with the goal of increasing the capacity of the refrigeration system. Cold suction gas is used to subcool the warm refrigerant leaving the condenser. As a result, less flash gas is generated in the expansion process and the useful refrigeration effect of the refrigerant stream entering the evaporator is increased. A penalty on the system is generated by this heat exchanger as it superheats the suction line gas and imposes a pressure drop on both suction and liquid lines. Superheat causes the volumetric efficiency of the compressor to decrease. Correspondingly, the capacity of the system drops. Liquid-suction heat exchangers are advantageous to use when the capacity benefit from subcooling exceeds the capacity penalty from the decreasing volumetric efficiency of the compressor as a result of pressure drop and superheating.

The advantage of liquid-suction line heat exchangers is highly dependent upon the type of refrigerant used [Klein et al, 2000]. In fact, with some refrigerants such as ammonia (R-717), capacity and efficiency of the system is reduced by adding liquid-suction heat exchangers. They are only mentioned in this section of the paper to point out that liquid-suction heat exchangers are not suitable for ammonia refrigeration applications.

### 5.1.3 Single-Stage Compression

Single-stage compression is most commonly used in single temperature applications with moderate to high suction temperatures. For ammonia systems with evaporative condensers, moderate to high suction temperatures are considered to be above 0°F. However, systems with screw compressors can have single-stage compression with suction temperatures well below 0°F. Screw compressors can handle lower suction temperatures because their allowable compression ratio (absolute discharge pressure / absolute suction pressure) can be as high as 24:1 where as a reciprocating compressor's maximum allowable compression ratio is 8:1. The difference in maximum allowable

compression ratios between screw and reciprocating compressors is due to mechanical design and oil cooling constraints between the two machines.
Single temperature applications typically have simple system designs and leave little room for exploring alternative component arrangements to optimize system performance.

### 5.1.4 Two-stage Compression

Two-stage compression is a possible alternative system design when high pressure lifts are required such as in low temperature applications (below 0°F for ammonia). By using two or more stages of compression, with provisions for cooling the discharge vapor back to near saturation after each stage, the total compression process more closely approximates an isothermal compression process instead of an isentropic compression process. Less work is required to compress a vapor isothermally than isentropically [Stoecker,1986]. Figure 5.1 shows a T-s diagram of a two-stage compression process, the compressor work saved by utilizing two compression stages is the shaded region. Figure 5.1 also demonstrates that much less superheat is generated with two-stage compression which helps reduce scaling in evaporative condensers. With two-stage compression, it is also important to mention that the system requires the use of two compressors which significantly adds to the initial cost of a system unless two compressors are already available because the system has a load at an intermediate temperature. The high stage compressor will however need to be sized to handle the increased volumetric flow from both the high and low temperature loads.

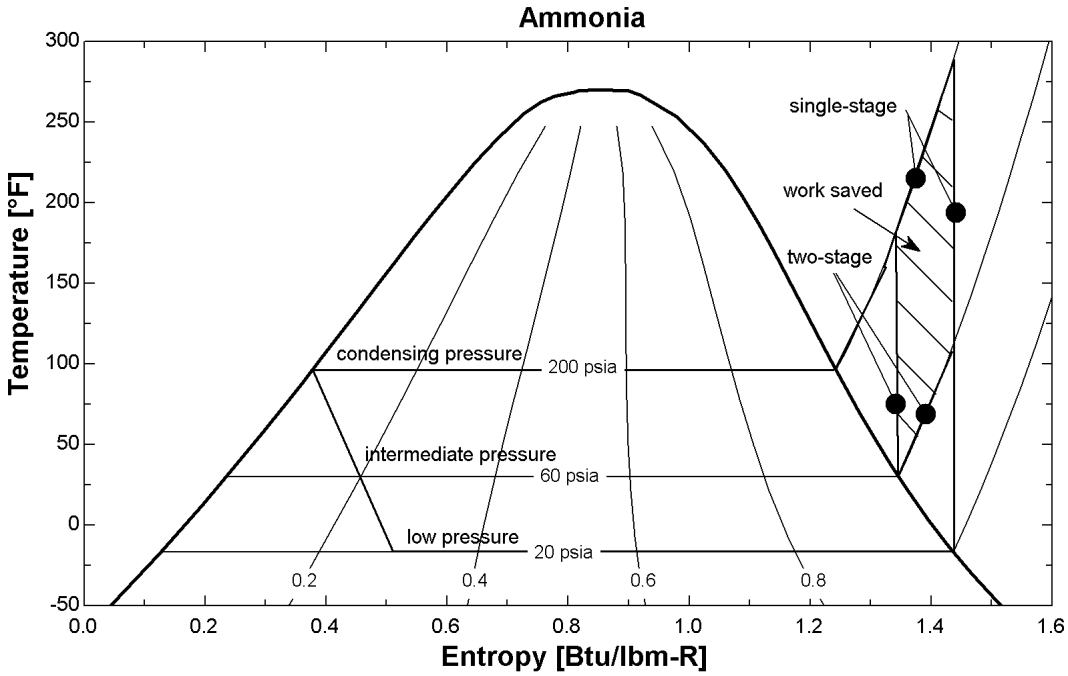


**Figure 5.1 Two-Stage vs. Single-Stage Work Savings (T-s diagram)**

### 5.1.5 Thermosiphon Cooling

In refrigeration applications where the load requires a relatively high refrigerant temperature, the possibility of using a thermosiphon system is an attractive alternative system design. In systems with evaporative condensers, the required refrigerant temperature must be at least 10°F above the outside air wet bulb temperature in order to provide sufficient temperature differences to exchange heat with the environment. In thermosiphon systems, saturated refrigerant is circulated through a system using its natural buoyancy characteristics. Vapor is cooled and condensed in the evaporative condenser. The dense liquid refrigerant "sinks" to the evaporator where it is boiled back to a vapor. The vapor bubbles, which are nearly 300 times less dense that the surrounding liquid, rise back up to the condenser pushing some of the liquid refrigerant along and the cycle begins again. No compressor is needed to circulate the refrigerant. In geographical regions that experience low wet bulb temperatures most of the year, refrigeration at high COP can be supplied by a properly designed thermosiphon system to high temperature loads such as fruit ripening applications.

## 5.2 Evaporative Condenser Over-sizing Penalty

At maximum load conditions, which occur at 5pm on the maximum July day, the evaporative condenser must reject approximately 3.3 million btu/hr. Using a design condensing temperature of 95°F and design wet bulb of 75°F, the current evaporative condenser (Evapco model# PMCB-885) can reject 10.2 million btu/hr. It was sized 3 times the size it had to be in anticipation of future system expansion. The PMCB-885 evaporative condenser can also be identified as having an 85°F design condensing temperature. Over-sizing the evaporative condenser produces two opposing energy consumption effects on the system. It allows the compressors to operate at a lower head pressure reducing the horsepower required by the compressors. It also requires more energy to operate since the condenser fan motors and cooling water pumps are all oversized along with the unit.

An evaporative condenser sized for a 95°F design condensing temperature is Evapco model# PMCB-295. Instead of 30 and 15 hp motors is has 10 and 5 hp motors. The horsepower of the cooling water pump drops from 25 to 3. A yearly simulation was run with the smaller evaporative condenser. Results are compared in Table 5.1. Definitions of the performance measures are provided in Section 4.2.4.

| Performance Measures | 85°F Design Condenser | | | 95°F Design Condenser | | |
|---|---|---|---|---|---|---|
| | High Temperature | Low Temperature | Combined | High Temperature | Low Temperature | Combined |
| ton-hr / ft²-yr | 19.4 | 11.6 | 15.2 | 19.4 | 11.6 | 15.2 |
| kWh / ton-hr | 1.2 | 1.8 | 1.4 | 1.1 | 1.8 | 1.4 |
| COP | 3.0 | 1.9 | 2.4 | 3.1 | 2.0 | 2.5 |
| hp/ton | 1.6 | 2.5 | 1.9 | 1.5 | 2.4 | 1.9 |
| hp(comp.)/ton | 0.9 | 1.6 | 1.2 | 1.0 | 1.6 | 1.2 |
| hp(cond.)/ton | 0.1 | 0.2 | 0.2 | 0.1 | 0.1 | 0.1 |
| hp(evap.)/ton | 0.2 | 0.3 | 0.2 | 0.2 | 0.3 | 0.2 |
| OnPeak kWh / yr | 379107 | 426176 | 805271 | 371417 | 414182 | 785604 |
| OffPeak kWh / yr | 655582 | 736493 | 1392118 | 641522 | 715164 | 1356681 |
| Peak kW | 194.4 | 218.4 | 412.8 | 198.0 | 221.8 | 419.7 |
| $ / ft² -yr | $0.92 | $0.88 | $0.90 | $0.90 | $0.85 | $0.88 |
| $ / cu.ft -yr | $0.05 | $0.04 | $0.04 | $0.05 | $0.03 | $0.04 |
| $ / ton-hr -yr | $0.05 | $0.08 | $0.06 | $0.05 | $0.07 | $0.06 |
| $ / yr | $42,158 | $47,402 | $89,667 | $41,452 | $46,102 | $87,659 |

**Table 5.1 Over-sized Condenser Comparison**

As shown in Table 5.1, the required compressor horsepower was smaller and evaporative condenser horsepower was higher for the over-sized condenser as predicted. For this particular system, using a smaller evaporative condenser results in an energy savings of 55,000 kWh or $2,000 per year. In both simulations, head pressure was allowed to float to a minimum pressure of 130 psia. The maximum head pressure that occurred during the year for the systems with 85°F and 95°F design condensing temperature was 160 psia and 197 psia respectively. If head pressure is not allowed to float, but rather set at an artificially high pressure as done in some industrial refrigeration systems because of a lack of a control system, there would be no compressor horsepower savings by over-sizing the condenser. The penalty for over-sizing a condenser for a system with elevated, set head pressure control would be even larger. If head pressure was controlled to an optimum the savings would be even larger and yet even more savings could be realized with optimum head pressure control if the condenser was left over-sized as examined in Section 6.2.5.

## 5.3 Two-Stage Compression System Arrangement

The facility that was modeled has intermediate and low pressure receivers to supply approximately 23°F and –12°F refrigerant to the cooler and freezer spaces respectively. However, it uses single-stage compressors from both the intermediate and low suction temperatures. This system seems like a likely candidate for two-stage compression. After simulating a two-stage system, it was learned that, due to a combination of compressor unloading characteristics and relatively small pressure lift requirements, the system would actually operate less efficiently with a two-stage compression system with flash intercooler. Flash intercooling is accomplished in most systems by simply bubbling the discharge gas from the low stage (booster) compressor(s) through the liquid in the intermediate pressure receiver vessel.

### 5.3.1 Simulation Results

The comparison between system performance measures of a single-stage and two-stage compression system is shown in Table 5.2. Definitions of the performance measures and electricity costs are provided in Section 4.2.4. In both systems, a floating, minimum head pressure algorithm is used. Also, the high suction temperature compressor is a

reciprocating compressor and the low suction temperature compressor is a single screw. An additional 66.7% (another 8 cylinders) of capacity needs to be added to the high-stage compressor of the current system if two-stage compression is used.

| Performance Measures | Single-Stage Compression | | | Two-Stage Compression | | |
|---|---|---|---|---|---|---|
| | High Temperature | Low Temperature | Combined | High Temperature | Low Temperature | Combined |
| ton-hr / ft²-yr | 19.4 | 11.6 | 15.2 | 19.4 | 11.6 | 15.2 |
| kWh / ton-hr | 1.2 | 1.8 | 1.4 | 1.6 | 1.2 | 1.5 |
| COP | 3.0 | 1.9 | 2.4 | 2.2 | 2.8 | 2.4 |
| hp/ton | 1.6 | 2.5 | 1.9 | 2.2 | 1.7 | 2.0 |
| hp(comp.)/ton | 0.9 | 1.6 | 1.2 | 1.5 | 0.8 | 1.2 |
| hp(cond.)/ton | 0.1 | 0.2 | 0.2 | 0.1 | 0.2 | 0.2 |
| hp(evap.)/ton | 0.2 | 0.3 | 0.2 | 0.2 | 0.3 | 0.2 |
| OnPeak kWh / yr | 379107 | 426176 | 805271 | 527763 | 286171 | 813931 |
| OffPeak kWh / yr | 655582 | 736493 | 1392118 | 912085 | 496515 | 1408604 |
| Peak kW | 194.4 | 218.4 | 412.8 | 276.0 | 130.7 | 406.7 |
| $ / ft² -yr | $0.92 | $0.88 | $0.90 | $1.29 | $0.58 | $0.91 |
| $ / cu.ft -yr | $0.05 | $0.04 | $0.04 | $0.07 | $0.02 | $0.04 |
| $ / ton-hr -yr | $0.05 | $0.08 | $0.06 | $0.07 | $0.05 | $0.06 |
| $ / yr | $42,158 | $47,402 | $89,667 | $58,991 | $31,353 | $90,453 |

**Table 5.2 Single vs. Two-Stage Compression – (floating head pressure control)**

### 5.3.2 Explanation of Two-Stage Performance Loss

Table 5.2 shows that the performance of a two-stage system under actual operating conditions is less efficient than a single-stage system. The inefficiencies arise from a combination of several reasons.

- Low Compression Ratio
- Compressor Type
- Constrained Intermediate Pressure
- Additional Pressure Losses

#### 5.3.2.1 Low Compression Ratio

Compression ratio is defined as the absolute compressor discharge pressure divided by the absolute compressor suction pressure. Due to the floating, minimum head pressure control and over-sized evaporative condenser, the average yearly condensing temperature is relatively low at 73°F. Low condensing temperatures/pressures reduce the compression ratio that the compressors are required to meet. As shown in Figure 5.2, the advantage that two-stage compression systems have over single-stage in compressor horsepower becomes smaller and eventually negative as the pressure lift decreases. This decrease is

due to the additional losses inherent with a two-stage system overshadowing the savings in compression work illustrated in Figure 5.1 and is true for both screw and reciprocating compressor systems. Figure 5.3 gives an overall look at the savings in compressor horsepower using screw and reciprocating compressors.

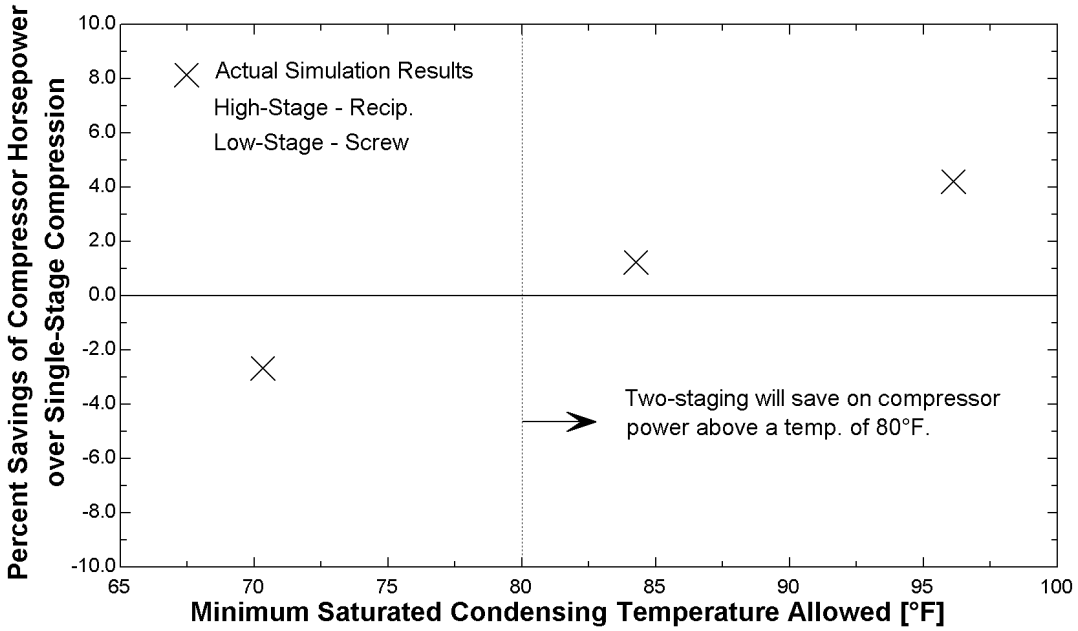


**Figure 5.2 Minimum Head Pressure Two-Stage Comparison**

5.3.2.2 Compressor Type

Also shown in Figure 5.3, screw compressors that have to operate at part load conditions loose their two-stage advantages over single-stage very quickly as the condensing temperature drops. The reason for this behavior is that the compressors operate less efficiently a part-load. In the particular system that was modeled, when the low suction temperature screw compressor (Model# VSS-451) is switched from high-stage to booster operation it must be unloaded even more and the overall performance of the system drops. The unloading penalty could be avoided if an appropriately sized compressor was used instead of the existing machinery. From interpolating Figure 5.3 a two-stage screw compressor system only needs to unload approximately 25 percent at a condensing temperature of 73°F to become less efficient than a single-stage compressor.

Another consideration with screw compressors is the actual compression process. The screw components are sealed by injecting oil during compression. A byproduct of the oil injection for mechanical purposes is a cooling effect on the refrigerant. The compression process in a screw compressor is more closely represented by isothermal compression, which is the whole point of two staging a compression process in the first place.

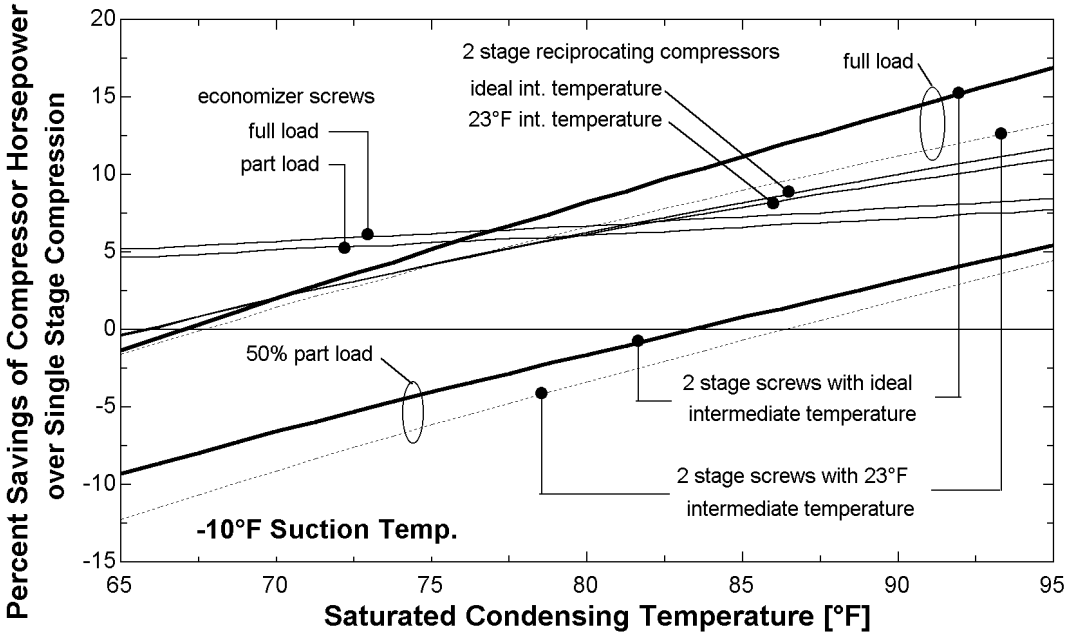


**Figure 5.3 Manufacturer's Two vs. Single-Stage Compressor Power Savings**

5.3.2.3 Constrained Intermediate Pressure

When two-stage systems are installed, an intermediate pressure must be set. Mitchell and Braun recommend an intermediate pressure equal to the square-root of the product of absolute suction and discharge pressures [Mitchell and Braun, 1998]. In this system, the intermediate pressure is dictated by the required refrigerant temperature of the cooler. Selecting intermediate pressures other than the optimum also contribute to the reduced effectiveness of two-stage compression. A comparison between ideal and non-ideal intermediate pressures is also shown in Figure 5.3. The penalty of using a non-ideal intermediate pressure is most significant with screw compressors. This result is explained with the help of Figure 5.4. This figure shows the saturation temperature that the intermediate pressure receiver should operate at to minimize the compressor horsepower

per ton of a two-stage system. The optimum intermediate pressure was found using internal EES optimization routines. Plots are shown for both single screw and reciprocating compressors. It is interesting to note that the optimized temperatures for the screw and reciprocating compressor systems straddle the “rule of thumb" ideal intermediate suggested by Mitchell and Braun, 1998.

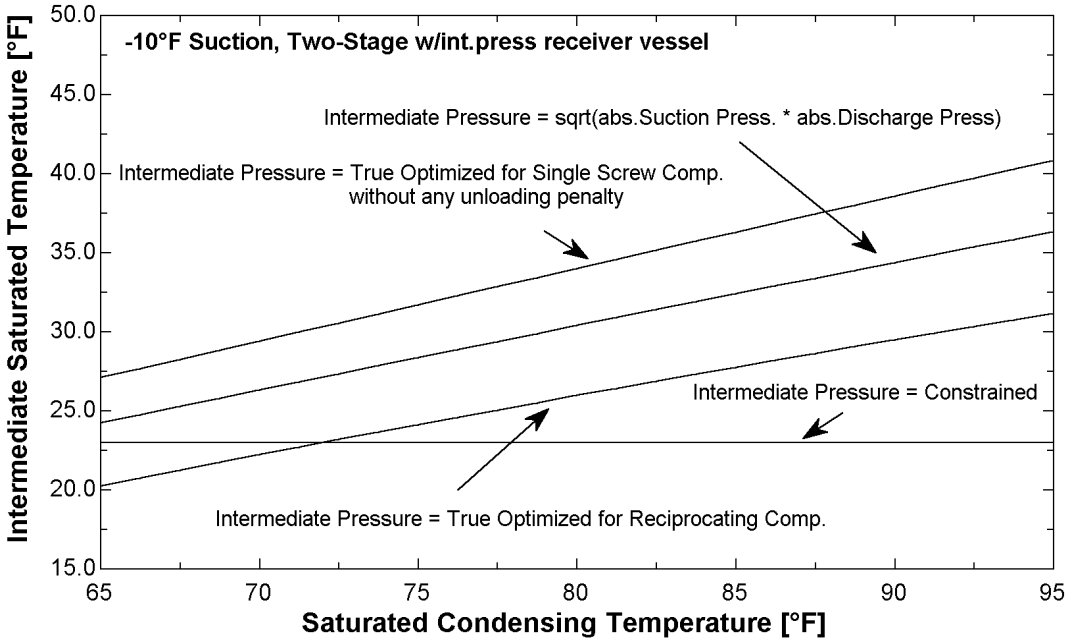


**Figure 5.4 Ideal Two-Stage Intermediate Pressure**

5.3.2.4 Additional Pressure Loss Effects

Finally, the performance degradation of additional pressure drops needs to be considered when using a two-stage system. With two-stage compression the pressure losses for an entire second compressor valve train and interconnecting piping must be rolled into the overall performance of the system. These losses would not be present if the compression was done in a single-stage. Also, these losses will become more significant in the overall system performance as the condensing temperature/pressure falls. Compressor performance degradation from the effects of additional pressure losses is demonstrated in Figure 5.5. Calculations were made using reciprocating compressors.

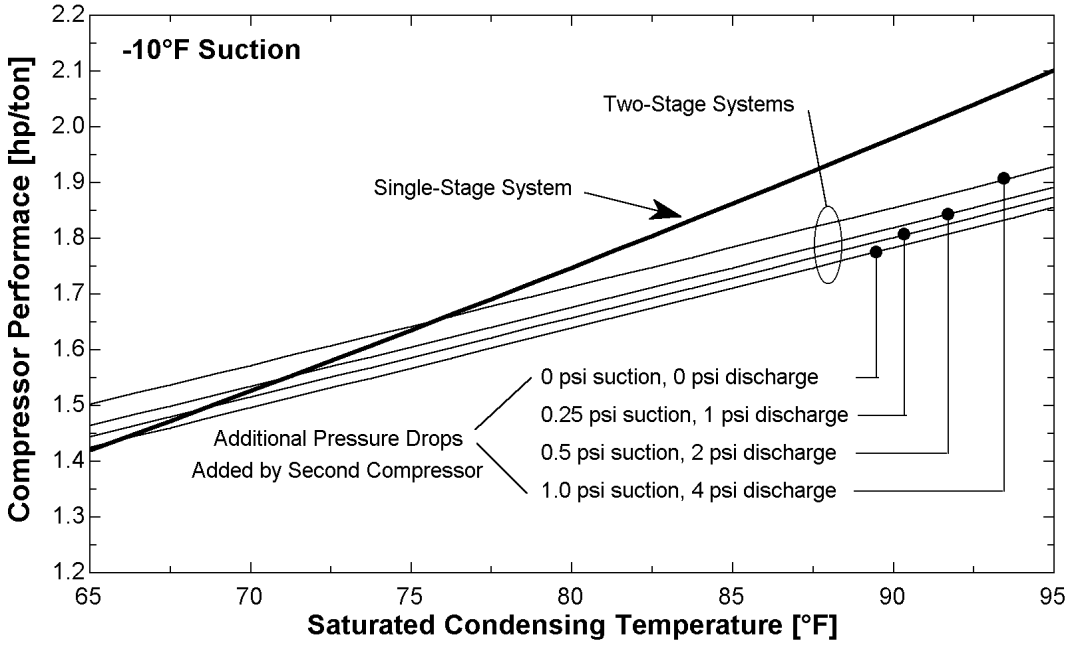


**Figure 5.5 Additional Pressure Loss Effects in Two-Stage Reciprocating Systems**

5.3.2.5 Additional Two-Stage System Comments

The comparison between a two-stage system design and the current facility's design is not an entirely complete comparison between a single and two-stage system. The difference arises from the fact that all the refrigerant used by both the cooler and freezer evaporators is first throttled to an intermediate pressure receiver. The entire flash gas load generated in the first throttling is handled by the high stage compressor. The design of the current facility does use single-stage compression; however, the actual design can be assimilated to one using an economizing screw compressor or one with a subcooling provision. Economized refrigeration cycles have higher efficiencies because not all the refrigerant is compressed from the lowest suction pressure. Some is compressed from an intermediate level which decreases the total amount of compressor work. The percent savings of an economized cycle over a single-stage cycle are also plotted in Figure 5.3. Two-stage systems loose their advantages over economized cycles at even higher compression ratios (saturated condensing temperatures) than they do over true single-stage systems. The current design with an intermediate pressure flash tank is another reason why no performance advantages were realized with the addition of two-stage

compression. An intermediate flash tank emulates some of the advantages of a refrigeration cycle that utilizes an economized compressor.

If a two-stage compression system were installed in the existing facility, additional or different compressors would have to be added to the high-stage compressor to handle the extra volume flow of refrigerant vapor from the low-stage compressor. Calculations showed that the current reciprocating compressor (Vilter Model# VMC-4412) would need an additional 66 percent of capacity. The facility would need to purchase an additional eight-cylinder compressor of similar construction to the existing one. Another option would be to disable the VMC-4412 and use one of the existing screw (Vilter Model# VSS-751) compressors for high stage duty. Unfortunately the VSS-751 would be grossly oversized and operate very inefficiently at part load most of the year.

Two-stage compression is not advantageous to operate on a year-round basis for this system mainly due to the low condensing pressures that are maintained. There are months however, particularly in the summer, where the condensing pressure must be elevated in order to reject energy at a sufficient rate. If a swing compressor arrangement was used, it would be possible to realize the potential compressor horsepower savings of two-stage systems during the summer months. During the cooler months in autumn, winter, and spring, the system would then be changed to operate as it is now.

## 5.4 Split System Arrangement

As introduced in Section 1.4, the system has three basic conditioned spaces to maintain at their desired temperatures. The freezer at 0°F, the cooler at 34°F, and the banana/tomato ripening rooms between 45 and 65°F. Only two suction temperatures, -12°F and 23°F, are maintained by the current system. The high temperature banana/tomato load is interconnected to a low suction temperature of 23°F which results in unnecessary compressor work. Another alternative system arrangement would be to add an additional, higher suction temperature level to serve the banana/tomato room load.

To investigate the potential energy savings of adding another suction level to the current system arrangement, the banana/tomato room loads were split off from the cooler and freezer loads. A completely separate refrigeration system utilizing a Vilter reciprocating compressor (Vilter model# VMC-454XL) along with a separate evaporative condenser (Evapco model# PMCB-190) were modeled to serve the banana/tomato room loads. One 5 and one 2.5 hp motor along with a 2 hp cooling water pump were used in the PMCB-190 model. A completely separate system was selected over just adding an additional intermediate pressure receiver and compressor to the existing system because it offered more options for system control such as multi-level head pressure settings and direct thermosiphon refrigeration possibilities.

### 5.4.1 Simulation Results

The comparison between system performance measures of the current system and split system is shown in Table 5.3. Definitions of the performance measures are the same as described in Section 4.2.4 except that the electrical energy consumed by the banana/tomato room system's compressor and evaporative condenser is added to the high temperature totals. In both systems, a floating head pressure algorithm is used. The minimum head pressure for the banana/tomato system was maintained at 130 psia in order to ensure proper operation of the dx evaporators. Since there was no need to maintain the minimum head pressure of the freezer/cooler system at 130 psia to ensure proper operation of the dx evaporators, the head pressure of the freeze/cooler system was allowed to float down to 95 psia. The new saturated suction temperature for the banana/tomato rooms was maintained at approximately 40°F (74 psia).

| Performance Measures | Current System | | | Split System | | |
|---|---|---|---|---|---|---|
| | High Temperature | Low Temperature | Combined | High Temperature | Low Temperature | Combined |
| ton-hr / ft²-yr | 19.4 | 11.6 | 15.2 | 19.4 | 11.6 | 15.2 |
| kWh / ton-hr | 1.2 | 1.8 | 1.4 | 1.0 | 1.8 | 1.3 |
| COP | 3.0 | 1.9 | 2.4 | 3.7 | 2.0 | 2.7 |
| hp/ton | 1.6 | 2.5 | 1.9 | 1.3 | 2.4 | 1.7 |
| hp(comp.)/ton | 0.9 | 1.6 | 1.2 | 0.7 | 1.3 | 0.9 |
| hp(cond.)/ton | 0.1 | 0.2 | 0.2 | 0.1 | 0.4 | 0.2 |
| hp(evap.)/ton | 0.2 | 0.3 | 0.2 | 0.2 | 0.3 | 0.2 |
| OnPeak kWh / yr | 379107 | 426176 | 805271 | 321434 | 421352 | 732334 |
| OffPeak kWh / yr | 655582 | 736493 | 1392118 | 549503 | 722933 | 1255898 |
| Peak kW | 194.4 | 218.4 | 412.8 | 181.5 | 222.6 | 397.5 |
| $ / ft² -yr | $0.92 | $0.88 | $0.90 | $0.79 | $0.87 | $0.83 |
| $ / cu.ft -yr | $0.05 | $0.04 | $0.04 | $0.04 | $0.03 | $0.04 |
| $ / ton-hr -yr | $0.05 | $0.08 | $0.06 | $0.04 | $0.08 | $0.05 |
| $ / yr | $42,158 | $47,402 | $89,667 | $36,391 | $47,177 | $82,610 |

**Table 5.3 Split System Performance Comparison (bi-level, floating head pressure)**

The comparison in Table 5.3 shows that adding a separate, dedicated vapor compression system to serve the banana/tomato rooms increases the performance of the system. Condenser power consumption did increase due to the addition of the second condenser. However, the addition of the second condenser allowed a significant reduction in head pressure of the freezer/cooler system. Also, a better hp/ton ratio was obtained for the banana/tomato loads. Both of these factors contributed to reducing the total system's compressor horsepower per ton ratio from 1.168 to 0.923. The end result was a savings of 209,157 kWh or $7,057 per year.

## 5.5 Thermosiphon Arrangement

A thermosiphon design is essentially the same as the split system described in Section 5.4. However, some additional evaporator piping would be added to allow natural circulation of the refrigerant between the high pressure receiver and the evaporator for certain times of the year. In Milwaukee, WI, five months of the year (Nov.-Mar.) have average outdoor conditions suitable for 45°F thermosiphon operation. During the rest of the year, the split system compressor would have to be operated. Also, due to the low condensing pressure, the capacity of the banana/tomato load evaporative condenser

would have to increase. Evapco model# PMCB-250 was used for this simulation. The PMCB-250 uses 10 and 5 hp fan motors with a 3 hp cooling water motor.

### 5.5.1 Simulation Results

The comparison between system performance measures of the current system and thermosiphon system is shown in Table 5.4. Definitions of the performance measures are the same as described in Section 4.2.4 except that the electrical energy consumed by the banana/tomato room system's compressor and evaporative condenser is added to the high temperature totals. Operation of the system was approached in the same manner as described in Section 5.4.1 except between the months of November to March where the banana/tomato system was allowed to operate as a thermosiphon. Evaporative condenser fan and cooing water power is still included in the high temperature power consumption when the system is in thermosiphon mode. Calculations using the maximum weather for each month indicated that there may be a few days in both November and March where the outdoor temperature/wet bulb increases to levels were a thermosiphon would likely not be able to maintain the required temperature.

| Performance Measures | Current System | | | Thermosyphon System | | |
|---|---|---|---|---|---|---|
| | High Temperature | Low Temperature | Combined | High Temperature | Low Temperature | Combined |
| ton-hr / ft²-yr | 19.4 | 11.6 | 15.2 | 19.4 | 11.6 | 15.2 |
| kWh / ton-hr | 1.2 | 1.8 | 1.4 | 0.9 | 1.8 | 1.2 |
| COP | 3.0 | 1.9 | 2.4 | 3.9 | 2.0 | 2.9 |
| hp/ton | 1.6 | 2.5 | 1.9 | 1.2 | 2.4 | 1.7 |
| hp(comp.)/ton | 0.9 | 1.6 | 1.2 | 0.6 | 1.3 | 0.9 |
| hp(cond.)/ton | 0.1 | 0.2 | 0.2 | 0.1 | 0.4 | 0.2 |
| hp(evap.)/ton | 0.2 | 0.3 | 0.2 | 0.2 | 0.3 | 0.2 |
| OnPeak kWh / yr | 379107 | 426176 | 805271 | 309392 | 421352 | 708070 |
| OffPeak kWh / yr | 655582 | 736493 | 1392118 | 524549 | 722933 | 1212070 |
| Peak kW | 194.4 | 218.4 | 412.8 | 186.2 | 222.6 | 396.7 |
| $ / ft² -yr | $0.92 | $0.88 | $0.90 | $0.78 | $0.87 | $0.81 |
| $ / cu.ft -yr | $0.05 | $0.04 | $0.04 | $0.04 | $0.03 | $0.04 |
| $ / ton-hr -yr | $0.05 | $0.08 | $0.06 | $0.04 | $0.08 | $0.05 |
| $ / yr | $42,158 | $47,402 | $89,667 | $35,644 | $47,177 | $80,655 |

**Table 5.4 Thermosiphon System Comparison (multi-level floating head pressure)**

Operating the system as a split system with thermosiphon capabilities results in an energy savings of 277,249 kWh or $9,012 per year over how the system is currently operated. The thermosiphon option reduces the energy costs by an additional $1,955 per year below the straight split system design.

## 5.6 System Design Conclusions

An annual performance summary of each alternative design considered is located in Section 7.2.

# *Chapter 6 -Optimum Control Strategies*

## 6.1 Compressor Loading

Compressor performance is commonly measured by calculating how much horsepower is required to produce a ton of refrigeration at a particular operating point or this parameter (hp/ton) can be averaged over a day, month, or year. The hp/ton measure can also be converted into another common performance parameter by taking the reciprocal and non-dimensionalizing it. The result of this manipulation is the coefficient of performance (COP) of the compressor. It is desirable to operate compressors at either the lowest hp/ton or highest COP that can be obtained while still meeting the system constraints, i.e. loads.

### 6.1.1 Reciprocating vs. Single Screw Compressors

Type of compressor, suction and discharge conditions, and unloading characteristics all affect a compressor's hp/ton measure and are discussed in Section 2.4.1. Figure 6.1 shows a comparison in hp/ton between a Vilter VSS-451 single screw and VMC-4412 reciprocating compressor for several different saturated discharge temperatures (SDT) at different part load conditions (%FLC) assuming a fixed suction condition at 0°F.

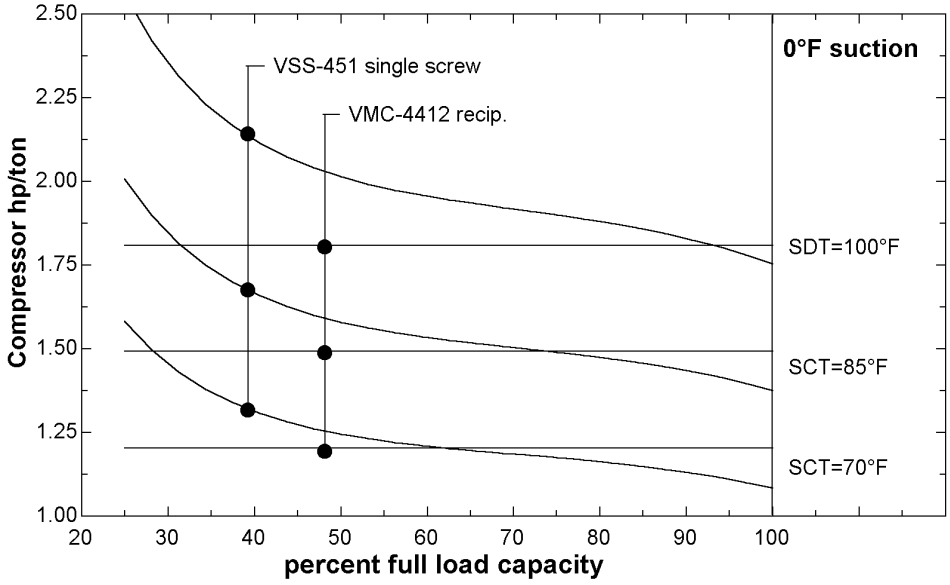


**Figure 6.1 Hp/ton Screw and Recip. Comparison**

Several observations can be made about compressor operation from Figure 6.1.

- A single screw compressor unloaded to 25 percent of its full load capacity uses nearly 50 percent more power per ton of refrigerating when compared to a reciprocating compressors. Reciprocating compressors unload nearly linearly.
- Screw compressors perform better than reciprocating compressors when operated near full load. The performance advantage of screws is greater at low condensing temperatures (assume variable vi compression).
- The penalty for unloading a screw compressor is greater when the pressure lift across that compressor is higher.

### 6.1.2 Load Sharing with Similar Compressors

When a system's load exceeds the capacity of a particular compressor, a secondary compressor must be cycled on to augment the capacity of the primary compressor. How best to split the load between the two compressors depends upon the magnitude of the load and type and size of the available compressors. Because of the linear unloading behavior of reciprocating compressors, the load should be split so that the pressure loss in each compressor's dry suction line is equalized. Screw compressors unload non-linearly and must be treated differently than reciprocating compressors. Figure 6.2 shows a plot of total system compressor performance (hp/ton) for a system with two equally sized single screw compressors operating in parallel. Each line on the plot represents a different system load. Starting at the far right of the plot for a given load, one compressor is fully loaded. The other compressor is unloaded until the aggregate capacity of the two compressors equals the total system load. By progressing to the left along the constant load line, the first compressor is unloaded and the second compressor is reloaded so the aggregate compressor capacity still equals the total refrigeration load.

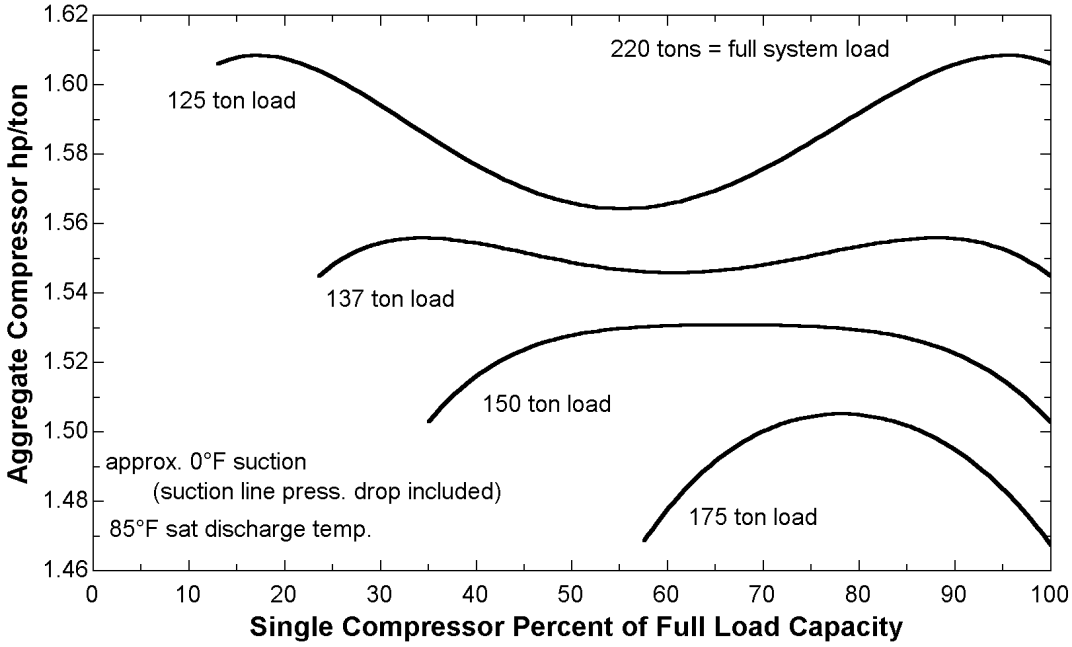


**Figure 6.2 Equal Sized Screw Compressor Load Sharing Characteristics**

As shown in Figure 6.2, for intermediate system loads (between 110 and 137 tons or 50 – 62 percent of available system capacity) it is best to split the load equally between the two compressors. For loads above 137 tons (62% of available system capacity), the system performance is best when one compressor is fully loaded and the other loaded to make up the difference. This crossover point is better shown in Figure 6.4. The minimum point in the middle of the top two load curves in Figure 6.2 begins to develop significance when the compressors are unloaded to around 55 – 60 percent of their full load capacity. This behavior can be explained by Figure 6.3, which shows that the performance (hp/ton) of a screw compressor begins to deteriorate very rapidly after it is unloaded below 50 percent of its full load capacity. The minimum point develops because if either compressor is unloaded too much at intermediate loads, the overall performance of the system drops rapidly. The crossover point shown in Figure 6.4 would likely change if compressors from other manufacturers were used due to different unloading characteristics.

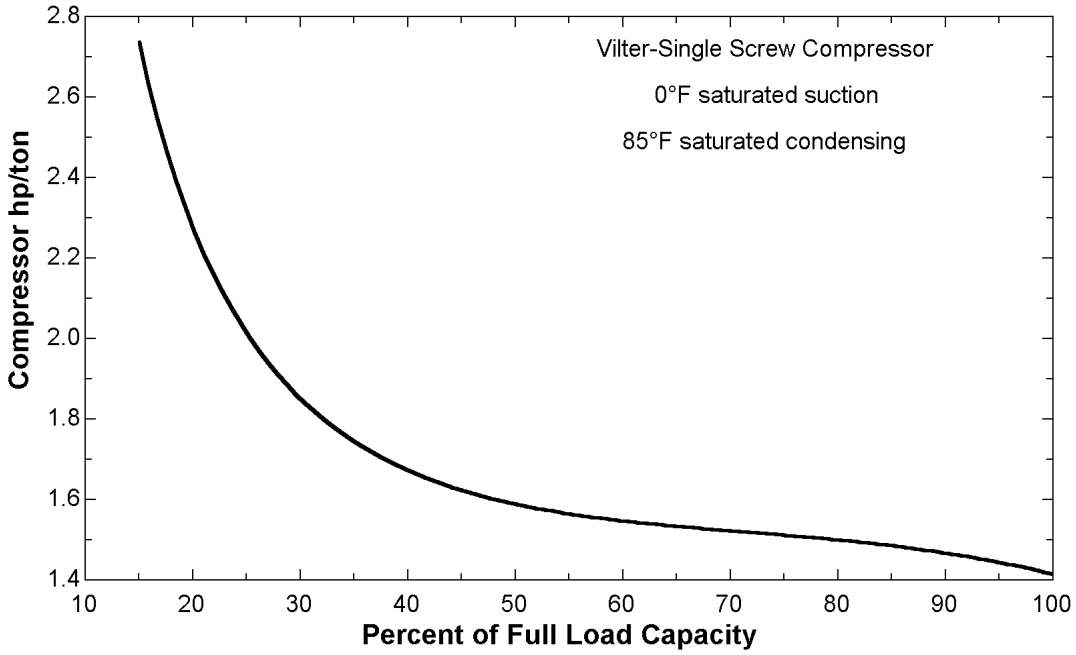


**Figure 6.3 Single Screw Unloading Performance Trace**

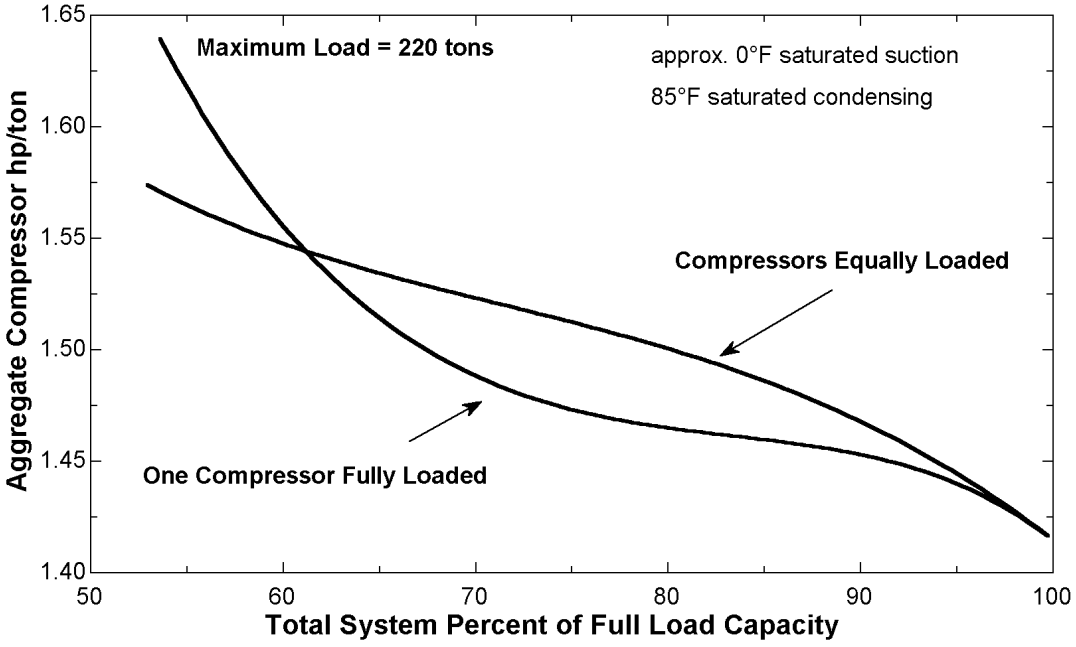


**Figure 6.4 Equal Sized Screw Compressor Load Sharing Characteristics**

The performance trace shown in Figure 6.4 was is compared to the performance trace of the same compressors at different suction and discharge conditions in Figure 6.5. The crossover point remains at nearly the same percent of available compressor capacity no

matter what the suction or discharge conditions are. If equally sized compressors from different manufacturers with different unloading characteristics were used, it is likely that the crossover point would change position. Modeling of more compressors was beyond the scope of this paper and was not pursued.

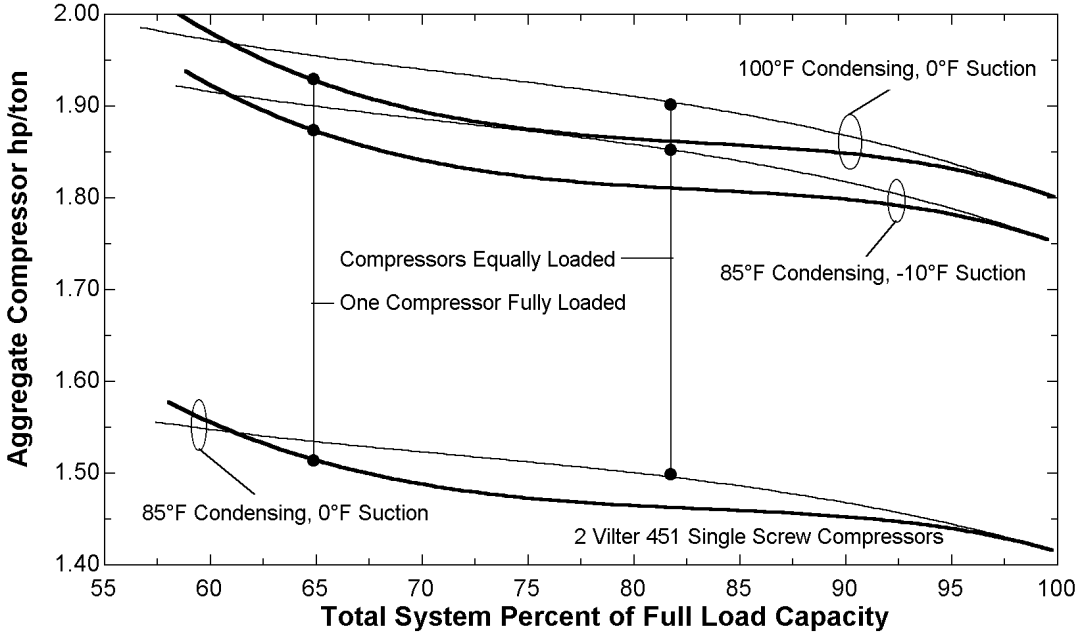


**Figure 6.5 Load Sharing Performance Characteristics at Different Suction and Discharge Conditions.**

### 6.1.3 Load Sharing with Dissimilar Compressors

When different sized screw compressors are used in parallel, a different set of load sharing characteristic curves develop. Figure 6.6 shows that it is no longer advantageous to share the load between the compressors at intermediate load levels (between 180 and 212 tons) as done with similar sized compressors. Instead, the larger compressor should be fully loaded when the total system loads are high (above 212 tons) and the smaller compressor fully loaded when there is an intermediate load. In this example, the larger compressor has approximately 64% more available capacity than the smaller compressor.

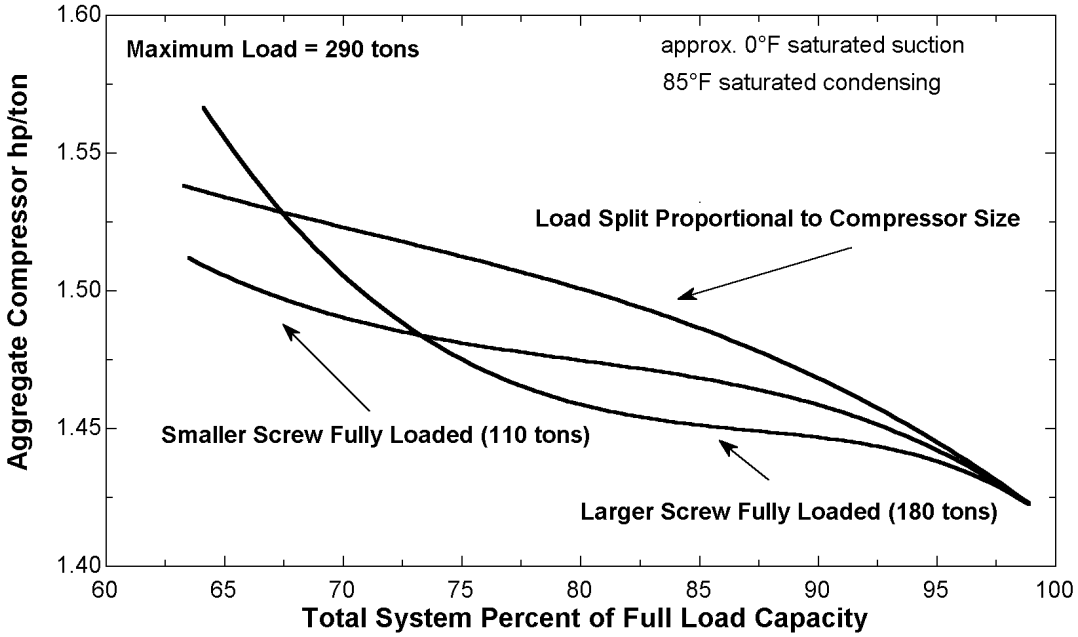


**Figure 6.6 Unequally Sized Screw Compressor Load Sharing Characteristics**

The trends in the characteristic load sharing curves in Figure 6.6 can again be understood with the aid of Figure 6.3, which is identical for both large and small single screw compressors. As the load exceeds the maximum capacity of the large screw, the smaller screw must be started. At intermediate loads (between 180 and 212) if the large compressor is kept fully loaded, the smaller compressor will be operating in the far-left performance regime of Figure 6.3 causing poor overall system performance. If the load is shifted to fully load the smaller compressor, the large compressor still operates near 50 to 60 percent of its full load capacity which preserves most of its performance integrity.

### 6.1.4 Compressor Optimizing Conclusions

- When a screw and reciprocating compressor are sharing a reducing load, the reciprocating compressor should be unloaded first.
- When two screw compressors are sharing a load, control strategies should avoid operating any screw compressor below 50 percent of its full load capacity.
- Unloading performance characteristics of systems with unequal sized compressors differ from systems with equally sized compressors.
- Screw compressors are better suited for base loading where they can be run at full load all the time.

## 6.2 Evaporative Condenser (head pressure)

### 6.2.1 Fixed vs. Floating Head Pressure Control

System condensing pressure, also referred to as head pressure, is typically controlled in one of two ways. Fixed head pressure control has the simplest control strategy, however this control strategy results in unnecessary compressor power due to the compressors operating with higher pressure lifts than required. The fixed level head pressure control strategy maintains the head pressure at a constant preset level regardless of system load and outside air conditions. This level could be adjusted several times a year in northern climates to improve performance during months of colder outdoor temperatures.

The second type of control strategy is termed “floating head pressure”. In this control strategy, the head pressure is allowed to “float” down to a minimum set value which is normally determined by system defrost pressure, expansion valve pressure drop requirements, or oil pressure requirements from oil injected screw compressor cooling. As the load on the system or the outdoor dry bulb (wet bulb in the case of evaporative condensers) temperature increases, the head pressure will rise, thereby, allowing the system to reject energy to the environment as needed to balance system heat rejection requirements.

The current system uses a floating head pressure control strategy with a minimum head pressure set point of 130 psia. A fixed head pressure control strategy was simulated using a set point pressure of 142.5 psia for the months of October through May and a set pressure of 166 psia from June through September. Figure 6.7 shows the resulting yearly head pressure profile using the maximum design day weather for each month.

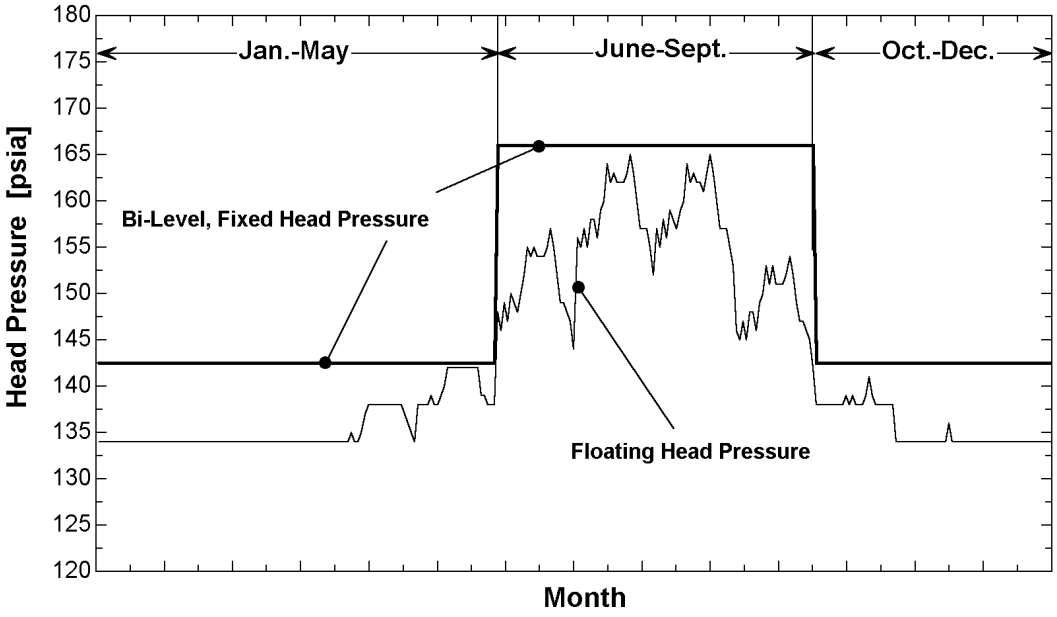


**Figure 6.7 Head Pressure Yearly Profile for Design Day of Each Month**

Yearly operating results comparing the energy use of the current system to the bi-level, fixed head pressure controlled system are presented in

| Performance Measures | Current System - Floating Head Pressure | | | Current System - Bi-Level, Fixed Head Pressure | | |
|---|---|---|---|---|---|---|
| | High Temperature | Low Temperature | Combined | High Temperature | Low Temperature | Combined |
| ton-hr / ft²-yr | 19.4 | 11.6 | 15.2 | 19.4 | 11.6 | 15.2 |
| kWh / ton-hr | 1.2 | 1.8 | 1.4 | 1.2 | 1.9 | 1.5 |
| COP | 3.0 | 1.9 | 2.4 | 2.9 | 1.8 | 2.4 |
| hp/ton | 1.6 | 2.5 | 1.9 | 1.6 | 2.6 | 2.0 |
| hp(comp.)/ton | 0.9 | 1.6 | 1.2 | 1.0 | 1.7 | 1.3 |
| hp(cond.)/ton | 0.1 | 0.2 | 0.2 | 0.1 | 0.2 | 0.1 |
| hp(evap.)/ton | 0.2 | 0.3 | 0.2 | 0.2 | 0.3 | 0.2 |
| OnPeak kWh / yr | 379107 | 426176 | 805271 | 394172 | 438694 | 832898 |
| OffPeak kWh / yr | 655582 | 736493 | 1392118 | 687807 | 764429 | 1452172 |
| Peak kW | 194.4 | 218.4 | 412.8 | 194.3 | 218.3 | 412.5 |
| $ / ft² -yr | $0.92 | $0.88 | $0.90 | $0.95 | $0.90 | $0.92 |
| $ / cu.ft -yr | $0.05 | $0.04 | $0.04 | $0.05 | $0.04 | $0.04 |
| $ / ton-hr -yr | $0.05 | $0.08 | $0.06 | $0.05 | $0.08 | $0.06 |
| $ / yr | $42,158 | $47,402 | $89,667 | $43,487 | $48,672 | $92,242 |

Table **6.1**. Performance measures and electrical costs are defined in Section 4.2.3.

| Performance Measures | Current System - Floating Head Pressure | | | Current System - Bi-Level, Fixed Head Pressure | | |
|---|---|---|---|---|---|---|
| | High Temperature | Low Temperature | Combined | High Temperature | Low Temperature | Combined |
| ton-hr / ft²-yr | 19.4 | 11.6 | 15.2 | 19.4 | 11.6 | 15.2 |
| kWh / ton-hr | 1.2 | 1.8 | 1.4 | 1.2 | 1.9 | 1.5 |
| COP | 3.0 | 1.9 | 2.4 | 2.9 | 1.8 | 2.4 |
| hp/ton | 1.6 | 2.5 | 1.9 | 1.6 | 2.6 | 2.0 |
| hp(comp.)/ton | 0.9 | 1.6 | 1.2 | 1.0 | 1.7 | 1.3 |
| hp(cond.)/ton | 0.1 | 0.2 | 0.2 | 0.1 | 0.2 | 0.1 |
| hp(evap.)/ton | 0.2 | 0.3 | 0.2 | 0.2 | 0.3 | 0.2 |
| OnPeak kWh / yr | 379107 | 426176 | 805271 | 394172 | 438694 | 832898 |
| OffPeak kWh / yr | 655582 | 736493 | 1392118 | 687807 | 764429 | 1452172 |
| Peak kW | 194.4 | 218.4 | 412.8 | 194.3 | 218.3 | 412.5 |
| $ / ft² -yr | $0.92 | $0.88 | $0.90 | $0.95 | $0.90 | $0.92 |
| $ / cu.ft -yr | $0.05 | $0.04 | $0.04 | $0.05 | $0.04 | $0.04 |
| $ / ton-hr -yr | $0.05 | $0.08 | $0.06 | $0.05 | $0.08 | $0.06 |
| $ / yr | $42,158 | $47,402 | $89,667 | $43,487 | $48,672 | $92,242 |

**Table 6.1 Floating vs. Fixed Head Pressure Comparison**

Although the condenser energy is reduced using fixed head pressure control due to less fan run-time, the compressor energy consumption increased significantly. Fixed, bi-level head pressure control results in an energy penalty of 87,681 kWh or $2,575 per year. (Dollar figures are based on the electric rates defined in Section 4.2.4.)

### 6.2.2 Condenser Fan Control

Fan motors can be designed to operate at single speed, multi-speed, or be controlled by variable frequency drives (VFD). Advantages of using multi-speed and VFD motors appear when a system is operating at part-load as discussed in Section 2.4.2.4. Condenser capacity control is accomplished by modulating or reducing the airflow through the unit with fan control and is also discussed in Section 2.4.2.4. As shown in Figure 2.11, given a specific system operating point, VFD motor control requires significantly less condenser fan power than simple on/off control when the condenser is operated between 30 and 90 percent of its full load capacity. Figure 2.11 also showed that a half-speed motor option also realizes significant power savings in that same operating range. Two opposing energy effects result from head pressure control with condenser fan modulation. First, if the head pressure is allowed to increase, the condenser fans have to run less often or at

lower speeds and a savings in condenser fan energy results. Secondly, high head pressure requires increased amounts of compressor energy to produce the extra pressure lift. Figure 6.8 is a plot of the combined compressor and condenser energy requirements [hp] as a function of head pressure. The point furthest to the left on the curves in Figure 6.8 represents the pressure at which the condenser is operating at 100 percent capacity. Any further decrease in condensing pressure would prevent the condenser from rejecting the required amount of energy from the system. The calculations were done for the current system operating on the peak hour of the average day in May. Figure 6.8 demonstrates that VFD fan control could save the system nearly 8% in combined compressor and condenser energy requirements if the head pressure were raised to 125 psia. VFD fan control looses its advantages at low head pressures because the fans must run at near full speed most of the time anyway. At high head pressures the fans in on/off control don't stay on long because of the high rate of heat transfer that occurs. However, at high head pressure an on/off control strategy would cycle the fans on and off frequently which would cause excessive wear on the motors and fan belts. Figure 6.8 shows that there is a different optimum head pressure for each type of condenser fan control. It is also interesting to note that half-speed fan motors have energy requirements that are only approximately one percent above the VFD motors at elevated head pressures. Since this system as a minimum allowed head pressure of 130 psia, VFD and half-speed motors may have very similar energy requirements for most of the year.

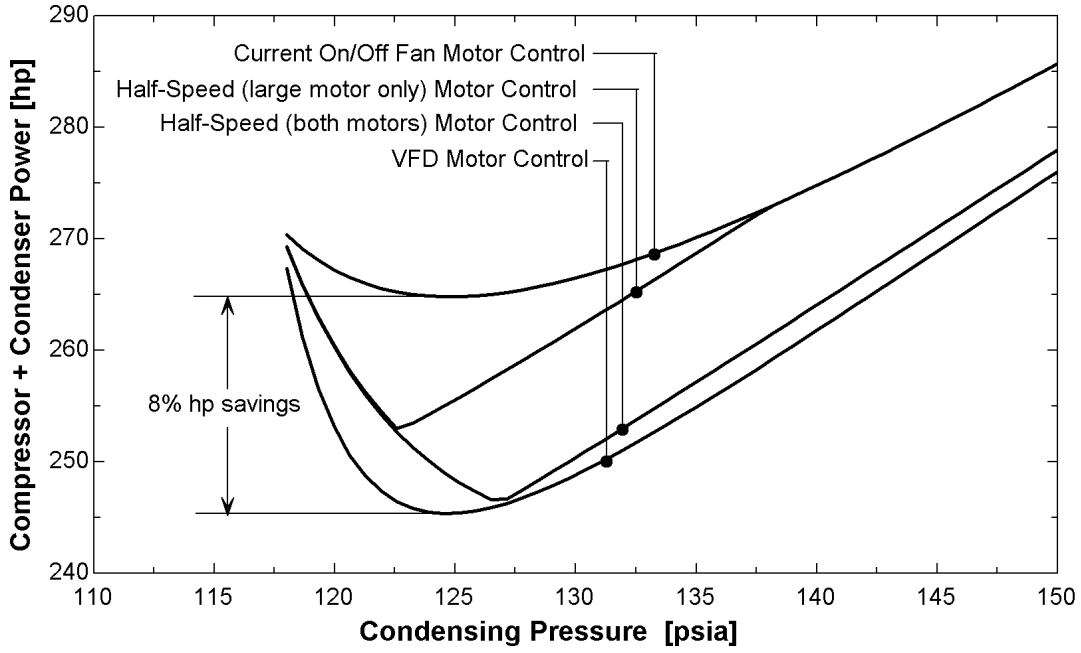


**Figure 6.8 Evaporative Condenser Fan Motor Control Strategies**

### 6.2.3 Optimized Floating Head Pressure Control

Figure 6.8 demonstrates that there is an optimum condensing pressure to operate the current system at for each type of fan control strategy. At this optimized pressure, the compressor power and condenser power sum to a minimum. Below this pressure the condenser fan power starts to increase significantly. Above this pressure the compressors must work unnecessarily hard.

The optimum pressure is dependent upon both the system load and size of condenser. Figure 6.9 shows the optimized head pressure using VFD fan control for the peak hour of the average day between the months of March and July. Each month represents an increasing load on the condenser. Outdoor temperatures dictated that the cooling water was on (i.e. evaporative condenser is wet) for each calculation. Each line in Figure 6.9 was made by calculating the sum of the compressor's and condenser's power draw as the head pressure was varied. The dark set of lines is for the condenser that is currently installed in the system. The current condenser requires a refrigerant temperature of 85°F on the design day to reject the required amount of energy. The compressor/condenser power with a smaller condenser, described in Section 5.2, that has a design condensing

temperature of 95°F is shown with the light lines. The point furthest to the left on each line represents the pressure at which the evaporative condenser has reached 100 percent capacity. Given that the load is constant, it would be physically impossible to achieve a lower head pressure without adding additional condensing capacity.

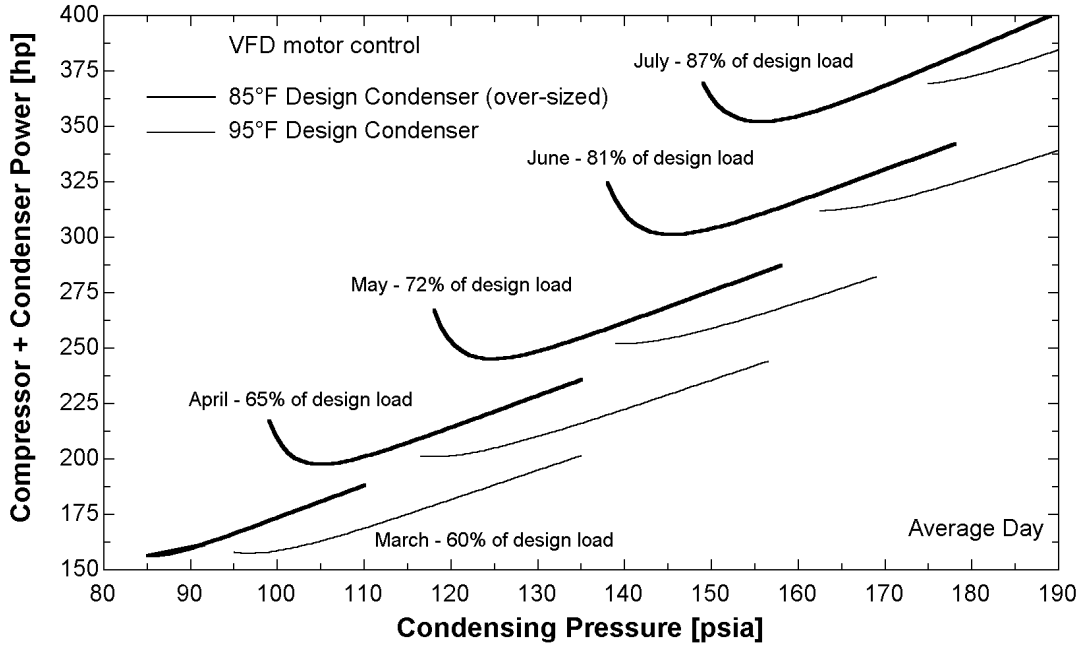


**Figure 6.9 Optimum Condensing Pressure for Increasing Loads**

In the actual operation of the system the head pressure is not allowed to go below 130 psia. Therefore, the system cannot possibly be operated at its ideal head pressure except for the months of June through September. It must be operated above its optimum head pressure resulting in excess compressor power. As shown by the thin lines in Figure 6.9, for systems with small condensers, it is best to operate the condenser fans at full speed except when an elevated head pressure must be maintained during cooler months. The point farthest left on the thin lines in Figure 6.9 corresponds with the fans at full speed. This is the point of lowest combined compressor and condenser energy for systems with smaller sized condensers.

### 6.2.4 Simulation Using VFD Evaporative Condenser Fan Motors

As suggested in Section 2.4.2.4 and demonstrated in Section 6.2.2, using variable frequency drives (VFD) for the evaporative condenser motors will reduce the condenser fan power consumption. An added benefit to VFD evaporative condenser fan control is

much less wear and required maintenance on the fan motors and drive belts. Table 6.2 compares the yearly simulation results between the current system using on/off control (the way it is currently done) and using VFD control.

Using VFD controlled motor under the current head pressure control scheme would save 61,684 kWh or $2,209 per year in electrical operating costs. Performance measures and electric rates are defined in Section 4.2.3.

| Performance Measures | Current System - On/Off Condenser Fan Control | | | Current System - VFD Condenser Fan Control | | |
|---|---|---|---|---|---|---|
| | High Temperature | Low Temperature | Combined | High Temperature | Low Temperature | Combined |
| ton-hr / ft²-yr | 19.4 | 11.6 | 15.2 | 19.4 | 11.6 | 15.2 |
| kWh / ton-hr | 1.2 | 1.8 | 1.4 | 1.1 | 1.8 | 1.4 |
| COP | 3.0 | 1.9 | 2.4 | 3.1 | 2.0 | 2.5 |
| hp/ton | 1.6 | 2.5 | 1.9 | 1.5 | 2.4 | 1.9 |
| hp(comp.)/ton | 0.9 | 1.6 | 1.2 | 0.9 | 1.6 | 1.2 |
| hp(cond.)/ton | 0.1 | 0.2 | 0.2 | 0.1 | 0.2 | 0.1 |
| hp(evap.)/ton | 0.2 | 0.3 | 0.2 | 0.2 | 0.3 | 0.2 |
| OnPeak kWh / yr | 379107 | 426176 | 805271 | 368997 | 414473 | 783401 |
| OffPeak kWh / yr | 655582 | 736493 | 1392118 | 637149 | 715086 | 1352304 |
| Peak kW | 194.4 | 218.4 | 412.8 | 193.4 | 217.4 | 410.7 |
| $ / ft² -yr | $0.92 | $0.88 | $0.90 | $0.90 | $0.86 | $0.88 |
| $ / cu.ft -yr | $0.05 | $0.04 | $0.04 | $0.05 | $0.03 | $0.04 |
| $ / ton-hr -yr | $0.05 | $0.08 | $0.06 | $0.05 | $0.07 | $0.06 |
| $ / yr | $42,158 | $47,402 | $89,667 | $41,146 | $46,244 | $87,458 |

**Table 6.2 On/Off vs. VFD Condenser Fan Control Performance Comparison**

### 6.2.5 Simulation With Optimized Condensing Pressure

A yearly simulation was performed for the current system arrangement using the optimum condensing pressure and VFD condenser fan control. The minimum condensing pressure that was allowed was 130 psia. The ideal head pressure was solved for using EES optimization procedures. The variable that was minimized for each hour of the yearly simulation was the sum of the compressor and condenser power. Figure 6.10 compares the yearly head pressure profile for the design day of each month between minimum (the way the system is currently operated) and optimized head pressure control.

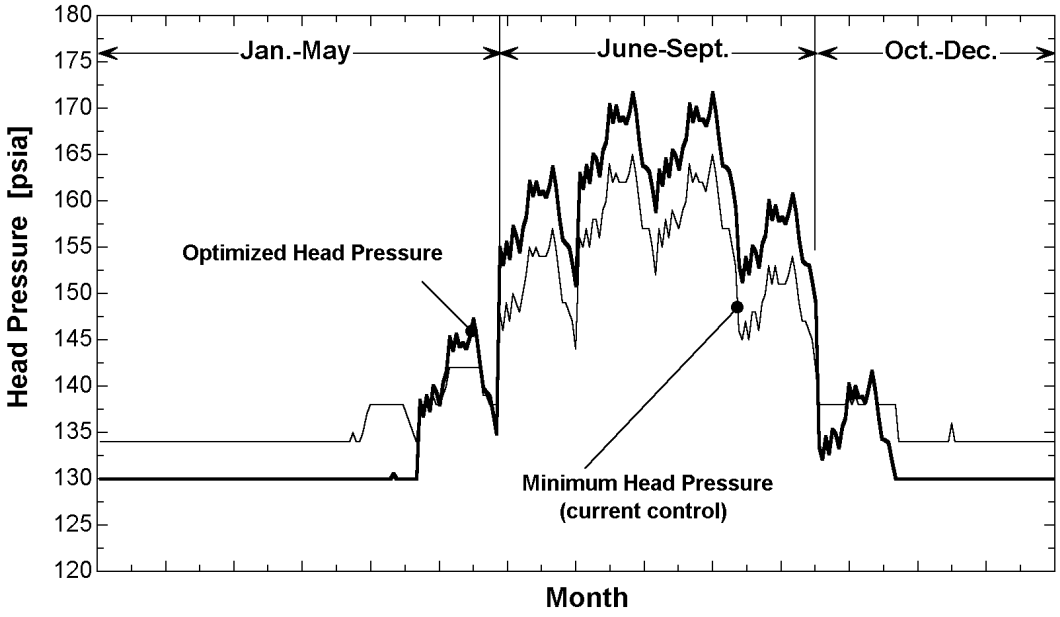


**Figure 6.10 Head Pressure Profiles for Design Days**

A performance comparison between the way the system is currently operated and if optimized head pressure and VFD condenser fan control were used is shown in Table 6.3. Performance measures and electric rates are defined in Section 4.2.3. Optimized head pressure control along with VFD condenser fan control would save 97,140 kWh or $3,856 per year in electrical operating costs.

| Performance Measures | Current System - On/Off Condenser Fan Control, Minimum Floating Head Pressure | | | Current System - VFD Condenser Fan Control, Ideal Floating Head Pressure | | |
|---|---|---|---|---|---|---|
| | High Temperature | Low Temperature | Combined | High Temperature | Low Temperature | Combined |
| ton-hr / ft²-yr | 19.4 | 11.6 | 15.2 | 19.4 | 11.6 | 15.2 |
| kWh / ton-hr | 1.2 | 1.8 | 1.4 | 1.1 | 1.8 | 1.4 |
| COP | 3.0 | 1.9 | 2.4 | 3.2 | 2.0 | 2.6 |
| hp/ton | 1.6 | 2.5 | 1.9 | 1.5 | 2.4 | 1.8 |
| hp(comp.)/ton | 0.9 | 1.6 | 1.2 | 0.9 | 1.5 | 1.1 |
| hp(cond.)/ton | 0.1 | 0.2 | 0.2 | 0.1 | 0.1 | 0.1 |
| hp(evap.)/ton | 0.2 | 0.3 | 0.2 | 0.2 | 0.3 | 0.2 |
| OnPeak kWh / yr | 379107 | 426176 | 805271 | 361974 | 407223 | 769193 |
| OffPeak kWh / yr | 655582 | 736493 | 1392118 | 626423 | 704629 | 1331056 |
| Peak kW | 194.4 | 218.4 | 412.8 | 187.7 | 211.6 | 399.3 |
| $ / ft² -yr | $0.92 | $0.88 | $0.90 | $0.88 | $0.84 | $0.86 |
| $ / cu.ft -yr | $0.05 | $0.04 | $0.04 | $0.05 | $0.03 | $0.04 |
| $ / ton-hr -yr | $0.05 | $0.08 | $0.06 | $0.05 | $0.07 | $0.06 |
| $ / yr | $42,158 | $47,402 | $89,667 | $40,319 | $45,412 | $85,811 |

**Table 6.3 Optimum vs. Minimum Head Pressure Control Comparison**

When calculations were being made to identify the optimum condensing pressure for the year, it was noticed that the optimum condensing pressure had a near linear relationship with the outside air wet bulb temperature. The curve fit and calculated optimum condensing pressure points are shown in Figure 6.11. The curve fit is given in Equation (6.1).

$$Optimum \quad Pressure = -27.6 + 2.55 \cdot T_{wet\ bulb} \tag{6.1}$$

A yearly simulation using Equation (6.1) in place of the EES optimization routines yielded negligible differences indicating that outdoor wet bulb temperature may be a good way to identify the optimum head pressure for a particular system. The curve plotted in Figure 6.11 does however shift slightly if parameters such as load profile, condenser size, condenser fan control, or system component arrangement change. Figure 6.11 also shows the optimum head pressure as a function of wet bulb for a yearly simulation of average days with the evaporator loads held constant at a combined total of 2.77 x $10^6$ btu/hr (indicated by the circles on the plot). The optimum head pressure curve does flatten out slightly. Each particular industrial refrigeration system would have its

own characteristic optimum head pressure curve. Also plotted in Figure 6.11 is the total heat rejected by the condenser as a function of wet bulb for both the normal system and with the evaporator load held constant. The definite scalar jump in the normal system data is the difference in load between second and first shifts of the warehouse as discussed in Section 2.5.3. The linear trend shown by the condenser energy data is expected since the load on the warehouse generally increases with increasing outdoor wet bulb temperatures. The slight increase in condenser load for the constant evaporator load data is due to increasing oil cooling requirements by the compressors as the head pressure increases.

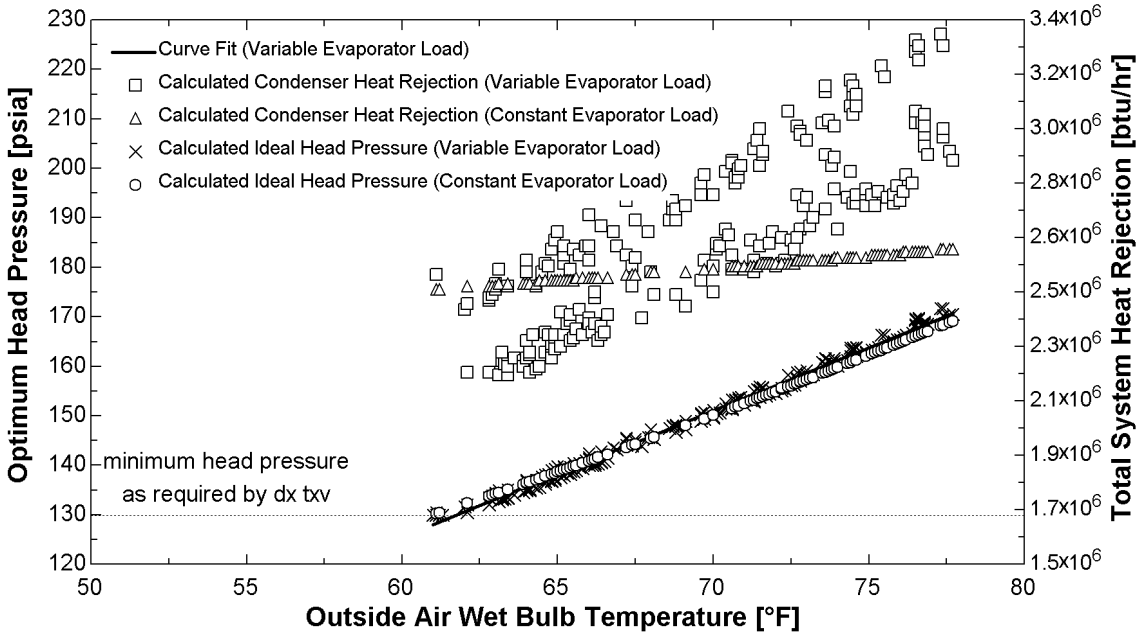


**Figure 6.11 Curve Fit for Ideal Head Pressure**

An additional simulation was done using the half-speed motors instead of VFD motors. A new curve fit was done for the optimum head pressure calculation and is shown in Equation (6.2).

$$Optimum\ Pressure = -33.3 + 2.69 \cdot T_{wet\ bulb} \tag{6.2}$$

Using optimum head pressure control and half-speed condenser fan motors the current system would save 85,006 kWh or $3,296 per year. VFD motors would save an additional $600 per year for this system.

### 6.2.6 Head Pressure Control Conclusions

- Fixed head pressure control, although very simple to implement, results in unnecessarily high system energy costs.
- All industrial refrigeration systems have a condensing pressure that results in a minimum energy requirement of the sum of compressor and condenser energy. This optimized pressure is a function of the system characteristics such as condenser size, component arrangement, condenser fan control schemes, and load profiles.
- Optimized head pressure has been shown to be a function of outdoor wet bulb temperature.
- Controlling to optimum head pressure is better than controlling to minimum head pressure when over-sized condensers are used.
- Condensers with variable frequency drives controlling the fan motors result in 8% fan energy savings over on/off fan control if the head pressure is controlled correctly. Half-speed motors also save significant amounts of energy over on/off control but are not as good as VFD controlled motors.
- It has been demonstrated that a over-sized condenser with VFD fan control can potentially save the system more in operating costs than a system with a smaller condenser.

An annual system performance summary of the main head pressure control schemes can be found in Section 7.2.

## 6.3 Evaporator Control

### 6.3.1 Evaporator Capacity Control Options

As mentioned in Section 2.4.3.6 when the load on a refrigerated space is reduced below its design load, the capacity of the system's evaporators must be reduced. The capacity of an evaporator can be altered by either reducing or cycling the refrigerant flow, reducing

or cycling the airflow, changing the temperature difference (TD) of the coil, or some combination of the three. TD is defined as the difference in temperature between the inlet air dry bulb and saturated refrigerant temperature.

### 6.3.2 Evaporator Fan Control

Fan motors can typically be specified to be single speed, multi-speed, or be controlled by variable frequency drives (VFD). Advantages of using multi-speed and VFD motors appear when the capacity of the evaporator is controlled by reducing the airflow. Evaporator capacity control is discussed in detail in Section 2.4.3.6. As shown earlier in Figure 2.17, given a specific system operating point, VFD motor control requires significantly less evaporator fan power than simple on/off control when the evaporator is operated between 30 and 90 percent of its full load capacity. Figure 2.17 also showed that a half-speed motor option also realizes significant power savings in that same operating range. The available capacity of an evaporator depends upon the TD of the coil and the coils unit load factor. The percent of full load that the coil operates at is defined as the actual capacity divided by the available capacity. Typically a system with pumped liquid overfeed coils (see Section 2.4.3.2 for a description of liquid overfeed coils) has a set refrigerant temperature and the actual capacity of an evaporator is changed by modulating the refrigerant and/or airflow.

Refrigerant set point temperature has a direct effect on both compressor and evaporator fan power consumption. A lower refrigerant temperature (and the resultant lower suction pressure) will result in a higher required pressure lift from the compressor and increase the amount of electrical energy consumed by the compressor. A lower refrigerant temperature increases the TD on the evaporator coil, which increases the capacity of the coil and reduces the amount of airflow to needed to meet a specific load. Consequently, the required evaporator fan power is reduced.

Figure 6.12 is a plot of the combined low temperature compressor and freezer evaporator energy requirements [hp] as a function of the low pressure receiver’s set point temperature/pressure. The farthest point to the right on the curves indicates that the

evaporator is at 100 percent of its full load capacity. If the refrigerant were any warmer, the evaporator would not be able to meet the load. The calculations were performed for the current system operating on the peak hour of the average day in July with a fixed head pressure. Figure 6.12 demonstrates that VFD fan control could save the system nearly 19% in combined compressor and evaporator energy requirements if the temperature of refrigerant in the low pressure receiver is –12°F. VFD fan control looses its advantages at high set temperatures because the fans must run at near full speed most of the time anyway. It is also interesting to note that half-speed fan motors have energy requirements that are only approximately 2.5 percent above the VFD motors at temperatures below the optimum of –12°F.

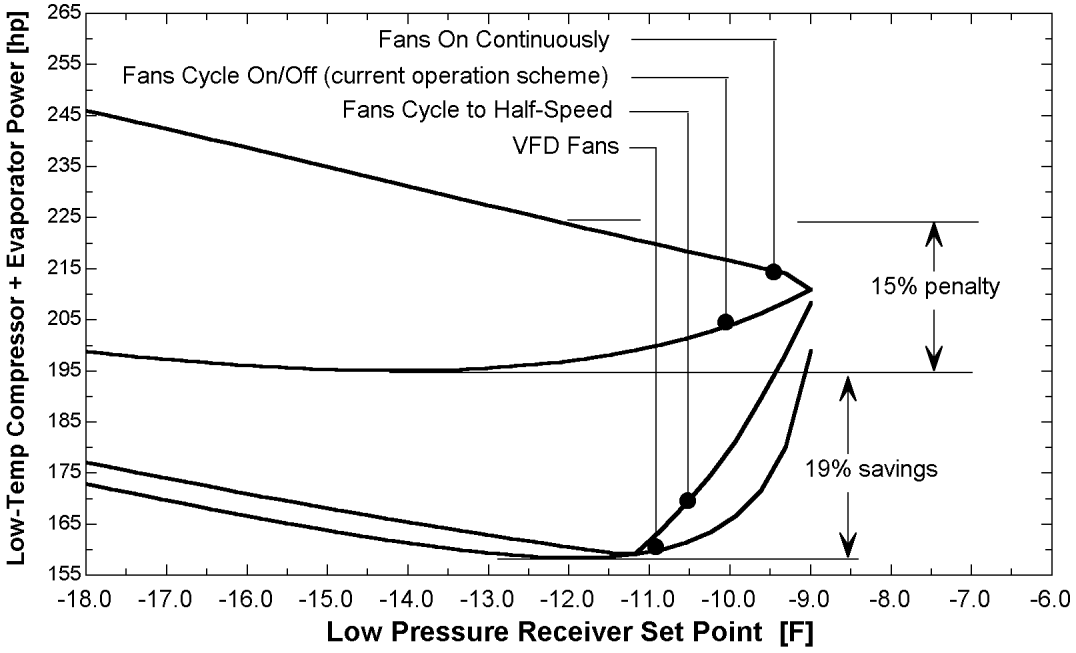


**Figure 6.12 Evaporator Fan Motor Control Strategies**

Figure 6.12 also suggests that controlling capacity by cycling refrigerant flow on and off and leaving the fans running for air circulation purposes would consume about 15% more combined compressor and evaporator fan energy than if the receiver temperature set point were to remain at –12°F.

### 6.3.3 On/Off Fan Control with Optimum Temperature Simulation

The optimum receiver set temperature changes depending on the type of fan control that is used for the evaporators. Also, the optimum set temperature will change as the loads on the evaporators change similar to the way the optimum head pressure changed with different system loads in Figure 6.9. In order to investigate the effects that receiver temperature set point control has on the system, a yearly simulation was done varying the set point temperature of the intermediate and low pressure receivers. Finding the ideal set temperatures using EES optimization procedures for each hour simulated proved to be very computationally intensive. Also, correlating the set point temperatures to another system parameter, as done with head pressure and wet bulb temperature in Figure 6.11, introduced too many non-linearities in the model and convergence problems were experienced. Instead of calculating the ideal set temperatures for each hour of the yearly simulation, the ideal set temperatures were calculated for one hour during each month of the simulation and that value was used for all other hours of that particular month. Careful attention had to be paid to the low pressure receiver set temperature. The optimization routines would tend to set the temperature very low in order to reduce the evaporator fan power. However, at lower temperatures, the VSS-451 screw compressor would not have sufficient capacity. Often the temperature would have to be reset to a higher value in order to avoid having to use the larger and less efficient VSS-751 screw compressor. The trend of optimum set point temperatures from month to month was constant for the on/off evaporator fan operation. The constant temperature trend is expected due to the flatness of the on/off curve in Figure 6.12. For instance, a change in set point temperature from –12°F to –18°F doesn't change the combined evaporator/compressor power consumption much. The slope is steeper for the VFD and half-speed motor curves and proper control of the optimum temperature will have a more significant effect. The monthly optimum set temperature trend for the $12^{th}$ hour of the average monthly days with the system evaporators operating in on/off mode is shown in Figure 6.13. On/off evaporator fan control is currently used in the system.

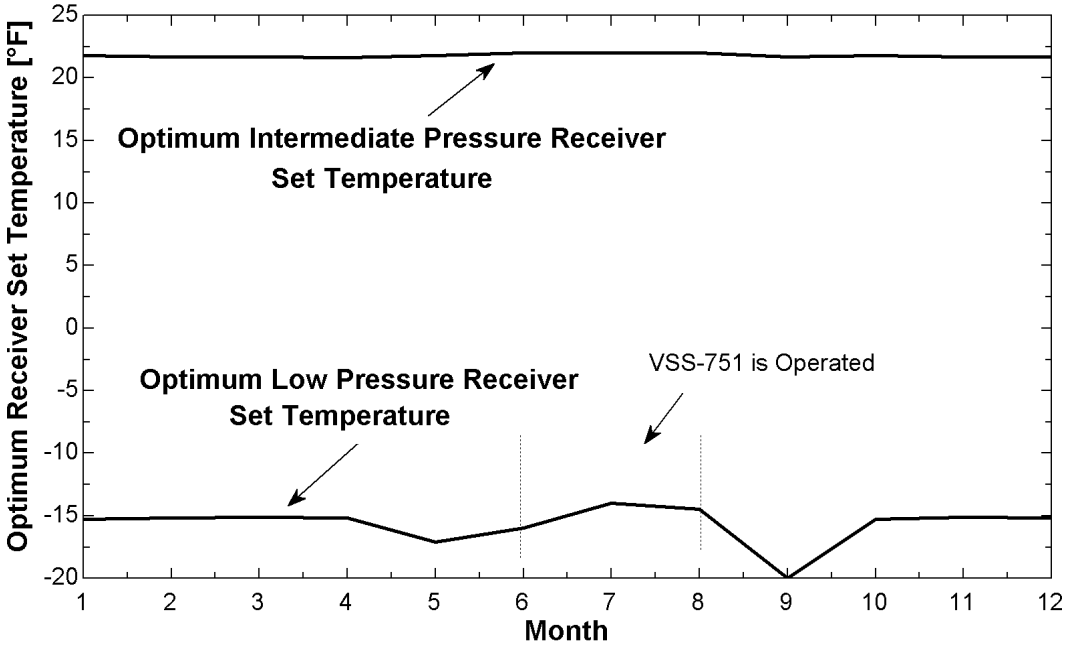


**Figure 6.13 Optimized Receiver Set Temperatures – On/Off Evap. Fan Control**

The actual temperature set points of the intermediate and low pressure receivers are 23°F and –12°F respectively. These set points are not too different from the optimized temperatures therefore not much performance improvement is expected by readjusting the set temperatures to their optimized values. The performance results from the simulation done with set temperatures like those shown in Figure 6.13 are displayed in Table 6.4. Performance measures and electric rates are defined in Section 4.2.3. Reducing the intermediate pressure receiver set point from 23°F to 22°F and the low pressure receiver set point from –12°F to –15°F would result in a savings of approximately $500 in electricity per year.

| Performance Measures | Current System - On/Off Evaporator Fan Control, Constant Receiver Set Temperature | | | Current System - On/Off Evaporator Fan Control, Optimum Receiver Set Temperature | | |
|---|---|---|---|---|---|---|
| | High Temperature | Low Temperature | Combined | High Temperature | Low Temperature | Combined |
| ton-hr / ft²-yr | 19.4 | 11.6 | 15.2 | 19.2 | 11.3 | 14.9 |
| kWh / ton-hr | 1.2 | 1.8 | 1.4 | 1.2 | 1.9 | 1.5 |
| COP | 3.0 | 1.9 | 2.4 | 3.0 | 1.9 | 2.4 |
| hp/ton | 1.6 | 2.5 | 1.9 | 1.6 | 2.5 | 2.0 |
| hp(comp.)/ton | 0.9 | 1.6 | 1.2 | 0.9 | 1.7 | 1.2 |
| hp(cond.)/ton | 0.1 | 0.2 | 0.2 | 0.1 | 0.2 | 0.2 |
| hp(evap.)/ton | 0.2 | 0.3 | 0.2 | 0.2 | 0.2 | 0.2 |
| OnPeak kWh / yr | 379107 | 426176 | 805271 | 378161 | 423587 | 801827 |
| OffPeak kWh / yr | 655582 | 736493 | 1392118 | 654004 | 733214 | 1387169 |
| Peak kW | 194.4 | 218.4 | 412.8 | 194.0 | 216.4 | 410.3 |
| $ / ft² -yr | $0.92 | $0.88 | $0.90 | $0.92 | $0.87 | $0.89 |
| $ / cu.ft -yr | $0.05 | $0.04 | $0.04 | $0.05 | $0.03 | $0.04 |
| $ / ton-hr -yr | $0.05 | $0.08 | $0.06 | $0.05 | $0.08 | $0.06 |
| $ / yr | $42,158 | $47,402 | $89,667 | $42,038 | $46,953 | $89,131 |

**Table 6.4 Receiver Set Temperature Control with On/Off Evaporator Fan Control Comparison**

### 6.3.4 Half-speed Fan Control with Ideal Temperature Simulation

Due to the large distances between individual evaporator units in the current warehouse, it is likely that if VFD evaporator fan control is implemented, each evaporator would have to have its own VFD controller. At most, two or three evaporator units could be placed on a single VFD controller. The large number of VFD controllers that are required for VFD control in the entire warehouse would significantly add to the capital cost of the system. Motors with half-speed operation might be a good alternative in this case. A yearly simulation was done using half-speed evaporator motors. The optimum receiver set temperatures were determined with the same method as described in Section 6.3.3. Optimum set temperatures demonstrate an inverse relationship with the load on the evaporators as shown in Figure 6.14. This figure shows the optimum set temperature for the peak load hour of each month for the design days. The optimum temperature drops when the load on the evaporator is high (summer months) in order to reduce the excessive full speed run time of evaporator fan motors. This savings in power from the

fan motors is greater than the penalty in compressor power as a result of lower suction pressures. Also with less fan energy, fan load on the space is reduced.

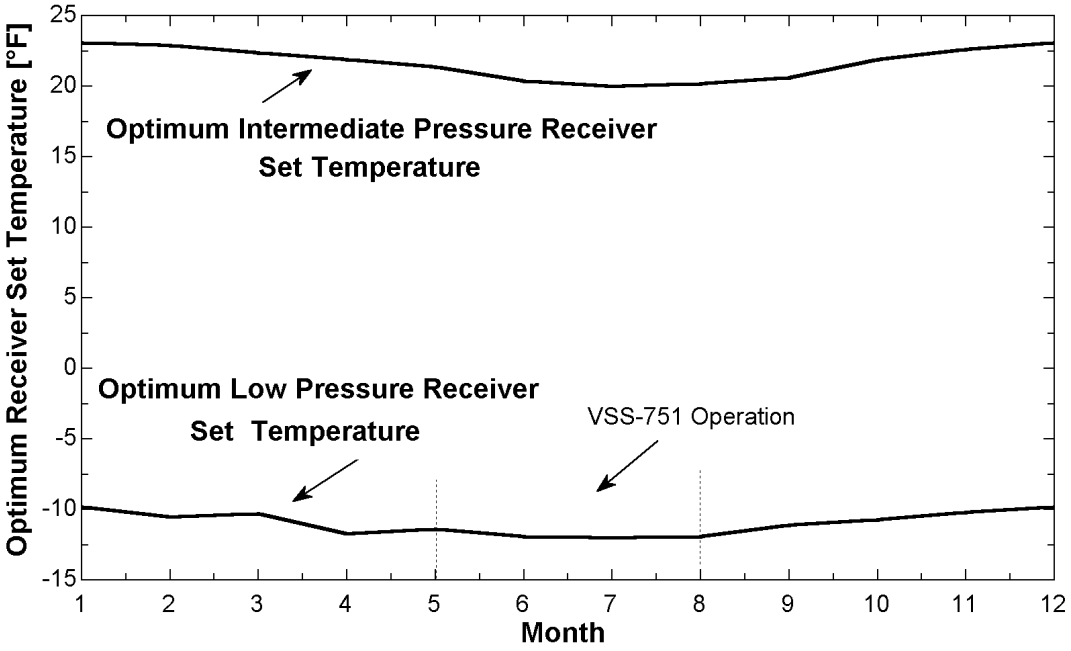


**Figure 6.14 Optimized Receiver Set Temperatures – Half-speed Evap. Fan Control**

The performance of the current system (on/off evaporator fan control) is compared to the performance of the system with half-speed evaporator fan motors and optimum head pressure control in Table 6.5. Performance measures and electric rates are defined in Section 4.2.3. Electrical energy saving of 314,436 kWh or $12,817 per year could be recognized if half-speed motors were used instead of single speed motors.

| Performance Measures | Current System - On/Off Evaporator Fan Control, Constant Receiver Set Temperature | | | Current System - Half-Speed Evaporator Fan Control, Optimum Receiver Set Temperature | | |
|---|---|---|---|---|---|---|
| | High Temperature | Low Temperature | Combined | High Temperature | Low Temperature | Combined |
| ton-hr / ft²-yr | 19.4 | 11.6 | 15.2 | 18.4 | 10.8 | 14.3 |
| kWh / ton-hr | 1.2 | 1.8 | 1.4 | 1.0 | 1.7 | 1.3 |
| COP | 3.0 | 1.9 | 2.4 | 3.4 | 2.1 | 2.7 |
| hp/ton | 1.6 | 2.5 | 1.9 | 1.4 | 2.3 | 1.8 |
| hp(comp.)/ton | 0.9 | 1.6 | 1.2 | 0.9 | 1.5 | 1.1 |
| hp(cond.)/ton | 0.1 | 0.2 | 0.2 | 0.1 | 0.2 | 0.2 |
| hp(evap.)/ton | 0.2 | 0.3 | 0.2 | 0.1 | 0.1 | 0.1 |
| OnPeak kWh / yr | 379107 | 426176 | 805271 | 328270 | 364473 | 692741 |
| OffPeak kWh / yr | 655582 | 736493 | 1392118 | 564106 | 626041 | 1190212 |
| Peak kW | 194.4 | 218.4 | 412.8 | 177.1 | 186.6 | 363.8 |
| $ / ft² -yr | $0.92 | $0.88 | $0.90 | $0.80 | $0.74 | $0.77 |
| $ / cu.ft -yr | $0.05 | $0.04 | $0.04 | $0.04 | $0.03 | $0.03 |
| $ / ton-hr -yr | $0.05 | $0.08 | $0.06 | $0.04 | $0.07 | $0.05 |
| $ / yr | $42,158 | $47,402 | $89,667 | $36,578 | $40,146 | $76,850 |

**Table 6.5 Receiver Set Temperature Control with Half-Speed Evaporator Fan Control Comparison**

### 6.3.5 Evaporator Control Conclusions

- If evaporator fans are run continuously at full speed for purposes of air circulation, an additional 15 percent of combined evaporator and compressor power would be needed to operate the system.
- Optimum receiver temperature/pressure set points are nearly constant through out the year in a refrigerated warehouse when evaporator fans are controlled by an on/off control strategy.
- Optimum receiver temperatures are inversely related to the evaporator loads when half-speed or VFD evaporator fan control is used.
- Half-speed evaporator fan motor control has been shown to save over 14 percent in entire system energy consumption when implemented with optimum receiver temperature/pressure control.

An annual system performance summary of the evaporator fan and refrigerant temperature control schemes can be found in Section 7.2.

## 6.4 Defrosting

The need for defrosting and various methods to defrost evaporator coils in industrial refrigeration applications are discussed in Section 2.4.3.7. The defrost in the current system is a time initiated and time terminated cycle with a few seasonal adjustments. Defrost cycles are initiated in evaporator units twice or three times a day all year long whether they need it or not. This type of defrost strategy can result in excessive energy use if the cycles are timed poorly or if the defrost need changes and the cycles are not adjusted accordingly [Stamm, 1985]. The system is penalized in two main ways when defrost cycles are improperly controlled. First, excessive defrosting (defrosting when there really is not a need for it) or improperly timed cycles simply add load to the conditioned space. The ASHRAE refrigeration handbook suggests that 50 percent or more of the energy used in defrosting escapes into the conditioned space during properly timed defrost cycles[ASHRAE Refrigeration Handbook, 1994]. An even larger amount of energy would escape into the space for improperly timed cycles. Secondly, poorly designed defrost piping and valve systems, in combination with excessive defrosting, result in a large amount of gas blow-by which falsely loads the compressors. Blow-by is the fraction of hot gas that is not condensed and passes through the coil into the wet suction return line. (See Section 2.4.3.7.)

The design load for this system occurs on the $17^{th}$ hour (5pm) of the design day for July. During this hour, calculations using the estimated latent component of the load show that approximately 89 pounds and 131 pounds of ice per hour need to be removed from the cooler and freezer spaces, respectively. There is almost one evaporator in its defrost cycle all the time so the ice melting load would be nearly constant. With the heat of fusion for water at atmospheric pressure equal to 144 Btu/lb, this translates into a total energy requirement of 12.8 and 18.8 MBH for the cooler and freezer spaces respectively. The mechanical contractor's design defrost total heat transfer is approximately 180 MBH for the cooler and 72 MBH for the freezer. (See Section 3.2.2 for a discussion on cold space defrost loads.) The difference between the energy supplied and the energy used to melt the ice is the energy that escapes into the space, energy that goes into boiling out some refrigerant left in the coil when hot gas enters, and energy used in warming the

evaporator coil and fins which is then an additional load on the system as the evaporator is filled with cold refrigerant after the defrost cycle is completed. The difference in energy values becomes even larger during winter months when the infiltration load is much lower.

This large discrepancy between the defrost energy needs and the increased load on the equipment for defrosting would suggest that there must be a better way to defrost than on a time initiated/terminated schedule. Another option would be to defrost only when the evaporator needed it. Ways to determine defrost need are mentioned in Section 2.4.3.7. A yearly simulation was done with the defrost load at half of what the mechanical contractor calculated which doesn't seem unreasonable given the large amount of energy that appears to be wasted by defrosting on a time initiated/terminated schedule. The results are shown in Table 6.6 with a savings of $3,775 per year.

Another minor concern with defrosting in this particular system is the large fraction of blow-by that the evaporators experience when they are defrosting. Blow-by was estimated to average around 10.75 percent by mass for a single evaporator in Section 3.2.1. The error analysis done on the model in Section 3.3.2 indicated that, of the "design" parameters analyzed, blow-by had one of the larger relative effects on total system power consumption. Although, for this system, a 50 percent increase in blow-by resulted in less than 1 percent increase in total system power. As long as blow-by is controlled to less than 20 percent for this large system, given only a single evaporator out of the 19 total is in defrost at any one time, blow-by will have a relatively small impact on overall system performance. For a smaller refrigeration systems or refrigeration systems where a single evaporator delivers a significant part of the total system capacity, excessive blow-by is more of a concern since the mass fraction of blow-by gas to the rest of the refrigerant in the wet suction return line is much higher and the compressor may run out of capacity during periods of defrost. This effect on smaller or large capacity evaporator refrigeration systems was beyond the scope of this research project and was not examined.

Liquid drainers on evaporator coils work like steam traps except with vapor refrigerant instead of steam when the coil is being defrosted. They can be incorporated into the design of top feed hot gas defrost piping. A schematic of top feed defrost piping with liquid drainers is shown in Figure 6.15. Liquid drainers prevent all hot gas from escaping into the wet suction return line and falsely loading the compressors. Table 6.6 also presents the performance results of a simulation with zero blow-by mass flow. An energy savings of $500 per year would result if liquid drainers were installed on all evaporator units.

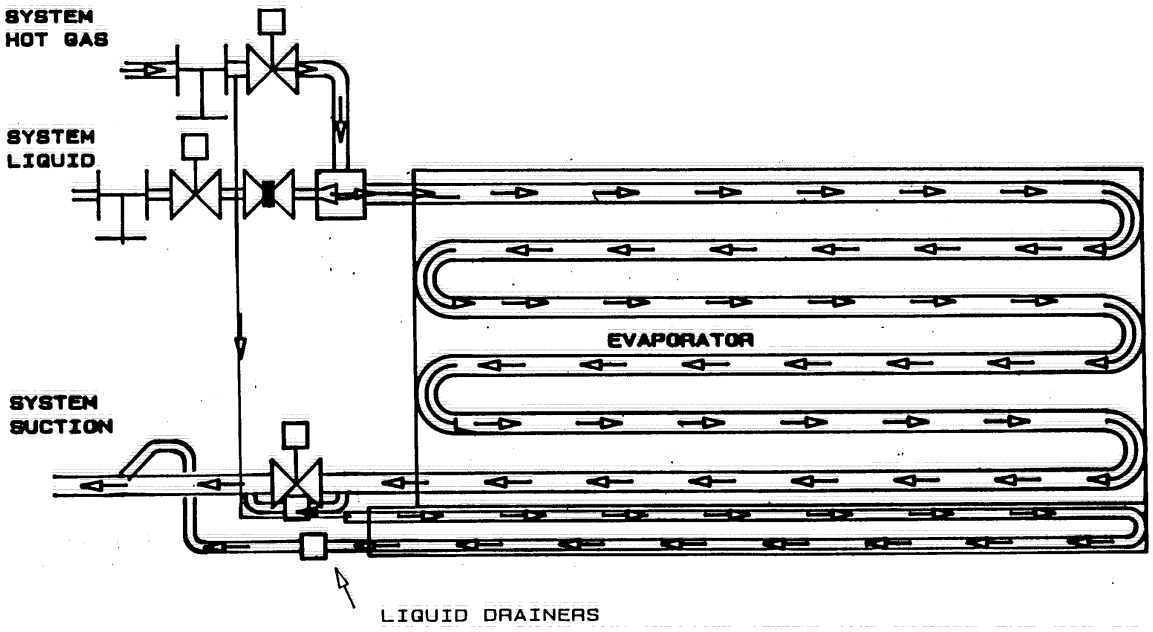


**Figure 6.15 Top Feed Hot Gas Defrost with Liquid Drainers**

| Performance Measures | Current Operation | Half Defrost Load | No Blow-By |
|---|---|---|---|
| ton-hr / ft²-yr | 15.2 | 14.2 | 15.2 |
| kWh / ton-hr | 1.4 | 1.5 | 1.4 |
| COP | 2.4 | 2.4 | 2.5 |
| hp/ton | 1.9 | 2.0 | 1.9 |
| hp(comp.)/ton | 1.2 | 1.2 | 1.2 |
| hp(cond.)/ton | 0.2 | 0.2 | 0.2 |
| hp(evap.)/ton | 0.2 | 0.2 | 0.2 |
| OnPeak kWh / yr | 805271 | 768436 | 798008 |
| OffPeak kWh / yr | 1392118 | 1328524 | 1379141 |
| Peak kW | 412.8 | 399 | 409.7 |
| $ / ft² -yr | $0.90 | $0.86 | $0.89 |
| $ / cu.ft -yr | $0.04 | $0.04 | $0.04 |
| $ / ton-hr -yr | $0.06 | $0.06 | $0.06 |
| $ / yr | $89,667 | $85,892 | $89,037 |

**Table 6.6 Defrost Modification System Effects**

## 6.5 Warehouse Doors and Infiltration

The error analysis presented in Section 3.3.2 revealed that the fraction of time that warehouse doors are left open has a very significant effect on the performance of the system. Larger door open fractions lead to significantly more infiltration load and more need for defrosting. Door open fractions were listed earlier in Table 3.4. As a demonstration of large effect of door infiltration effects, a yearly simulation was done on the current system with the door open fraction values reduced by half and the defrost load reduced by 25 percent. Results of this simulation are compared to the normal operation of the system in Table 6.7. Performance measures and electric rates are defined in Section 4.2.3.

If the doors were open half the time in this particular system, an estimated savings of $7,850 per year in electricity could be saved!

| Performance Measures | Current System Operation | | | Door Open Time Fractions are Reduced by Half | | |
|---|---|---|---|---|---|---|
| | High Temperature | Low Temperature | Combined | High Temperature | Low Temperature | Combined |
| ton-hr / ft²-yr | 19.4 | 11.6 | 15.2 | 17.7 | 10.3 | 13.7 |
| kWh / ton-hr | 1.2 | 1.8 | 1.4 | 1.2 | 1.9 | 1.5 |
| COP | 3.0 | 1.9 | 2.4 | 3.0 | 1.9 | 2.4 |
| hp/ton | 1.6 | 2.5 | 1.9 | 1.6 | 2.6 | 2.0 |
| hp(comp.)/ton | 0.9 | 1.6 | 1.2 | 0.9 | 1.6 | 1.2 |
| hp(cond.)/ton | 0.1 | 0.2 | 0.2 | 0.2 | 0.2 | 0.2 |
| hp(evap.)/ton | 0.2 | 0.3 | 0.2 | 0.2 | 0.3 | 0.2 |
| OnPeak kWh / yr | 379107 | 426176 | 805271 | 352335 | 390082 | 742421 |
| OffPeak kWh / yr | 655582 | 736493 | 1392118 | 611097 | 677649 | 1288771 |
| Peak kW | 194.4 | 218.4 | 412.8 | 171.9 | 180.0 | 351.9 |
| $ / ft² -yr | $0.92 | $0.88 | $0.90 | $0.85 | $0.79 | $0.82 |
| $ / cu.ft -yr | $0.05 | $0.04 | $0.04 | $0.05 | $0.03 | $0.04 |
| $ / ton-hr -yr | $0.05 | $0.08 | $0.06 | $0.05 | $0.08 | $0.06 |
| $ / yr | $42,158 | $47,402 | $89,667 | $38,905 | $42,823 | $81,816 |

**Table 6.7 Effect of Door Infiltration Loads on System Performance**

## 6.6 Optimized System Simulation

The estimated savings attributable to the different system arrangements and optimization techniques discussed in Chapters 5 and 6 are, unfortunately, not always additive. For example, this system would not benefit from installing a variable frequency drive on an evaporative condenser that is sized for 95°F design condensing temperature because the optimum head pressure requires the fans to run at full speed most of the time anyway. Several of the optimization strategies discussed in Chapters 5 and 6 that appeared to have the biggest effects in reducing the overall power consumption of the system were simultaneously implemented in a yearly simulation.

The following design configuration and operating techniques were implemented in the optimized design:

- The banana and tomato ripening rooms were split to their own separate system. A discussion of a split system is in Section 5.4. This division of the system increased the number of suction levels, and therefore compressors, from two to three. It also allowed multi-level head pressure control since two separate evaporative condensers were used. It was decided not to implement the thermosiphon option

due to the very high first cost associated with distribution of thermosiphon refrigerant to each individual banana or tomato ripening room.

- The main system's evaporative condenser was left at its current size (over-sized). The banana/tomato room system's evaporative condenser was sized at a design of 95°F. Since the banana/tomato room rarely operate at even half of the design load, this condenser could be considered over-sized as well. Variable frequency drives (VFD's) were used on both evaporative condensers. The advantages of VFD's are discussed in Section 6.2.2.
- Ideal head pressure control, discussed in Section 6.2.3, was implemented on both evaporative condensers.
- Multi-level head pressure control was used. The minimum head pressure allowed in the banana/tomato system with direct expansion evaporators was kept at 130 psia as done in the current system. The head pressure in the main system was allowed to drift as low as 95 psia. Multi-level heat pressure control is discussed in Section 5.4.1.
- Half-speed evaporator motor control was also simulated. Advantages of half-speed motor operation are discussed in Section 6.3.2.
- Ideal receiver set temperature/pressure as discussed in Section 6.3.4 and was also implemented in the optimized system simulation. Optimized temperatures were only set for the intermediate and low pressure receivers in the main system. Optimum temperatures were not calculated for the banana/tomato rooms since the fruit ripening process requires delicate control of the refrigerant temperature.
- It was demonstrated in Section 6.4 that a significant improvement could be made on the defrosting control of the system. For instance, defrosting should be done on demand instead of on a time initiated and time terminated schedule. The defrost load on the system along with the blow-by was reduced by 25% in the optimized simulation. Calculations done in Section 6.4 suggest the defrost load could be reduced even more however.

Figure 6.16 below shows the new optimum head pressure control curves. A discussion on the current system's optimum head pressure control is in Section 6.2.5.

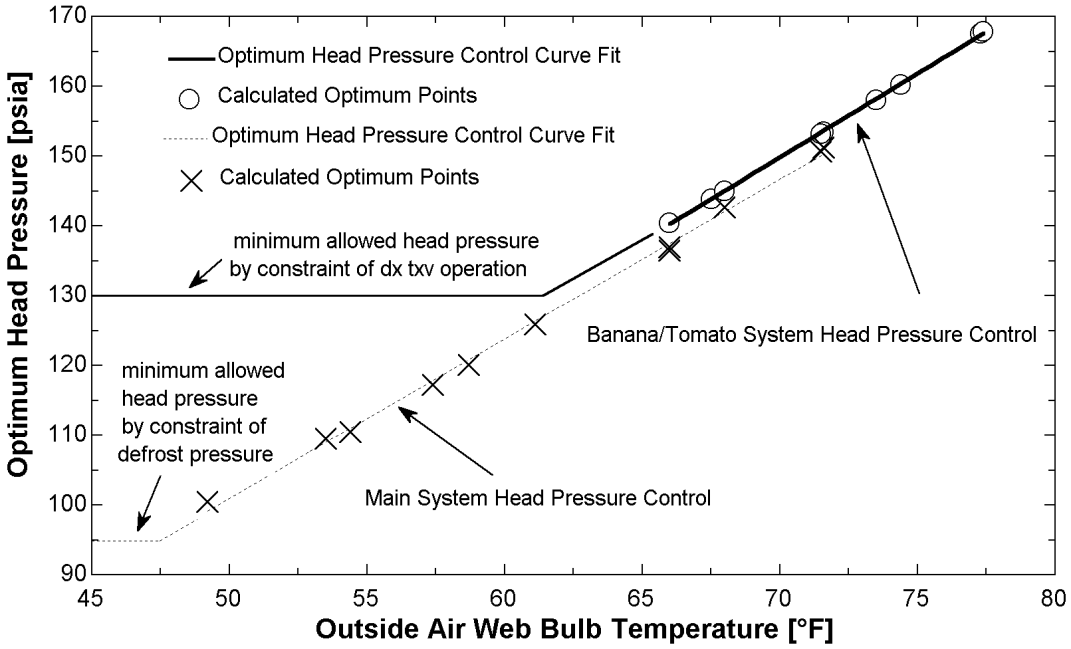


**Figure 6.16 Optimized System Head Pressure Control Curves**

Optimum receiver set temperature/pressure monthly trends for both the average and maximum simulation days are shown in Figure 6.17. A discussion about the calculation of optimum temperatures is located in Section 6.3.4.

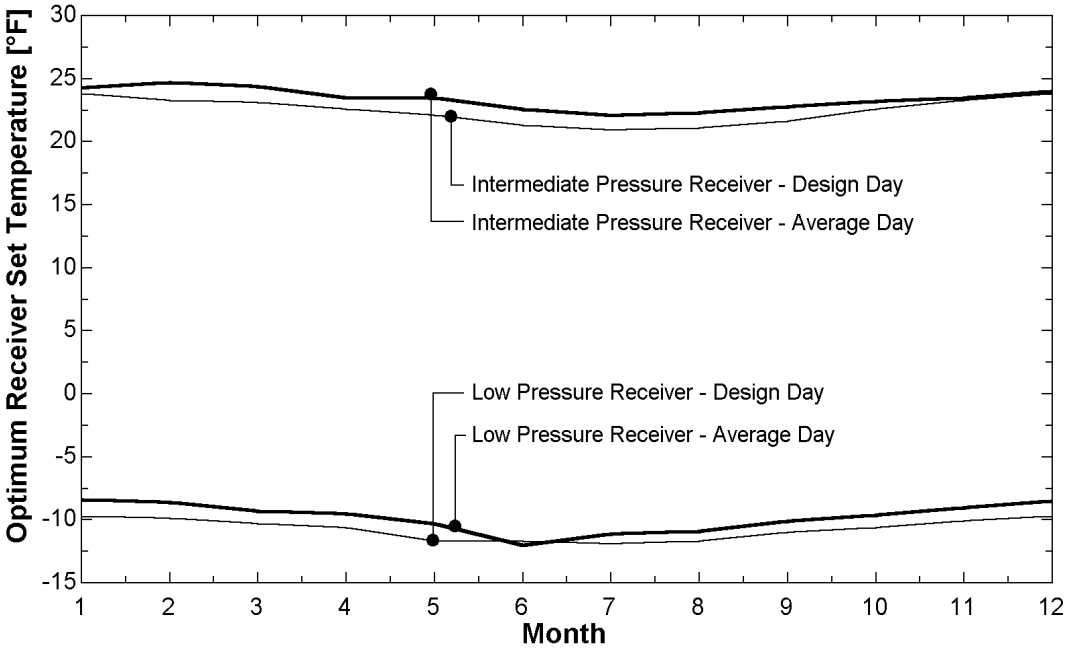


**Figure 6.17 Optimum Receiver Set Point Temperatures**

Yearly simulation performance measures from the optimized system are compared to how the system is currently operated in Table 6.8. Performance measures and electricity costs are defined in Section 4.2.3. Adding an additional small compressor and small evaporative condenser along with VFD condenser fan control and half-speed motors on the evaporators would save the system $25,795 per year in energy costs. This savings is based on relatively inexpensive electricity costs around the Milwaukee, WI area. The saving would be much larger for areas where electricity is more expensive.

| Performance Measures | Current System Operation | | | Optimized System Operation | | |
|---|---|---|---|---|---|---|
| | High Temperature | Low Temperature | Combined | High Temperature | Low Temperature | Combined |
| ton-hr / ft²-yr | 19.4 | 11.6 | 15.2 | 17.1 | 10.6 | 13.6 |
| kWh / ton-hr | 1.2 | 1.8 | 1.4 | 0.8 | 1.5 | 1.1 |
| COP | 3.0 | 1.9 | 2.4 | 4.4 | 2.3 | 3.2 |
| hp/ton | 1.6 | 2.5 | 1.9 | 1.1 | 2.0 | 1.5 |
| hp(comp.)/ton | 0.9 | 1.6 | 1.2 | 0.6 | 1.2 | 0.9 |
| hp(cond.)/ton | 0.1 | 0.2 | 0.2 | 0.1 | 0.2 | 0.1 |
| hp(evap.)/ton | 0.2 | 0.3 | 0.2 | 0.1 | 0.1 | 0.1 |
| OnPeak kWh / yr | 379107 | 426176 | 805271 | 239539 | 322955 | 557870 |
| OffPeak kWh / yr | 655582 | 736493 | 1392118 | 407525 | 551588 | 951195 |
| Peak kW | 194.4 | 218.4 | 412.8 | 143.0 | 185.3 | 325.6 |
| $ / ft² -yr | $0.92 | $0.88 | $0.90 | $0.60 | $0.68 | $0.64 |
| $ / cu.ft -yr | $0.05 | $0.04 | $0.04 | $0.03 | $0.03 | $0.03 |
| $ / ton-hr -yr | $0.05 | $0.08 | $0.06 | $0.04 | $0.06 | $0.05 |
| $ / yr | $42,158 | $47,402 | $89,667 | $27,443 | $36,811 | $63,872 |

**Table 6.8 Current vs. Optimized System Performance Comparison**

# *Chapter 7 -Recommendations and Conclusions*

## 7.1 Instrumentation Package Recommendation

Industrial refrigeration performance optimization can not be accomplished without adequate instrumentation and data acquisition capabilities. The operator needs sufficient information in order to calculate how the system is performing. This information also needs to be recorded in order to provide the opportunity for historical trending of system performance. Throughout this paper, system performance was identified by the performance measures defined in Section 4.2.3. All these measures are different forms and totals of two main parameters. These two main parameters are electrical energy consumed [kWh] and total amount of refrigeration done [ton-hr]. With an accurate measurement of these two values, a system operator can not only judge how the system is currently performing, but how much of an effect that changing the system component arrangement or operating procedures had on the system performance.

Control of the system is also an important task. Proper instrumentation should also be provided for control. This may include pressure and/or temperature measurements at critical areas such as in low and high pressure receiver vessels or in conditioned spaces.

### 7.1.1 Electric Power

Electrical power consumption [kW] may be the easiest but not necessarily the least expensive to record. Figure 7.1 shows the distribution of where all the power for the current system is being used on the peak hour of an average day in July. Figure 7.2 shows the same for an average day in January.

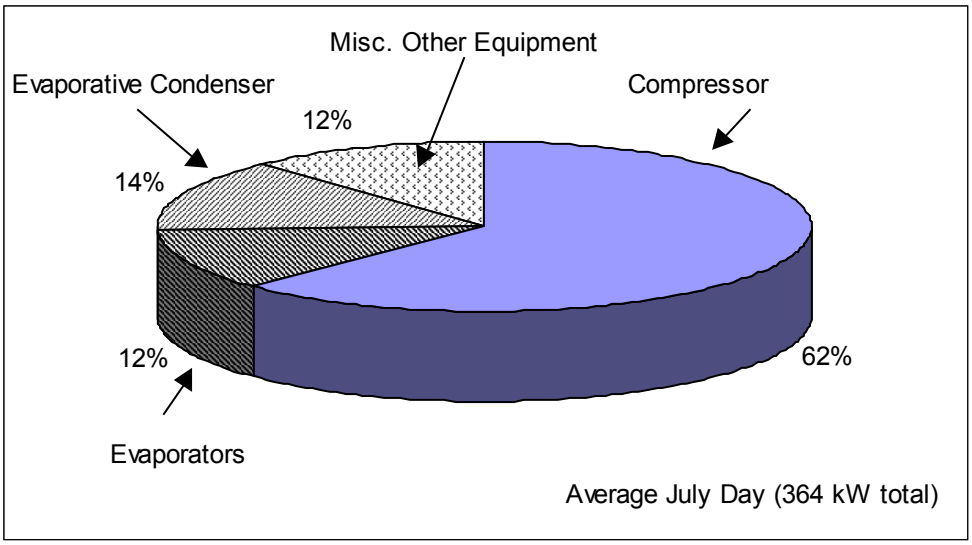


**Figure 7.1 July Distribution of Total Refrigeration System Power**

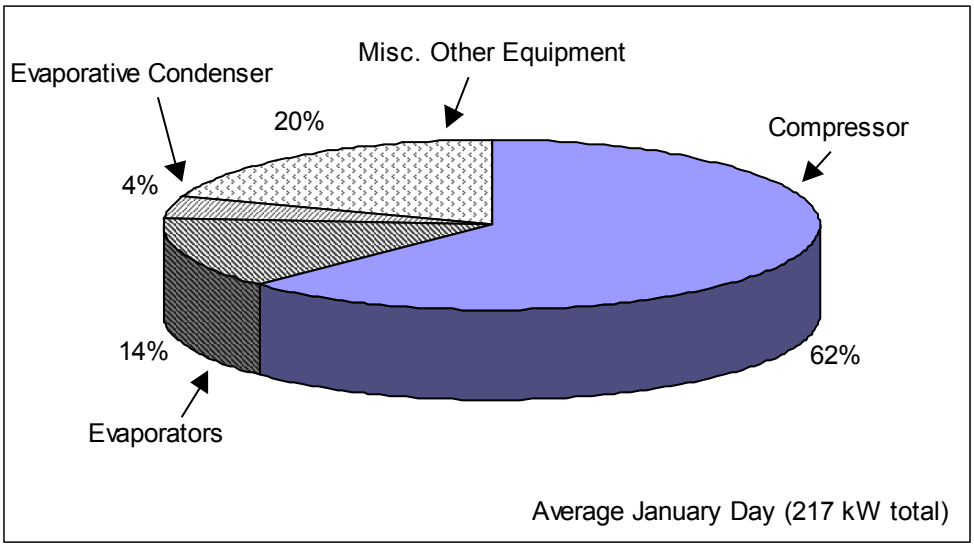


**Figure 7.2 January Distribution of Total Refrigeration Power**

Figure 7.1 and Figure 7.2 suggest that it would be most important to monitor the power to the compressors since they account for more than half of the total power consumed throughout the year. Evaporator power is also a significant portion of the total annual power and important in total system performance optimization. Condenser power is relatively small when outdoor conditions are very cold, however it increases to a significant portion of the total system power when outdoor conditions warm and require the condenser to operate wet. Miscellaneous other equipment includes power from

circulating pumps, mechanical room lights, computers, and control equipment. Miscellaneous power will likely not change with system optimization and is therefore unimportant to closely monitor. If multiple compressors and/or condensers are used and are not operated with identical control strategies, it would be advantageous to monitor the power consumption of each machine separately. Monitoring the power consumption for each separate compressor when more than one screw compressor is sharing a load will also help identify the characteristic operating curves discussed in Section 6.1.

### 7.1.2 Refrigeration Loads

Refrigeration effect [ton or ton-hrs] is also an important parameter to record accurately. In refrigeration systems with constant loads, the refrigeration load may be easy to calculate from knowledge of the cooling process. For instance, the load placed on a refrigeration system cooling a tank of milk could be calculated with knowledge of the specific heat and before and after temperatures of the milk. In other systems, such as the warehouse facility examined in this study, the loads may vary significantly from day to day depending upon the weather and the movement of refrigerated product. In this situation, the instantaneous loads placed on the compressors are most accurately determined by calculating the product of mass flow of refrigerant through the system and its change in specific enthalpy from when it exits the high pressure receiver as a liquid to when it enters the suction line of the compressor as a gas. For systems with multiple suction levels, multiple stages of compression or performance enhancement devices such as subcoolers, intercoolers, or suction line heat exchangers, the determination of the correct specific enthalpies to use in the load calculation must be carefully considered in order to calculate the true refrigeration effect.

An accurate knowledge of mass flow for each load of a system must be obtained in order to calculate the actual load. For simple systems, such as the low temperature side of the system looked at in this paper, the mass flow could be calculated with aid of the compressor maps and accurate knowledge of suction and discharge pressure and any unloading imposed upon the compressor. Mass flow can be calculated by dividing the actual capacity of the compressor defined in Equation (2.5) by the actual change in

enthalpy across the evaporator ($\Delta h_{actual}$) also defined in Section 2.4.1.2. The accuracy of this calculation will be limited by the accuracy of the compressor manufacturer's data.

If the system is more complicated, such as the high temperature load of the current system, alternative ways of obtaining mass flow must be used. One possible alternative is direct measurement with a mass flow meter. Most flow meters require the fluid stream that they are measuring to be a single-phase fluid. This limits the possible locations for a flow meter in a refrigeration system. In systems with liquid overfeed evaporators, a flow meter located in the liquid recirculation line leading from the receiver to the evaporator would not be useful unless the enthalpy of the two-phase refrigerant in the wet suction return line could be determined. The best place for a flow meter would be in the high pressure liquid lines between the receiver vessels as done in the system studied in this project. Again, with more complex systems, careful attention must be paid to calculating the actual mass flow of refrigerant vaporized in the evaporators as well as the associated specific enthalpies used in the load calculation. For instance, to calculate the mass of refrigerant vaporized in the high temperature evaporators, the mass flow into the low pressure receiver as well as the flash gas generated by the low temperature refrigerant as it is throttled to the intermediate pressure and the refrigerant used in the direct expansion evaporators must be subtracted from the total amount of refrigerant measured in the high pressure liquid line which is supplying refrigerant to both the high and low temperature loads.

### 7.1.3 Summary of Recommended System Instrumentation

Beyond the suggested measurements of electricity consumption and mass flow, additional measurements must be made throughout the system in order to aid in system control or to finish the load calculations by computing the required refrigerant specific enthalpies. Table 7.1 is a summary of all the necessary measurements needed to get a basic understanding of system performance. These measurements will also enable an operator to recognize when a change made in system operation actually resulted in performance improvement.

| Location | Minimum Measurement | Preferred Measurement | Usefulness |
|---|---|---|---|
| Condenser | Pressure | | Condenser Fan Control |
| Condenser | Mechanical Room Power | Fan and Pump Power | Electricity Consumption |
| Compressor(s) Suction | Dry Suction Line Pressure | Individual Machine Suction Flange Pressure | Capacity, Horsepower, and Mass Flow Calculations |
| Compressor(s) Discharge | Discharge Line Pressure | Individual Machine Discharge Flange Pressure | Capacity, Horsepower, and Mass Flow Calculations |
| Compressor(s) | Part Load Operation | | Capacity, Horsepower, and Mass Flow Calculations |
| Compressor(s) | Mechanical Room Power | Individual Machine Power Draws | Electricity Consumption |
| Evaporator | Coil Refrigerant Temperature/Pressure, Inlet Air Temperature | Supply and Coil Refrigerant Temp./Press., Inlet and Outlet Air Temperature | Coil Capacity Calculations |
| Evaporator | | Static Pressure Drop or Time Clock Measuring Liquid Solenoid Feed Time | Defrost Demand Determination |
| Evaporator | Evaporator Fan Power | | Electricity Consumption |
| Receiver Vessels | Temperature/Pressure | | Set Point Control, Load Calculations |
| Receiver Vessels | | High Pressure Liquid Supply Line Mass Flow | Load Calculations |
| Cold Space | Temperature | | Control |
| Outdoor Air | Dry Bulb, Wet Bulb | | Condenser Fan Control |
| Entire System | Electric Bill | | Monthly Analysis |

**Table 7.1 Recommended Performance Monitoring Measurements**

## 7.2 Energy Comparison of System Designs and System Control Techniques

Table 7.2 compares the yearly simulation results of each system design and control technique explored in Chapters 5 and 6. Listed in Table 7.2 is the peak electrical demand for the year, the total electrical energy used for on and off peak hours for the year, the yearly electrical energy cost, and the amount of energy savings compared to how the system is currently operated in dollars. A negative number in the energy savings column would indicate an increase in electrical energy cost for the year. The cost of electrical energy is defined in Section 4.2.3.

| System Design Option | Section Number | Peak kW | On-Peak kWh | Off-Peak kWh | Electric Cost per year | Electric Savings per year |
|---|---|---|---|---|---|---|
| Current System | | 413 | 805,271 | 1,392,188 | $89,667 | $0 |
| Smaller Condenser | 5.2 | 420 | 785,604 | 1,356,681 | $87,659 | $2,008 |
| Two-stage Compression | 5.3 | 407 | 813,931 | 1,408,604 | $90,453 | -$786 |
| Split System | 5.4 | 398 | 732,334 | 1,255,896 | $82,610 | $7,057 |
| Split System with Thermosiphon | 5.5 | 397 | 708,070 | 1,212,072 | $80,655 | $9,012 |
| Optimization Technique | | | | | | |
| Bi-Level, Fixed Head Pressure | 6.2.1 | 413 | 832,898 | 1,452,172 | $92,242 | -$2,575 |
| VFD Condenser Fans, Minimum Head Pressure | 6.2.4 | 411 | 783,410 | 1,352,304 | $87,458 | $2,209 |
| VFD Condenser Fans, Optimum Head Pressure | 6.2.5 | 399 | 769,193 | 1,331,056 | $85,811 | $3,856 |
| On/Off Evaporator Fans, Optimum Receiver Temp. | 6.3.3 | 410 | 801,827 | 1,387,169 | $89,131 | $536 |
| Half-speed Evaporator Fans, Optimum Reciever Temp. | 6.3.4 | 364 | 692,741 | 1,190,212 | $76,850 | $12,817 |
| Hot Gas Defrost Control | 6.4 | 399 | 768,436 | 1,328,524 | $85,892 | $3,775 |
| Warehouse Door Infiltration | 6.5 | 352 | 742,421 | 1,288,771 | $81,816 | $7,851 |
| Optimized System - Split System, VFD Evap.Cond.Fans, Half-speed Evap.Fans, Reduced Defrost | 6.6 | 325 | 557,870 | 951,195 | $63,872 | $25,795 |

**Table 7.2 Energy Savings Comparison Between Optimization Techniques**

It is important to recognize that many of the savings presented in Table 7.2 are not additive. For instance, it would not make sense to install a reduced sized condenser on this system and then expect to save an additional $3,900 in energy costs by implementing variable frequency drive control on the fan motors because the fans on the reduced sized condenser will have to run at full speed most of the year anyway. The bottom row of Table 7.2 compares the operating costs for an optimized system that takes advantage of as many of the significant optimizing techniques as possible that could realistically be implemented at the facility. A detailed description of this optimized system is provided in Section 6.6. An optimized refrigeration system meeting the cooling needs of a two-temperature cold storage food warehouse and distribution facility has been shown to operate at a cost of $0.04 per ft² per year for a 34°F storage space and $0.06 per ft² per year for a 0°F storage space. Product is received at storage temperature so there is no "product" load associated with those cost figures.

## 7.3 Research Conclusions

Figure 7.1 demonstrates that compressors, evaporative condensers, and evaporators in an industrial refrigeration system together consume about 88 percent of the total energy

used. Most optimization techniques examined in this paper focused on saving operating costs from one or more of the main energy consuming components.

### 7.3.1 Compressors

Compressors consume over 60 percent of the total system energy. Total compressor power for a system is a function of its suction pressure, discharge pressure, total system load, and unloading in the case of screw compressors which do not unload linearly.

Compressor suction pressure is largely governed by the temperature of refrigerant that is required in the evaporators. A lower required refrigerant temperature results in lower suction pressure and increased compressor power requirements. Refrigerant temperature set point has also been shown to have an effect on evaporator power consumption. A lower refrigerant temperature results in less power consumed by the evaporator fans. There is an optimum refrigerant set point that produces a minimum combined compressor and evaporator power draw. It was shown that this optimum temperature is evaporator fan control scheme dependent and has a slight inverse relationship with the total cooling load on the system (receiver set point temperatures should be lowered slightly as the load on the evaporators increase).

A second parameter that has a direct effect on compressor suction pressure and therefore required power is the pressure drop in the wet and dry suction lines. Excessive pressure losses due to undersized piping, fittings, and valve trains will significantly reduce the available capacity of the compressor and require increased compressor power. It has been shown that pressure losses in suction lines affect the system much more than in discharge lines.

Compressor discharge pressure is largely governed by the control of the system's condenser. A lower condensing pressure results is a lower compressor discharge pressure and less compressor power. However, to maintain low condensing pressures, the fans on the condenser must operate more which increases the energy consumption of the condenser. There is an optimum condensing pressure that minimizes the combined

compressor and condenser power consumption. It was shown that the optimum condensing pressure is dependent on the type of condenser fan control strategy used. It was also discovered that the optimum condensing pressure had a linear relationship with the outdoor wet bulb temperature. This relationship is a result of the evaporative condenser's wet bulb performance dependency and the general proportional trend of the total system load with wet bulb temperature for this cold storage facility.

Compressors in cold storage refrigeration systems without any thermal storage capability are rarely operated at their design conditions. When part load operation is required, which is most of the time, the compressors must be unloaded in order to balance the cooling capacity of the system with the evaporator load. Reciprocating compressors have linear unloading curves and therefore introduce small power consumption penalties when operated at part load. This is not the case however for screw compressors. As screw compressors are unloaded they require more power per unit of cooling capacity. It is recommended that screw compressors be sized appropriately so they can be operated at or near full capacity most of the time. Screw compressors should be used for base loading and reciprocating compressors should be used to meet the transient portion of a varying load.

If two screw compressors are sharing a load there exists a point where it is better to fully load one compressor rather than split the load equally. In the case of two equally sized Vilter screw compressors, it is best for the compressors to share the load up to an identifiable cross-over point which occurs when the load on the system is 62 percent of the available capacity of the compressors. Beyond that point it is best to fully load one of the screws and make up the difference with the other. The cross-over point can be identified using figures similar to those developed in Section 6.1. When load sharing between two unequal sized screw compressors is required, calculations have shown that it is best to first fully load the smaller of the two, then at a certain identifiable cross-over point, it is best to fully load the larger of the two compressors and make up the difference with the smaller of the two. Calculations with unequal sized Vilter screw compressors (the big compressor is 66% larger than the small compressor), indicated that this cross-

over point occurred when the load was 73 percent of the available capacity of the compressors. Cross-over points do not change locations with different suction and discharge conditions, they may however change locations with compressors from manufacturers other than Vilter because they have different unloading curves.

Finally, compressor power can be reduced by simply reducing the load on the system. Table 7.2 suggests that either cutting the amount of parasitic defrost load that enters the space or the time that the doors of the warehouse are open by half will save this system 4.2 and 8.8 percent in electrical costs per year respectively. Also, using multi-speed evaporator fan control significantly cuts down on the internal heat gains of the cold space.

### 7.3.2 Evaporative Condensers

Assuming a design condensing temperature of 95°F, the evaporative condenser in the system that was studied, using on/off fan control, was sized nearly 3 times the size it had to be. The existing unit in the system currently has an 85°F design condensing temperature. A smaller sized, 95°F design evaporative condenser unit, also using on/off fan control, has much smaller fan and pump motors and would save this system 2.2 percent per year in electric costs. However, it was demonstrated that by installing a variable frequency driven (VFD) motor on the current, over-sized evaporative condenser fans, the system would operate with 2.5 percent less power use per year. This additional savings is partly due to the fact that the head pressure can be reduced most of the year saving on compressor power. If both the VFD motor control was installed and optimum head pressure control strategies were implemented, the system would save 4.3 percent in electric costs per year. VFD motor control on the smaller evaporative condenser unit would not save much energy since the fans need to run at full speed most of the time anyway. Generally speaking, it would be best to install an over-sized evaporative condenser with VFD motor control on an industrial refrigeration system.

### 7.3.3 Evaporators

The optimum control, design, and operation of evaporators resulted in some of the most significant energy savings of all the optimization techniques examined. This is largely

due to the fact that between all the conditioned spaces in the warehouse there are 40 individual evaporator units, each with a couple of electric motors. Even though the motors are small, the shear number of them results in significant energy consumption and sensible heat gain to the space.

It was demonstrated that operating the evaporators with a half-speed motor option saved the system nearly 14 percent in annual power costs. Variable frequency driven (VFD) motors would save even more, however due to the large number of individual evaporator units, the option of controlling each of them with VFD was deemed financially unfeasible.

Another concern with the operation of evaporators identified in this paper is the defrosting process. All evaporators that operate with refrigerant temperatures below the freezing point of water and dew point of the conditioned space will condense and freeze water out of the passing air stream and build a layer of frost on the airside of the coil. The frost layer leads to performance degradation of the evaporator due to reduced heat transfer and airflow. 13 percent or approximately $10,000 per year of the current system's total electrical energy use is due to its defrost needs. The type of defrost control currently utilized in the system is time initiated - time terminated. Each evaporator in the cooler, loading dock, and freezer space is set to defrost twice or three times a day regardless of the actual amount of frost that has accumulated on the coil. Based upon the load calculations of the installing mechanical contractor and the system model, the amount of energy being provided to defrost the coils is nearly 15 times the amount of energy needed to melt the ice. If defrosting was done on demand instead of on a time schedule, it was theorized that the amount of defrost throughout the year could be reduced by half. A reduction in defrost energy by half resulted in an electric cost savings of 4.2 percent per year.

Another defrost related parameter that was examined in this paper is termed blow-by. Blow-by is the mass fraction of vapor refrigerant that passes through the evaporator without condensing, over the total refrigerant flow through the evaporator during defrost.

Blow-by results in a false load on the compressor and reduces the performance of the refrigeration system. Blow-by for this system was estimated at 11 percent based on the installing contractor's defrost load calculations and experimental data. However, only one evaporator is in defrost at a time and the small amount of blow-by generated by the single evaporator compared to the total amount of vapor loading the compressors affected the system power requirement less than 1 percent. For smaller refrigeration systems or large refrigeration systems with single evaporator units delivering a significant portion of the total system capacity, a single evaporator with a blow-by of 11 percent may result in so much compressor capacity reduction that the system can not meet the required refrigeration load. Defrost piping designs, such as top fed hot gas with liquid drainers, exist that prevent blow-by all together and should be used if possible.

### 7.3.4 Warehouse Operation

All cooler, loading dock, and freezer spaces in this model have doors that lead directly to the outside. The model's infiltration load was based on the fraction of time that the doors remained open. Door open times were adjusted until the design infiltration load matched that of the installing mechanical contractor's design load calculations. To examine the effect that warehouse doors have on system performance, a yearly simulation was done with all door open fractions reduced by half. Reducing the door open fractions by half resulted in an 8.8 percent annual electric cost savings. Infiltration through doors has a significant impact on overall system performance in refrigerated warehouses and should be kept to a minimum if possible.

### 7.3.5 System Component Arrangement

When a cold storage facility with two suction pressures has a higher suction pressure about halfway between the low suction pressure and the average condensing pressure, it seems, at first, like a good opportunity to use two-stage compression. However, it was discovered that if the current system were converted to a two-stage system, that the annual electrical energy cost would actually increase. This is due to several unavoidable losses introduced to the system associated with a change over to two-stage compression including unfavorable compressor unloading penalties and increased pressure losses due to the required piping arrangement and additional equipment. These parasitic losses were

slightly larger than the compressor work saved by implementing two-stage compression. The average low temperature compression ratio for this system was a modest 4.5:1 due to the minimum head pressure control algorithm and a relatively warm low suction temperature of 0°F. For systems with higher head pressures or lower suction temperatures, two-stage compression would be a good option to consider. Two-stage compression for this system would be advantageous when the compression ratio exceeds 5:1.

Another alternative component arrangement considered in this study was based on the simple fact that the current system has two suction levels but three distinct evaporator temperatures. The system has suction levels at -12°F to serve the freezer space, and 23°F to serve the cooler, loading dock, and banana/tomato ripening rooms. The current suction levels are appropriate for operation of the freezer, cooler, and loading dock spaces, however back pressure regulators are used to maintain the refrigerant temperature in the fruit ripening rooms between 45-55°F. This system is providing approximately 50°F refrigeration to the banana/tomato rooms at the increased cost of 23°F refrigerant. It made sense to add another suction level to the system for this reason. It was also learned that the head pressure of the entire system had to be maintained at artificially high levels in order to control the direct expansion evaporators in the banana/tomato rooms properly. The head pressure requirements of the banana/tomato rooms plus the obvious need for an additional suction level suggested it may be best to meet the banana/tomato room loads with a completely separate system. A yearly simulation was done with the banana/tomato rooms operating on a separate refrigeration system. The simulation suggested that the annual electrical cost of the system would decrease by 7.9 percent or $7,000. However, an additional compressor, evaporative condenser, and associated equipment would have to be purchased.

## 7.4 Future Work Recommendations

Industrial vapor compression refrigeration systems have been around for more than 100 years. However, still very little knowledge about the interaction between components and actual performance of entire system is documented. Throughout the course of this

research several key areas of refrigeration systems were identified as potential places for system optimization. Further research would best be directed toward the following efforts.

- Using the recommended measurements in this study, accurately assess the performance of an industrial refrigeration system, develop standardized procedures for documenting or commissioning the performance of any industrial refrigeration system.
- Establish a database of industrial refrigeration system performance data and classify systems according to design and load characteristics in order to establish baseline performance data. Other systems with similar characteristics could then be compared to the established baseline for a quick assessment of their comparative performance.
- Develop procedures to identify optimum head pressure and suction pressure set points to be used in optimized control of systems.
- It was demonstrated in this study that some design and operational changes involving the evaporators and evaporator defrosting could save the system significant amounts of energy. A detailed study involving evaporator fan control and evaporator design would provide useful information regarding evaporator control. Aspects of evaporator defrost to examine more closely include proper hot gas pressure, proper defrost piping designs, defrost cycle timing, defrost demand assessment, detailed defrost energy accounting, and parasitic space loads associated with defrosting.

# *Appendix A-Compact Disc File Directory*

:\CDfiles\Thesis\

Thesis, supporting table and graphics files, and other research related documents.

:\CDfiles\YearSimulations\

**CurrentSystemMdl.ees**

Model of the current system. Calls AvgMaxWeather.txt and HeatFluxs.txt files to input the outdoor air conditions and transmission heat gains, respectively.

**TwoStageMdl.ees**

Two-stage compression model. Calls AvgMaxWeather.txt and HeatFluxs.txt files to input the outdoor air conditions and transmission heat gains, respectively.

**SplitSystemMdl.ees**

Model of system with the fruit ripening rooms split off on their own separate system. Calls AvgMaxWeather.txt and HeatFluxs.txt files to input the outdoor air conditions and transmission heat gains, respectively.

**SplitSystemwithTS.ees**

Model of system with the fruit ripening rooms split off on their own separate system and operating as a thermosiphon for half of the year. Calls AvgMaxWeather.txt and HeatFluxs.txt files to input the outdoor air conditions and transmission heat gains, respectively.

**AvgMaxWeather.txt**

A text file that contains hourly weather data generated by the Extremes program for Milwaukee, WI. Weather data is for one 24hour "average" and one 24hour "maximum" day per month. (12 months)

**HeatFluxs.txt**

A text file that contains hourly wall heat flux data which was obtained from the steady state solution of files RoofSurHeatFlux.EES and WallSurHeatFlux.EES in the :\CDfiles\LoadCalcs\ directory. The following is an example identification label for a particular wall: mW0R40M68Es where m=maximum day (a=average), W=wall (R=roof), 0-0°F inside air temperature, R40=Rvalue of 40, M68=Average mass of wall or room is 68 lb/ft², E=east facing wall, s= wall is shaded from the sun.

:\CDfiles\YearSimulations\SimResults\

**SysPerformSym1.xls**

Yearly Simulation with 1 Stage Compression, Minimum Head Pressure, Set Receiver Temps., 85°F Condenser.

**SysPerformSym2.xls**

Yearly Simulation with 1 Stage Compression, Minimum Head Pressure, Set Receiver Temps., 85°F Condenser, No Unloading Penalty for Screw Compressors.

**SysPerformSym3.xls**

Yearly Simulation with 2 Stage Compression, Minimum Head Pressure, Set Receiver Temps., 85°F Condenser.

**SysPerformSym4.xls**

Yearly Simulation with 2 Stage Compression, Minimum Head Pressure, Set Receiver Temps., 85°F Condenser, No Unloading Penalty for Screw Compressors.

**SysPerformSym5.xls**

Yearly Simulation with 1 Stage Compression, Minimum Head Pressure, Set Receiver Temps., 95°F Condenser.

**SysPerformSym6.xls**

Yearly Simulation with 2 Stage Compression, Minimum Head Pressure, Set Receiver Temps., 95°F Condenser.

**SysPerformSym7.xls**
Yearly Simulation with 1 Stage Compression, Fixed Level Head Pressure, Set Receiver Temps., 95°F Condenser.

**SysPerformSym8.xls**
Yearly Simulation with 2 Stage Compression, Fixed Level Head Pressure, Set Receiver Temps., 95°F Condenser.

**SysPerformSym9.xls**
Yearly Simulation with 1 Stage Compression, Fixed Level Head Pressure, Set Receiver Temps., 95°F Condenser, No Unloading Penalty for Screw Compressors.

**SysPerformSym10.xls**
Yearly Simulation with 2 Stage Compression, Fixed Level Head Pressure, Set Receiver Temps., 95°F Condenser, No Unloading Penalty for Screw Compressors.

**SysPerformSym11.xls**
Yearly Simulation with 1 Stage Compression, Bi-Level Minimum Head Pressure, Set Receiver Temps., 85°F Condenser, Fruit Ripening Rooms Are Separate System.

**SysPerformSym12.xls**
Yearly Simulation with 1 Stage Compression, Bi-Level Minimum Head Pressure, Set Receiver Temps., 85°F Condenser, Fruit Ripening Rooms Are Separate System with Thermosiphon Capabilities.

**SysPerformSym13.xls**
Yearly Simulation with 1 Stage Compression, Fixed Level Head Pressure(166,142 psia), Set Receiver Temps., 85°F Condenser.

**SysPerformSym14.xls**
Yearly Simulation with 1 Stage Compression, Minimum Head Pressure, Set Receiver Temps., 85°F Condenser, VFD Condenser Fan Control.

**SysPerformSym15.xls**
Yearly Simulation with 1 Stage Compression, Optimum Head Pressure, Set Receiver Temps., 85°F Condenser, VFD Condenser Fan Control.

**SysPerformSym16.xls**
Yearly Simulation with 1 Stage Compression, Curve Fit Optimum Head Pressure, Set Receiver Temps., 85°F Condenser, VFD Condenser Fan Control.

**SysPerformSym17.xls**
Yearly Simulation with 1 Stage Compression, Minimum Head Pressure, Set Receiver Temps., 85°F Condenser, Evaporator Fans with Half-Speed Control.

**SysPerformSym18.xls**
Yearly Simulation with 1 Stage Compression, Minimum Head Pressure, Optimum Receiver Temps., 85°F Condenser, Evaporator Fans with Half-Speed Control.

**SysPerformSym19.xls**
Yearly Simulation with 1 Stage Compression, Minimum Head Pressure, Optimum Receiver Temps., 85°F Condenser.

**SysPerformSym20.xls**
Yearly Simulation with 1 Stage Compression, Minimum Head Pressure, Set Receiver Temps., 85°F Condenser, Defrost Load at Half.

**SysPerformSym21.xls**
Yearly Simulation with 1 Stage Compression, Minimum Head Pressure, Set Receiver Temps., 85°F Condenser, No Blow-By.

**SysPerformSym22.xls**
Yearly Simulation with 1 Stage Compression, Minimum Head Pressure, Set Receiver Temps., 85°F Condenser, Concrete Wall Construction in Freezer and Cooler.

**SysPerformSym23.xls**
Yearly Simulation with 1 Stage Compression, Minimum Head Pressure, Set Receiver Temps., 85°F Condenser, Doors Open Half The Time, Defrost Reduced by 25%.

**SysPerformSym24.xls**
Yearly Simulation with 1 Stage Compression, Bi-Level Optimum Head Pressure, Optimum Receiver Temps., 85°F Condenser, Fruit Ripening Rooms On Separate System, VFD on Condenser Fans, Half-Speed on Evaporator Fans, 25% Less Defrost and Blow-By.

**SysPerformSym25.xls**
Yearly Simulation with 1 Stage Compression, Minimum Head Pressure, Set Receiver Temps., 85°F Condenser, No Defrosting.

:\CDfiles\LoadCalcs\

**AvgMaxWeather.txt**
Text file containing hourly dry bulb, wet bulb, and irradiation data for Milwaukee, WI. The data is for the average and maximum day of each month.

**Weatherdata.lkt**
EES look-up table containing hourly dry bulb, wet bulb, and irradiation data for Milwaukee, WI. The data is for the average and maximum day of each month.

**Hrtmydat.xls**
Excel file containing hourly dry bulb, wet bulb, and irradiation data for Milwaukee, WI. The data is for the average and maximum day of each month.

**SolAirTemps.ees**
EES file used to calculate the sol-air temperatures of the building surfaces.

**AvgSolAirTemp.txt**
The calculated sol-air temperatures for all N,S,E,W surfaces of a building in Milwaukee,WI. The data is for the average day of each month.

**AvgSolAirTemp.txt**
The calculated sol-air temperatures for all N,S,E,W surfaces of a building in Milwaukee,WI. The data is for the maximum day of each month.

**RoofSurHeatFlux.ees**
EES file calculating the heat flux through the roof of a building knowing the sol-air temperature, indoor temperature, and wall construction.

**WallSurHeatFlux.ees**
EES file calculating the heat flux through the walls of a building knowing the sol-air temperature, indoor temperature, and wall construction.

:\CDfiles\ExpDataFiles\

**Feb7-13.xls**
Averaged system data at 5 min. intervals from the data acquisition system. (1998)

**Feb7-13_EnthHi.xls**
A time log of the high temperature mass flow meter pulses. 60lbs of refrigerant per pulse. (1998)

**Feb7-13_EnthLo.xls**
A time log of the low temperature mass flow meter pulses. 30lbs of refrigerant per pulse. (1998)

**FebDemand.xls**
Electrical demand data. 15 min. increments. (1998)

**Jan9-16.xls**
Averaged system data at 5 min. intervals from the data acquisition system. (1998)

**Jan9-16_EnthHi.xls**
A time log of the high temperature mass flow meter pulses. 60lbs of refrigerant per pulse. (1998)

**Jan9-16_EnthLo.xls**
A time log of the low temperature mass flow meter pulses. 30lbs of refrigerant per pulse. (1998)

**JanDemand.xls**
Electrical demand data. 15 min. increments. (1998)

**Mdot_Smoothing.xls**
File used to time average the mass flow pulse data.

**VarName.xls**
Contains the names and descriptions of all the experimental variables recorded by the data acquisition system.

:\CDfiles\Thesis\Plots\
Files used to create many of the figures used in the thesis.

:\CDfiles\ComponentModeling\Compressors\

Files associated with modeling the compressors. Includes an Excel file with all the manufacturer's data obtained from Vilter.

:\CDfiles\ComponentModeling\EvapCond\

Files associated with modeling an Evapco evaporative condenser.

:\CDfiles\ComponentModeling\Evaporator\

Files associated with modeling an evaporator.

:\CDfiles\ComponentModeling\Piping\

Files associated with modeling the pressure drop in the dry suction return lines of the system.

:\CDfiles\ComponentModeling\SubCooler\

File examining some experimental data from Feb.08,1998 regarding the effectiveness of the high temperature subcooler.

:\CDfiles\EESLibrary\

**AllocateLoad_AA_1_L1000.lib**

Allocates the entire load of two parallel compressors to a single compressor

**Defrost.lib**

Calculates the amount of refrigerant needed to meet the defrost load as well as the state of the ammonia exiting the coil after being defrosted.

**DX_Evap.lib**

Models the dx oil cooler in the reciprocating compressor.

**DX_EvapMod.lib**

Models the dx evaporators in the banana rooms.

**DX_EvapModBan.lib**

Models the dx evaporators in the banana rooms.

**EvapCond.lib**

Enthalpy based effectiveness of the PMCB-885 Evapco evaporative condenser.

**EvapCondFHPreal.lib**

Algorithm to select condensing pressure that emulates the current control strategy.

**EvapCondBan.lib**

Enthalpy based effectiveness of the PMCB-190 Evapco evaporative condenser used in the split system simulation.

**EvapCondBanFHP.lib**

Algorithm to select condensing pressure that emulates the current control strategy.

**EvapCondBanTS.lib**

Enthalpy based effectiveness of the PMCB-190 Evapco evaporative condenser used in the split system with thermosiphon simulation.

**EvapCondBanTS.lib**

Algorithm to select condensing pressure that emulates the current control strategy.

**HandXValve.lib**

Models a hand expansion valve.

**LoadFcts_DefBan.lib**

Contains functions that give the yearly defrost load profiles based on what month the simulation is on.

**LoadProf2.lib**

Reports the internal and wall transmission heat gains for the cooler, freezer, and loading dock spaces for the average day of each month.

**LoadProf2max.lib**

Reports the internal and wall transmission heat gains for the cooler, freezer, and loading dock spaces for the maximum day of each month.

**LOF_EvapMod.lib**
Models a liquid over-feed evaporator.
**PartLoadEvapCondHP.lib**
Estimates the part load hp requirements of the PMCB-885 Evapco evaporative condenser.
**PartLoadEvapCondBanHP.lib**
Estimates the part load hp requirements of the PMCB-190 Evapco evaporative condenser used in the split system simulation.
**PartLoadEvapCondBanTSHP.lib**
Estimates the part load hp requirements of the PMCB-190 Evapco evaporative condenser used in the split system with thermosiphon system simulation.
**PartLoadEvapHP.lib**
Estimates the part load hp requirements of the evaporators.
**RecSetTemps.lib**
Contains functions that set the optimum intermediate and low pressure receiver temperature set points for the current system with half-speed evaporator fan control.
**RecSetTempsAC.lib**
Contains functions that set the optimum intermediate and low pressure receiver temperature set points for a split system with half-speed evaporator fan control.
**RecSetTempsOnOff.lib**
Contains functions that set the optimum intermediate and low pressure receiver temperature set points for the current system with on/off evaporator fan control.
**SubCooler.lib**
Models an effectiveness based shell and tube heat exchanger.
**Thermal_Syphon.lib**
Calculates the mass flow of refrigerant required for the screw compressor thermosiphon oil coolers.
**TSPowerTrick.lib**
A procedure to trick the split system with thermosiphon into thinking the compressor is off for the average day of each month.
**TSPowerTrickmax.lib**
A procedure to trick the split system with thermosiphon into thinking the compressor is off for the maximum day of each month.
**UnderFloorHeatX.lib**
Models the under floor heat exchanger.
**Vmc4412.lib**
Models a Vilter model# VMC 4412 high-stage reciprocating compressor.
**Vmc4412booster.lib**
Models a Vilter model# VMC 4412 booster reciprocating compressor.
**Vmc4412plus.lib**
Models a Vilter model# VMC 4412 high-stage reciprocating compressor with an option to increase the size of the compressor.
**Vmc454.lib**
Models a Vilter model# VMC 454XL high-stage reciprocating compressor.
**Vmc454TS.lib**
Models a Vilter model# VMC 454XL high-stage reciprocating compressor for the thermosiphon system.
**Vss451.lib**
Models a Vilter model# VSS 451 high-stage single screw compressor.
**Vss451booster.lib**
Models a Vilter model# VSS 451 booster single screw compressor.
**Vss451boosterwoul.lib**
Models a Vilter model# VSS 451 booster single screw compressor with out any unloading penalty.
**Vss451woul.lib**
Models a Vilter model# VSS 451 high-stage single screw compressor with out any unloading penalty.

**Vss751.lib**

Models a Vilter model# VSS 751 high-stage single screw compressor.

**Vss751booster.lib**

Models a Vilter model# VSS 751 booster single screw compressor.

**Vss751boosterwoul.lib**

Models a Vilter model# VSS 751 booster single screw compressor with out any unloading penalty.

**Vss751woul.lib**

Models a Vilter model# VSS 751 high-stage single screw compressor with out any unloading penalty.

:\CDfiles\MdlValidation\

**CurrentSystemMdl_Feb08.ees**

Model of the current system which calls 15 minute experimental data from a lookup table called Feb08_15min.lkt and compares it with the actual mass flow and power consumption data stored in Feb08HiFlow.lkt, Feb08LoFlow.lkt, and Feb08Demand.lkt

**Feb08_15min.lkt**

Look up table storing 15 minute averaged experimental data from the system for February 8th.

**Feb08HiFlow.lkt**

Look up table storing mass flow measurements for the high temperature flow meter for February 8th.

**Feb08LoFlow.lkt**

Look up table storing mass flow measurements for the low temperature flow meter for February 8th.

**Feb08Demand.lkt**

Look up table storing kW and kWh data for the mechanical room for February 8th.

# *Appendix B- Regression Coefficients for Compressor Maps*

Compressor: VMC-4412
Type: High Stage, Recip. Suction Range: -25 to 35°F Discharge Range: 61 to 108°F
Capacity (C)[tons] Regression Coefficient Stats: No.Pts. = 90, $r^2$ = 99.94%, rms = 1.27
Power (P)[BHP] Regression Coefficient Stats: No.Pts. = 90, $r^2$ = 99.01%, rms = 2.65

| | | | | |
|---|---|---|---|---|
| C1 | 1.417794E+02 | P1 | 1.391940E+01 | Oil Load |
| C2 | -7.282728E-01 | P2 | 1.769032E+00 | 12,000 btu/hr per |
| C3 | 7.112363E-04 | P3 | -5.856508E-03 | cylinder head |
| C4 | 3.955366E+00 | P4 | -1.091229E+00 | 2cyl. = 1 cyl.head |
| C5 | 2.834690E-02 | P5 | -1.823856E-02 | |
| C6 | -1.342394E-02 | P6 | 2.840168E-02 | |

Compressor: VMC-4412
Type: Booster, Recip. Suction Range: -55 to 10°F Discharge Range: 11.3 to 52°F
Capacity (C)[tons] Regression Coefficient Stats: No.Pts. = 104, $r^2$ = 99.95%, rms = 0.69
Power (P)[BHP] Regression Coefficient Stats: No.Pts. = 104, $r^2$ = 99.71%, rms = 0.67

| | | | | |
|---|---|---|---|---|
| C1 | 1.196463E+02 | P1 | 2.647984E+01 | Oil Load |
| C2 | -2.683934E-01 | P2 | 1.455031E+00 | 12,000 btu/hr per |
| C3 | -3.693544E-03 | P3 | -4.388386E-03 | cylinder head |
| C4 | 2.931189E+00 | P4 | -8.850628E-01 | 2cyl. = 1 cyl.head |
| C5 | 1.949577E-02 | P5 | -1.207509E-02 | |
| C6 | -3.427118E-03 | P6 | 2.208473E-02 | |

Compressor: VSS-451
Type: High Stage, Screw Suction Range: -40 to 40°F Discharge Range: 75 to 105°F
Capacity (C)[tons] Regression Coefficient Stats: No.Pts. = 36, $r^2$ = 99.96%, rms = 1.66
Power (P)[BHP] Regression Coefficient Stats: No.Pts. = 36, $r^2$ = 99.38%, rms = 2.93
Oil Cooling Load (O)[tons] Regression Coefficient Stats: No.Pts. = 36, $r^2$ = 96.73%, rms = 1.18

| | | | | | |
|---|---|---|---|---|---|
| C1 | 1.479726E+02 | P1 | -8.024030E+00 | O1 | 1.251999E+01 |
| C2 | -2.384444E-01 | P2 | 1.892000E+00 | O2 | -3.017778E-01 |
| C3 | -1.444444E-03 | P3 | 6.111111E-04 | O3 | 3.888889E-03 |
| C4 | 3.741200E+00 | P4 | -1.338408E+00 | O4 | -3.461500E-01 |
| C5 | 2.771861E-02 | P5 | -8.148539E-03 | O5 | -3.469156E-03 |
| C6 | -7.196667E-03 | P6 | 2.640500E-02 | O6 | 2.210000E-03 |

Compressor: VSS-451
Type: Booster, Screw Suction Range: -70 to 10°F Discharge Range: 0 to 30°F
Capacity (C)[tons] Regression Coefficient Stats: No.Pts. = 26, $r^2$ = 99.97%, rms = 0.51
Power (P)[BHP] Regression Coefficient Stats: No.Pts. = 26, $r^2$ = 98.48%, rms = 1.18
Oil Cooling Load (O)[tons] Regression Coefficient Stats: No.Pts. = 22, $r^2$ = 99.87%, rms = 0.08

| | | | | | |
|---|---|---|---|---|---|
| C1 | 1.424953E+02 | P1 | 3.706316E+01 | O1 | -5.306015E+00 |
| C2 | -3.145059E-01 | P2 | 1.135181E+00 | O2 | 1.603894E-01 |
| C3 | -4.036120E-04 | P3 | 1.980317E-03 | O3 | 7.793372E-04 |
| C4 | 3.005527E+00 | P4 | -3.719673E-01 | O4 | -2.247171E-01 |
| C5 | 1.761754E-02 | P5 | -4.299868E-03 | O5 | -1.045195E-03 |
| C6 | -3.301035E-03 | P6 | 1.170343E-02 | O6 | 9.461581E-04 |

Compressor: VSS-751
Type: High Stage, Screw Suction Range: -40 to 40°F Discharge Range: 75 to 105°F
Capacity (C)[tons] Regression Coefficient Stats: No.Pts. = 36, $r^2$ = 99.96%, rms = 2.76
Power (P)[BHP] Regression Coefficient Stats: No.Pts. = 36, $r^2$ = 99.38%, rms = 4.88
Oil Cooling Load (O)[tons] Regression Coefficient Stats: No.Pts. = 36, $r^2$ = 96.75%, rms = 1.92

| | | | | | |
|---|---|---|---|---|---|
| C1 | 2.444451E+02 | P1 | -1.230368E+01 | O1 | 2.066645E+01 |
| C2 | -3.722222E-01 | P2 | 3.117111E+00 | O2 | -4.986667E-01 |
| C3 | -2.527778E-03 | P3 | 1.138889E-03 | O3 | 6.388889E-03 |
| C4 | 6.202342E+00 | P4 | -2.222375E+00 | O4 | -5.636333E-01 |
| C5 | 4.598133E-02 | P5 | -1.354302E-02 | O5 | -5.652597E-03 |
| C6 | -1.189500E-02 | P6 | 4.384167E-02 | O6 | 3.586667E-03 |

Compressor: VSS-751
Type: Booster, Screw Suction Range: -70 to 10°F Discharge Range: 0 to 30°F
Capacity (C)[tons] Regression Coefficient Stats: No.Pts. = 26, $r^2$ = 99.97%, rms = 0.85
Power (P)[BHP] Regression Coefficient Stats: No.Pts. = 26, $r^2$ = 98.48%, rms = 1.95
Oil Cooling Load (O)[tons] Regression Coefficient Stats: No.Pts. = 22, $r^2$ = 99.90%, rms = 0.11

| | | | | | |
|---|---|---|---|---|---|
| C1 | 2.364679E+02 | P1 | 6.149361E+01 | O1 | -8.811185E+00 |
| C2 | -5.266080E-01 | P2 | 1.879501E+00 | O2 | 2.764575E-01 |
| C3 | -6.428571E-04 | P3 | 3.386161E-03 | O3 | 9.854286E-04 |
| C4 | 4.988951E+00 | P4 | -6.178774E-01 | O4 | -3.700167E-01 |
| C5 | 2.925893E-02 | P5 | -7.136719E-03 | O5 | -1.719645E-03 |
| C6 | -5.553571E-03 | P6 | 1.937388E-02 | O6 | 1.699100E-03 |

Compressor: VMC-454xl
Type:High Stage, Recip. Suction Range: -25 to 55°F Discharge Range: 61 to 108°F
Capacity (C)[tons] Regression Coefficient Stats: No.Pts. = 90, $r^2$ = 99.94%, rms = 1.27
Power (P)[BHP] Regression Coefficient Stats: No.Pts. = 90, $r^2$ = 99.01%, rms = 2.65

| | | | | |
|---|---|---|---|---|
| C1 | 5.069950E+01 | P1 | 2.185788E+00 | Oil Load |
| C2 | -3.790672E-02 | P2 | 9.342884E-01 | 12,000 btu/hr per |
| C3 | -1.067513E-03 | P3 | -3.452822E-03 | cylinder head |
| C4 | 1.449601E+00 | P4 | -8.224665E-01 | 2cyl. = 1 cyl.head |
| C5 | 1.816389E-02 | P5 | -1.176638E-02 | |
| C6 | -5.295278E-03 | P6 | 1.822679E-02 | |

# *Appendix C-Regression Coefficients for Piping Losses*

| Piping Section | High Temperature, Dry Suction, Section 1 | High Temperature, Dry Suction, Section 2 | Low Temperature, Dry Suction, Section 1 | Low Temperature, Dry Suction, Section 2 |
|---|---|---|---|---|
| mass flow range | 500-4000 [lbm/hr] | 500-4000 [lbm/hr] | 500-4000 [lbm/hr] | 500-4000 [lbm/hr] |
| temperature range | 19 to 31°F | 20 to 31°F | -6 to -15°F | -6 to -15°F |
| PL1 | -3.283145E-03 | -3.968793E-02 | 1.424612E-02 | 3.456024E-01 |
| PL2 | 4.426028E-05 | -7.376233E-05 | 1.467649E-03 | 3.673461E-02 |
| PL3 | 4.766203E-06 | 2.375219E-05 | 2.641958E-05 | 6.562170E-04 |
| PL4 | 8.776170E-06 | 5.061285E-05 | -1.041767E-05 | -3.058960E-04 |
| PL5 | 2.928733E-09 | 1.880267E-08 | 7.632792E-09 | 2.005375E-07 |
| PL6 | -2.980726E-07 | -1.841325E-06 | -9.398284E-07 | -2.362885E-05 |
| No.Pts. | 83 | 83 | 83 | 83 |
| $r^2$ | 99.97% | 99.97% | 99.95% | 99.94% |
| rms | 0.00027 | 0.0018 | 0.00084 | 0.0022 |

# *Appendix D-Mechanical Piping Legend*

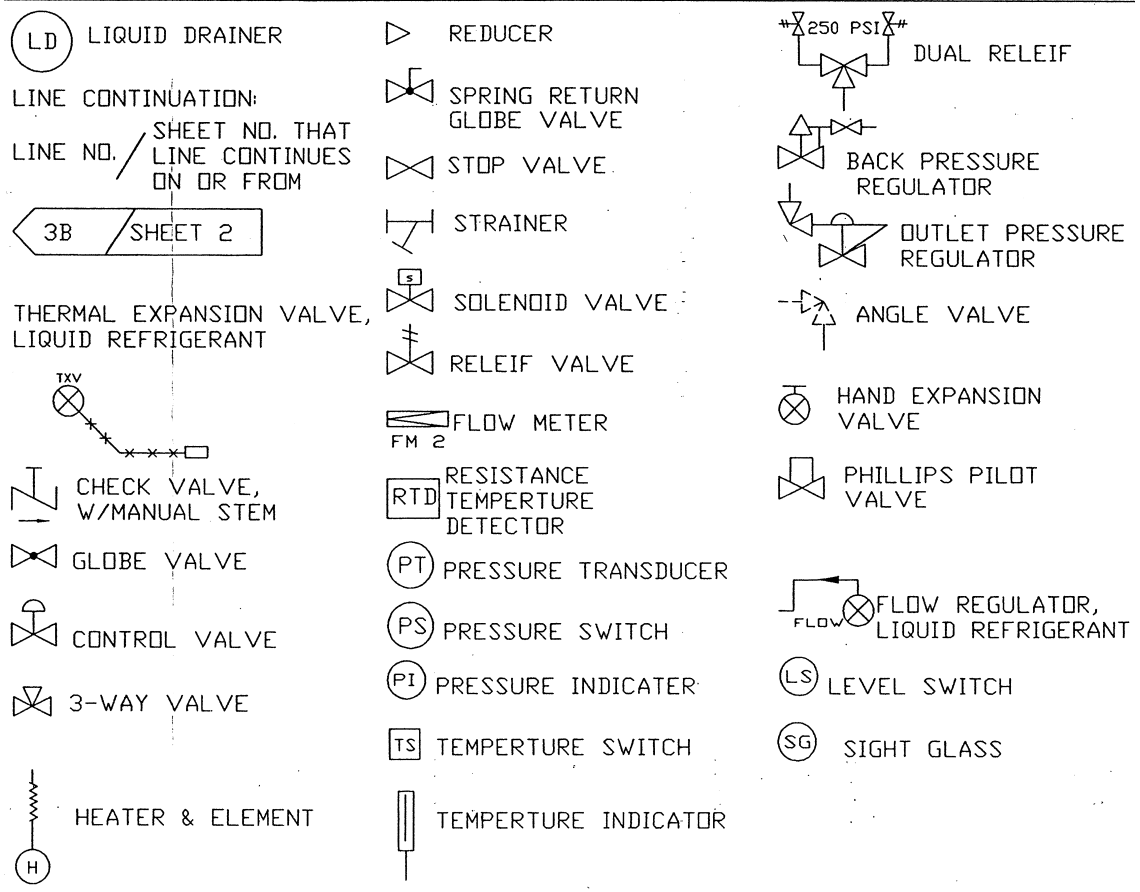

# *Appendix E-Internal Space Load Profiles*

| Daily Space Load Profiles [btu/hr] | | | | |
|---|---|---|---|---|
| Space | Source | Sensible [Btu/hr] | Latent [Btu/hr] | Loading Multiplier for First Shift Operation |
| Freezer | people | 4830 | 9730 | 0.5 |
| | product | 0 | 0 | 1 |
| | fork lifts | 118000 | 0 | 0.5 |
| | lights | 83060 | 0 | 1 |
| | sub-floor heating | 2.5/ft² | 0 | 1 |
| Cooler | people | 3450 | 6950 | 0.5 |
| | product | 0 | 1201 | 1 |
| | fork lifts | 118000 | 0 | 0.5 |
| | lights | 73700 | 0 | 1 |
| Dock | people | 3450 | 6950 | 0.5 |
| | product | 0 | 0 | 1 |
| | fork lifts | 55500 | 0 | 0.5 |
| | lights | 27528 | 0 | 1 |

| Monthly Space Load Profiles [MBH] | | | | | | | | | | | | |
|---|---|---|---|---|---|---|---|---|---|---|---|---|
| Month | 1 | 2 | 3 | 4 | 5 | 6 | 7 | 8 | 9 | 10 | 11 | 12 |
| Freezer, Hot Gas Defrost | 60 | 60 | 60 | 60 | 60 | 72 | 72 | 72 | 60 | 60 | 60 | 60 |
| Freezer, Warming Room Load | 120 | 120 | 120 | 120 | 156 | 156 | 156 | 156 | 120 | 120 | 120 | 120 |
| Cooler, Hot Gas Defrost | 144 | 144 | 144 | 144 | 144 | 180 | 180 | 180 | 180 | 144 | 144 | 144 |
| Cooler, Electric Defrost | 48 | 48 | 48 | 48 | 48 | 48 | 60 | 60 | 60 | 48 | 48 | 48 |
| Dock, Air Defrost | 60 | 60 | 60 | 60 | 60 | 120 | 120 | 120 | 120 | 60 | 60 | 60 |

# *References*

American Society of Heating, Refrigeration, and Air Conditioning Engineers (ASHRAE) Handbook, Refrigeration Volume, American Society of Heating, Refrigeration and Air Conditioning Engineers, Atlanta, GA, 1990.

American Society of Heating, Refrigeration, and Air Conditioning Engineers (ASHRAE) Handbook, Refrigeration Volume, American Society of Heating, Refrigeration and Air Conditioning Engineers, Atlanta, GA, 1994.

Altweis, Joy, "Electrical Demand Reduction in Refrigerated Warehouses," M.S. Thesis, Mechanical Engineering, Solar Energy Laboratory, University of Wisconsin-Madison, 1998.

Avallone, Eugene A (editor), Baumeister III, Theodore (editor), Marks' Standard Handbook For Mechanical Engineers, Ninth Edition, McGraw-Hill, New York, NY, 1987.

Brownell, K.A., "Investigation of the Field Performance for Industrial Refrigeration Systems," M.S. Thesis, Mechanical Engineering, Solar Energy Laboratory, University of Wisconsin- Madison, 1998.

Crane Co., "Flow of Fluids Through Valves, Fittings, and Pipe." Technical Paper No. 410, Joliet, IL, 1988.

Fisher, M., Engineer, Vilter Manufacturing Company, Milwaukee, WI, private communication, 1998.

Kastello R., Engineer, J.F. Ahern Co., Fondulac, WI, private communication, 1999.

Klein, S.A., ALvarado, F.L. "EES-Engineering Equation Solver," F-Chart Software, Middleton, WI, 1999.

Klein, S.A., Reindl D.T., and Brownell, K.A., Refrigeration System Performance using Liquid-Suction Heat Exchangers, *International Journal of Refrigeration,* Accepted for Publication January 2000.

Krack Corporation, "Refrigeration Load Estimating Manual." Manual RLE-593, Addison, IL, 1992.

Kollasch, J., Engineer, EVAPCO Inc., Westminster, MD, private communication, 1999.

Mitchell, John W. and Braun, James E., Design, Analysis, and Control of Space Conditioning Equipment and Systems, University of Wisconsin-Madison, 1998.

Nicoulin et al, Computer Modeling Of Commercial Refrigerated Warehouses *Proceedings ACEEE*, Washington D.C., pp. 15-27, 1997.

Schmidt, D., Klein, S., Reindl, D., American Society of Heating, Refrigeration, and Air Conditioning Engineers (ASHRAE) Research Project RP-962.

Stamm R.H., Engineer, Industrial Refrigeration, Inc., Sandy, OR, private communication, 1999.

Stamm, R.H., Industrial Refrigeration: Frost Removal, *Heating/Piping/Air Conditioning*, April,1985.

Stoecker, W.F., Industrial Refrigeration, Business News Publishing Company, Troy MI, 1988.

Struder, G., Engineer, EVAPCO Inc., Westminster, MD, private communication, 1999.

Taylor B.N. and Kuyatt, C.E., Guidelines for Evaluating and Expressing the Uncertainty of NIST Measurement Results, National Institute of Standards and Technology Technical Note 1297, 1994.